

ISTANBUL TECHNICAL UNIVERSITY ★ ENERGY INSTITUTE

**IDENTIFICATION OF CLOSED CAVITY FAÇADES IN TERMS OF
CONDENSATION RISK AND ENERGY PERFORMANCE**

M.Sc. THESIS

Ahmet BILER

Energy Science and Technology Division

Energy Science and Technology Programme

MAY 2015

ISTANBUL TECHNICAL UNIVERSITY ★ ENERGY INSTITUTE

**IDENTIFICATION OF CLOSED CAVITY FAÇADES IN TERMS OF
CONDENSATION RISK AND ENERGY PERFORMANCE**

M.Sc. THESIS

**Ahmet BILER
301121001**

Energy Science and Technology Division

Energy Science and Technology

Thesis Advisor: Assoc. Prof. Dr. Hatice SOZER

MAY 2015

İSTANBUL TEKNİK ÜNİVERSİTESİ ★ ENERJİ ENSTİTÜSÜ

**KAPALI BOŞLUKLU – ÇİFT CİDARLI CEPHELERİN YOĞUŞMA RİSKİ VE
ENERJİ PERFORMANS ANALİZLERİ**

YÜKSEK LİSANS TEZİ

**Ahmet BİLER
(301121001)**

Enerji Bilim ve Teknoloji Anabilim Dalı

Enerji Bilim ve Teknoloji Programı

Tez Danışmanı: Doç. Dr. Hatice SÖZER

MAYIS 2015

Ahmet BILER, a **M.Sc.** student of ITU **Institute of Energy** student ID 301121001, successfully defended the **thesis** entitled “**IDENTIFICATION OF CLOSED CAVITY FAÇADES IN TERMS OF CONDENSATION RISK AND ENERGY PERFORMANCE** ”, which he prepared after fulfilling the requirements specified in the associated legislations, before the jury whose signatures are below.

Thesis Advisor : **Assoc. Prof. Dr. Hatice SÖZER**

Istanbul Technical University

Jury Members : **Prof. Dr. Ahmet DURMAYAZ**

Istanbul Technical University

Prof. Dr. Zeynep Düriye BİLGE

Yildiz Technical University

Date of Submission : 4 May 2015

Date of Defense : 27 May 2015

To science,

FOREWORD

Condensation prevention is highly crucial to keep materials sustainable, to conserve them from corrosion and other environmental effects and to supply visual aesthetics in building envelopes. Energy efficiency in buildings has also significant role to decrease environmental pollution as well as for the minimization of initial cost and operating cost together. Moreover, high energy efficiency without condensation risk in building envelopes is highly essential to supply thermal comfort conditions at indoor environment with lower cost. On the other hand, the application of double skin façades under Turkey conditions is quite untouched topic. Therefore, there were supposed to be done a scientific study in this field to show decision makers probable risks and advantageous.

The purpose of thesis is to propose an appropriate configuration of a new generation closed-cavity façade which has maximum thermal performance without condensation risk.

I am grateful to Assoc. Prof. Dr. Hatice Sözer for her valuable assistance, continuous advice and well guidance in this study.

Special thanks to **METAL YAPI** for providing the licensed Solidworks Flow Simulation CFD program, supplying all the materials related to glass and frame, configuring experiment mock-up, providing sufficient time for this scientific study as employer and encouraging me to finalize master thesis.

Special thanks to **FTI** (Façade Testing Institute) for supplying experiment filters from a company in France and permitting me to use all measuring devices and charging staff to arrange experiment chambers for this scientific study.

Key words: Double skin façade, evaluation of condensation, closed cavity façade, façade respirante, CFD for double skin façade, solidworks flow simulation, August-Roche Magnus formula, filter modelling of closed cavity façade, Bisco, Vitrage Decision, cooling load, heating load, thermal transmittance

May 2015

Ahmet Biler
(Civil Engineer)

TABLE OF CONTENTS

	<u>Page</u>
FOREWORD	ix
TABLE OF CONTENTS	xi
ABBREVIATIONS	xv
LIST OF TABLES	xvii
LIST OF FIGURES	xix
SUMMARY	xxi
1. INTRODUCTION	1
1.1 Purpose of Thesis	3
2. FAÇADE RESPIRANTE	5
2.1 Literature Review	6
3. CONFIGURATION METHODS OF FR TEST MOCK-UP	11
3.1 Determination of Appropriate Façade Respirante Profile Detail	11
3.2 Constitution of Façade Respirante Profile	11
3.3 Test Model Constitution of Designed Façade Respirante Details.....	12
4. ANALYSIS METHODS	15
4.1 Analysis of FR in Laboratory Environment	15
4.1.1 Setting the boundary Conditions	15
4.1.2 Setting the boundary conditions of configured façade respirante condensation test	17
4.2 Analysis of FR with CFD Model	17
4.2.1 Setting boundary conditions of CFD Model.....	17
4.3 Analysis of FR in terms of Energy Performance	19
4.3.1 Setting boundary conditions of energy performance analysis	19
4.3.2 Condensation risk analysis of frames	19
4.3.3 Thermal transmittance analysis of frames	20
4.3.4 Energy performance.....	20
5. DETERMINATION OF FR MODELLING BY CFD (COMPUTATIONAL FLUID DYNAMICS)	23
5.1 General Features of CFD Model	23
5.1.1 Specific system definitions for CFD model.....	23
5.1.1.1 Glass combination.....	23
5.1.1.2 Support of specimen	23
5.1.1.3 Filters	23
5.1.1.4 Venetian blinds	24
5.1.2 Simplifications.....	24
5.1.2.1 Glass simplifications.....	24
5.1.2.2 Filter simplification.....	24
5.1.2.3 Blind simplification	25
5.2 General Settings of CFD Models	25
5.2.1 Determination of the initial conditions	25

5.2.2	Boundary conditions	26
5.2.2.1	Indoor conditions	26
5.2.2.2	Outdoor conditions.....	26
5.2.2.3	Turbulence model	26
5.2.2.4	Other settings	26
5.2.3	Mesh settings	27
5.3	Results	28
5.3.1	Specified points.....	29
5.3.2	Velocity, temperature and RH values from specified points	30
5.3.3	Value comparison charts between three different models	32
5.3.4	Cut plots from the middle of right plane.....	35
5.3.5	Validation with August-Roche Magnus approach.....	38
5.3.6	Effect of different filter distance to exterior glass	41
5.4	Next Step	43
6.	TESTING THE FR FOR CONDENSATION RISK	45
6.1	Methodology of Experiment.....	46
6.1.1	Setting the boundary conditions	46
6.2	Description of Mock-Up.....	47
6.2.1	General features of glazing combination	47
6.2.1.1	Inner glass combination	47
6.2.1.2	Outer glass.....	47
6.2.2	Venetian blinds	48
6.2.3	Filters	50
6.2.4	General views of façade respirante details	51
6.3	Selection of Experiment Equipments	53
6.3.1	Identification of experiment equipments	53
6.3.1.1	Thermocouple (Thermal Sensor)	53
6.3.1.2	Hygrometers (Humidity Sensors)	55
6.3.1.3	Data logger	57
6.3.1.4	Humidity control	57
6.3.2	Calibration	58
6.3.2.1	Hygric sensors.....	58
6.3.2.2	Thermal sensors	58
6.4	Set Cases.....	59
6.5	Results	60
6.5.1	Venetian blind with vertically positioned (Slats are closed)	61
6.5.2	Venetian blind with horizontally positined (Slats are open).....	64
6.5.3	Venetian blinds are removed	67
6.5.4	One filter is sealed	70
6.5.5	Two filters are sealed	73
7.	ANALYZING THE FR BASED ON ITS ENERGY PERFORMANCE.....	77
7.1	Thermal Analysis.....	77
7.1.1	Referenced standards and norms	77
7.1.2	Technical features in terms of building physics	78
7.1.3	Boundary conditions and initial conditions	78
7.1.4	General views of constituted closed cavity façade details.....	80
7.1.5	Condensation risk assessment.....	82
7.1.5.1	Determination of interior glass air gap thermal conductivity	82
7.1.5.2	Horizontal profile -1 (Bottom).....	83
7.1.5.3	Horizontal profile -2 (Top)	84

7.1.5.4 Vertical profile	85
7.1.6 Determination of U_w value	86
7.1.6.1 U_g of glazing combination	86
7.1.6.2 Horizontal profile-1 (Bottom).....	89
7.1.6.3 Horizontal profile-2 (Top)	90
7.1.6.4 Vertical profile	91
7.1.6.5 Global U_w value	92
7.2 Energy Performance	94
7.2.1 Thermal transmittance through conduction and convection.....	94
7.2.2 Solar heat gain calculation.....	96
7.2.3 Cooling load comparison considering solar radiation	99
7.2.3.1 South direction	99
7.2.3.2 North direction	100
7.2.3.3 West/East direction	101
7.2.4 Heating load considering solar radiation	102
7.2.4.1 South direction	102
7.2.4.2 North direction	104
7.2.4.3 West/East direction	105
7.2.5 Carbon footprint.....	106
7.3 Result.....	107
8. CONCLUSION	109
8.1 Evaluation of CFD Results.....	109
8.2 Evaluation of Lab Results	110
8.3 Evaluation of Energy Performance Analysis	110
ACKNOWLEDMENT	113
REFERENCES	115
CURRICULUM VITAE	117

ABBREVIATIONS

1/U	: Total thermal resistance ($\text{m}^2.\text{K}/\text{W}$)
A	: Area (m^2)
A_f	: Area of frame (m^2)
A_g	: Area of glazing (m^2)
A_i	: Total window area in “i” direction (m^2)
A_s	: Area of spandrel zone (m^2)
CCF	: Closed Cavity Façade
CFD	: Computational Fluid Dynamics
CSTB	: Centre Scientifique et Technique du Bâtiment
CTBUH	: Council on Tall Buildings and Urban Habitat
D	: Thickness of frame component (m)
FR	: Façade Respirante
FTI	: Façade Testing Institute
g_{i,month}	: Monthly average solar factor (SHGC) of transparent surfaces in “i” direction
HVAC	: Heating, Ventilating and Air Conditioning Systems
I_{i,month}	: Monthly average solar radiation intensity of vertical surfaces in “i” direction (W/m^2),
M-Free	: Moisture Free
R	: Thermal resistance ($\text{m}^2.\text{K}/\text{W}$),
R_e	: Thermal resistance of exterior surface ($\text{m}^2.\text{K}/\text{W}$)
RH_{outdoor}	: Outdoor relative humidity value
RH_{cavity}	: Relative humidity value in cavity
RH_{indoor}	: Indoor relative humidity
R_i	: Thermal resistance of interior surface ($\text{m}^2.\text{K}/\text{W}$),
r_{i,month}	: Monthly average shading factor of transparent surfaces in “i” direction
RW	: Reference Window
SHGC	: Solar Heat Gain Coefficient
T_{ext glass}	: Exterior glass interior surface temperature ($^{\circ}\text{C}$)
T_{inner cavity}	: Temperature between blind and interior glass ($^{\circ}\text{C}$)
T_{indoor}	: Indoor temperature ($^{\circ}\text{C}$)
T_{outer cavity}	: Temperature between exterior glass and blind ($^{\circ}\text{C}$)
U	: Thermal transmittance ($\text{W}/\text{m}^2.\text{K}$)
U_f	: Thermal transmittance of the frame section ($\text{W}/\text{m}^2.\text{K}$)
U_g	: Thermal transmittance of the glazing section ($\text{W}/\text{m}^2.\text{K}$)
U_s	: Thermal transmittance of the spandrel section ($\text{W}/\text{m}^2.\text{K}$)
U_w	: Thermal transmittance of the window modulus ($\text{W}/\text{m}^2.\text{K}$)
λh	: Thermal conductivity ($\text{W}/\text{m}.\text{K}$)
Ψ	: Linear thermal transmittance $\text{W}/(\text{m}.\text{K})$

LIST OF TABLES

	<u>Page</u>
Table 4.1 : Initial conditions and final situations data table.....	16
Table 4.2 : Condensation risk assessment experiment results of specified Façade Respirante system.....	18
Table 4.3 : Dew points of experimental values.....	19
Table 4.4 : Monthly average ambient air temperatures	21
Table 4.5 : Solar radiation values from different directions	21
Table 5.1 : Total iteration number and total mesh number	28
Table 5.2 : Explanation of specified points.....	30
Table 5.3 : “Model without porous media” results from specified points in cavity .	30
Table 5.4 : “Model without porous media” results from specified points on exterior glass surface	31
Table 5.5 : “Model with porous media” results from specified points in cavity	31
Table 5.6 : “Model with porous media” results from specified points on exterior glass surface	31
Table 5.7 : “Model with linear channel” results from specified points in cavity.....	32
Table 5.8 : “Model with linear channel” results from specified points on exterior glass surface	32
Table 5.9 : Experiment results at 400 th minute	38
Table 5.10 : Dew point value changes with respect to relative humidity and temperature	40
Table 5.11 : Condensation risk assessment in “Model without porous media”	40
Table 5.12 : Condensation risk assessment in “Model with porous media”	41
Table 5.13 : Condensation risk assessment in “Model with linear channel”	41
Table 5.14 : Effect of “25 mm distance to exterior glass” in cavity	41
Table 5.15 : Effect of “25 mm distance to exterior glass” on exterior glass surface	42
Table 5.16 : Effect of “38 mm distance to exterior glass” in cavity	42
Table 5.17 : Effect of “38 mm distance to exterior glass” on exterior glass surface”	42
Table 5.18 : Effect of “56 mm distance to exterior glass” in cavity	42
Table 5.19 : Effect of “56 mm distance to exterior glass” on exterior glass surface	43
Table 6.1 : Initial conditions and final situations data table.....	46
Table 6.2 : The zones where thermal sensors (Thermocouple) are located and height of them.....	55
Table 6.3 : Hygrometer positions in experiment.....	57
Table 6.4 : Hygric calibrations.....	58
Table 6.5 : Thermal calibrations	59
Table 6.6 : Condensation risk experiment result table of venetian blind with vertically positioned	62

Table 6.7 : Condensation risk experiment result table of venetian blind with horizontally positioned (Slats are opened)	65
Table 6.8 : Venetian blinds are removed.....	68
Table 6.9 : Mean pressure difference value between P_{cvp} and P_{svp} in last 100 minute	70
Table 6.10 : One Filter is sealed.....	71
Table 6.11 : Two filters are sealed	74
Table 6.12 : Mean pressure difference value between P_{cvp} and P_{svp} in last 100 minute	76
Table 7.1 : Thermal conductivity values of various materials	78
Table 7.2 : Dew point Table respect to RH vs. indoor temperature.....	79
Table 7.3 : Calculation of thermal conductivity of glass air gap	82
Table 7.4 : Monthly average ambient air temperatures.....	95
Table 7.5 : Heat flow through closed cavity façade (W/m^2).....	95
Table 7.6 : Heat flow through reference window (W/m^2).....	96
Table 7.7 : Solar radiation values from different directions.....	98
Table 7.8 : Solar radiation values for CCF and Reference window with respect to solar directions	98
Table 7.9 : Total heat flow and solar heat gain from south through closed cavity façade.....	99
Table 7.10 : Total heat flow and solar heat gain from south through reference window.....	100
Table 7.11 : Total heat flow and solar heat gain from north through closed cavity façade	100
Table 7.12 : Total heat flow and solar heat gain from north through reference window.....	101
Table 7.13 : Total heat flow and solar heat gain from east and west through closed cavity façade	101
Table 7.14 : Total heat flow and solar heat gain from east and west through reference window	102
Table 7.15 : Total heat flow and solar heat gain from south through closed cavity façade	103
Table 7.16 : Total heat flow and solar heat gain from south through reference window.....	103
Table 7.17 : Total heat flow and solar heat gain from north through closed cavity façade	104
Table 7.18 : Total heat flow and solar heat gain from south through reference window.....	105
Table 7.19 : Total heat flow and solar heat gain from east and west through closed cavity façade	105
Table 7.20 : Total heat flow and solar heat gain from south through reference window.....	106
Table 7.21 : Annual total heating and cooling load together just because of heat flow and solar radiation.....	107
Table 7.22 : Annual savings with respect to regions.....	107

LIST OF FIGURES

	<u>Page</u>
Figure 1.1 : Active façade	1
Figure 1.2 : Naturally ventilated façade.....	1
Figure 1.3 : Interactive façade.....	2
Figure 1.4 : Closed cavity façades	2
Figure 2.1 : Façade Respirante.....	6
Figure 3.1 : General view of Constituted Façade Respirante test mock-up after analysis.....	12
Figure 3.2 : Longitudinal section and cross section view of filters	13
Figure 4.1 : The section of experiment prototype based on Façade Respirante (CLC 12-260039255) detail from CSTB	16
Figure 4.2 : Experimental mock-up view of Façade Respirante.....	17
Figure 5.1 : 3D view of CFD model with discrete blinds.....	26
Figure 5.2 : Mesh distribution of CFD model (from left to right Y-Z axis view, filter mesh, X-Z axis view, X-Y view).....	27
Figure 5.3 : Specified points	29
Figure 5.4 : Relative humidity values at glass surface (above), cavity between exterior glass and blind (bottom left), cavity between blind and interior glass (bottom right).....	33
Figure 5.5 : Temperature values at glass surface (above), cavity between exterior glass and blind (bottom left), cavity between blind and interior glass (bottom right).....	34
Figure 5.6 : Velocity values at glass surface (above), cavity between exterior glass and blind (bottom left), cavity between blind and interior glass (bottom right).....	34
Figure 5.7 : Model without porous media (left), model with porous media (middle), model with linear channel (right) velocity distributions.....	35
Figure 5.8 : Model without porous media (left), model with porous media (middle), model with formed crack (right) temperature distribution	36
Figure 5.9 : Model without porous media (left), model with porous media (middle), model with linear channel (right) relative humidity distributions	37
Figure 6.1 : Section view of experiment stand.....	47
Figure 6.2 : Glazing combinations of Façade Respirante	48
Figure 6.3 : Technical features of inner glass combination [Guardian Glass Configurator]	49
Figure 6.4 : Hella Blind.....	49
Figure 6.5 : Plan and section and view of filters.....	50
Figure 6.6 : General view of constituted façade respirante test mock-up after analysis.....	51
Figure 6.7 : Horizontal frame-1 (Bottom).....	52
Figure 6.8 : Horizontal frame-2 (Top)	52

Figure 6.9 : Vertical frame	52
Figure 6.10 : Experimental mock-up view of Façade Respirante	53
Figure 6.11 : Section detail (left) and plan detail (right) placement of thermocouples and hygrometers	54
Figure 6.12 : Omega T type thermocouple	54
Figure 6.13 : Dixell XH20P hygrometer	56
Figure 6.14 : OMET T3111P hygrometer	56
Figure 6.15 : HP Agilent 34972A data logger	57
Figure 6.16 : Olefini-12 NA dehumidifier	58
Figure 6.17 : General view of experiment stand	60
Figure 6.18 : Condensation risk experiment result chart of venetian blind with vertically position	63
Figure 6.19 : Condensation risk experiment result chart of venetian blind with horizontally positioned (slats are open)	66
Figure 6.20 : Venetian blinds are removed	69
Figure 6.21 : One filter is sealed	72
Figure 6.22 : Two filters are sealed	75
Figure 7.1 : The change of dew point value according air temperature vs. dew point temperature	79
Figure 7.2 : General view of Constituted Façade Respirante test mock-up after CFD analysis	80
Figure 7.3 : Horizontal frame-1 (Bottom)	81
Figure 7.4 : Horizontal frame-2 (Top)	81
Figure 7.5 : Vertical frame	82
Figure 7.6 : Temperature distribution on the detail with isothermal lines (Red)	83
Figure 7.7 : Temperature distribution on the detail with isothermal lines (Red)	84
Figure 7.8 : Temperature distribution on the detail with isothermal Lines (Red)	85
Figure 7.9 : Glazing combinations of Façade Respirante	87
Figure 7.10 : Technical features of glazing combinations	88
Figure 7.11 : Temperature distribution on detail with isothermal lines (Red)	89
Figure 7.12 : Temperature distribution on detail with isothermal lines (Red)	90
Figure 7.13 : Temperature distribution on detail with isothermal lines (Red)	91
Figure 7.14 : Closed cavity mock-up distribution of system components	92
Figure 7.15 : Thermal and light characteristics of reference window	97

IDENTIFICATION OF CLOSED CAVITY FAÇADES IN TERMS OF CONDENSATION'S RISK AND ENERGY PERFORMANCE

SUMMARY

The condensation risk and energy performance of closed cavity façade, so called Façade Respirante was analysed in this thesis. The research is composed of three different parts which are condensation risk assessment based on computational fluid dynamics (CFD) modelling, testing condensation risk in Lab environment and energy performance analysis of tested closed cavity façade.

Condensation risk assessment on CFD is based on the methodology and the data obtained from CSTB (Centre Scientifique et Technique du Bâtiment) test with CLC 12-260039255 code. The methodology and the result of this test is used in order to validate the outputs of three different filter modelling which are “Model with porous media”, “Model without porous media” and “Linear channel” approach. These approaches are modelled separately as 3 different CFD models. The values obtained from interior cavity match up with each 3 models in quite high level in terms of relative humidity, temperature and velocity. Dew point values at “model with linear channel” is lower with respect to other models. The reason is having higher velocities leads to lower dew points. Higher velocities with ignorable level are observed at the model with linear channel. The dew points which are obtained with August-Roches Magnus approach in the middle of cavity between venetian blind and exterior glass are considerably lower than temperature on glass surface with same height. Therefore, there is no condensation in all specified CFD models with indicated conditions. There is also analysis with respect to filter distance change to exterior side. When filter gets closer to interior side, relative humidity next outer glass becomes higher. Filter position influences more bottom part of cavity from temperature, velocity and relative humidity aspect. As a result, Façade Respirante model is developed without any condensation under specified conditions by considering comprehensive CFD results.

Closed cavity façade (Façade Respirante) experiment module is configured based on comprehensive CFD results. Configured closed cavity façade is tested at FTI (Façade Testing Institute) Labs in Istanbul Turkey.

Experiment results indicates that there is high tendency to condensation formation at venetian blinds vertically positioned case. On the other hand, when the blinds are removed, there is less probability to form condensation on outer glass surface. Moreover, as long as number of filter decrease, there is higher condensation risk. There is no condensation formation on glass surfaces, if there is at least 5 filters at bottom side of configured façade respirante system.

Energy performance analysis is composed of two parts which are façade's thermal and energy performance analyses. The simulation for thermal analyses on specified aluminium surfaces of Façade Respirante shows that there is no condensation. Final U_w value of closed cavity façade module is determined as $1.56 \text{ W/m}^2\text{K}$ and 0.39 solar factor with respect to specified standards. The comparison with reference

window which has $2.40 \text{ W/m}^2\text{K}$ and 0.42 solar heat gain coefficient based on TS 825 standard are made to evaluate the heat transfer due to temperature difference and solar radiation intensity. Consequently, there is monthly up to 6.4 W/m^2 and annually up to 17.8 W/m^2 saving in cooling load by applying closed cavity façade (CCF) system. Besides, there is monthly up to 23.6 W/m^2 and annually up to 130.5 W/m^2 saving in heating load by applying CCF system. There is up to 130.5 W/m^2 heat transfer rate difference in Turkey. It means, it can be up to 339.3 kWh annual saving for each m^2 of window. Configured CCF system with 339.3 kWh for each m^2 energy saving potential, decrease 234 kg CO_2 emission in a year which corresponds to 6 trees CO_2 emission toleration.

KAPALI BOŞLUKLU-ÇİFT CİDARLI CEPHELERİN YOĞUŞMA RİSKİ VE ENERJİ PERFORMANSI ANALİZLERİ

ÖZET

Bu tez kapsamında çift cidarlı cephe sistemlerinden ara boşlukları kısmi olarak havalandırılan kapalı boşluklu-çift cidarlı cephelerin yoğuşma riski ve enerji performansı açılarından değerlendirilmesi ele alınmıştır. Tez, daha önce Fransa’da yapılmış benzer bir cephe sisteminin deney verileri kullanılarak sistemin hesaplamalı akışkanlar dinamiği (CFD) aracılığıyla modellenmesi, kapsamlı CFD sonuçları ile oluşturulan yeni cephe modülünün FTI (Façade Testing Institute) laboratuvarlarında yoğuşma riski açısından test edilmesi ve yeni oluşturulan cephe modülünün enerji performansının analiz edilmesi olmak üzere üç farklı aşamadan oluşmaktadır.

Façade Respirante (Nefes alabilir cephe) kapalı boşluklu bir çift cidarlı cephe türüdür. Cephede camlar arası alt bölgeye hava filtreleri yerleştirilerek dış cam iç yüzeydeki yoğuşma oluşumunun engellenmesi amaçlanmaktadır. Façade Respirante sisteminde hiç yoğuşma olmadan maksimum ısı performansına ulaşmak ana hedeflerden bir tanesidir. Sistem, camlar arası bölgede üst taraftan ve yan taraflardan tamamen kapatılmış, alt taraftan ise filtreler aracılığı ile kısmi olarak hava girişi sağlanmaktadır. Yoğuşma oluşumu filtrelerin ağ yapısı ve filtre sayısı ile oynanarak kontrol edilmektedir. Filtre sayısının azalması ve filtre ağlarının küçülmesi camlar arası boşluk bölgesinde taşınım (convection) ile ısı geçişini minimize etmekte; toz, kir ve uçucu bileşenlerin içeri girişini azaltarak hijyen sağlanmasına yardımcı olmaktadır. Ancak, bu durumda yetersiz hava hareketi yoğuşmaya sebep olmaktadır. İdeal filtre sayısı yapılan testler ile yoğuşmanın olmadığı en düşük filtre sayısı olarak belirlenmektedir. Filtre sayısı ve filtre ağ yapısı sistem boyutları, sistemin uygulanacağı bölge ve sistem bileşenlerinin higroskopik (nem-tutma) özelliklerine göre değişkenlik göstermektedir.

CSTB'nin (Centre Scientifique et Technique du Batiment) yaptığı Façade Respirante yoğuşma deneyi test metodolojisinde başlangıç ve sınır koşulları olarak iç ortam sıcaklığı 20°C'de ve %50 bağıl nemde sabit tutulur ve yine iç ortama 50 Pa pozitif basınç verilir. Dış ortamda ise başlangıç koşulu olarak sıcaklık 20°C'ye ve bağıl nem %80'e şartlanır. Sıcaklık her 20 dakika'da bir 1 °C düşürülerek 400. dakikanın sonunda 0°C'ye ulaştırılır. Higrometre ve ısı çiftleri (thermocouple) ile iç ortam, ara boşluk ve dış ortamda sıcaklık ve nem değişiminin takibi yapılır. Sonuç olarak, ölçülen camlar arası boşluk kısmi buhar basıncı değeri, dış camın iç yüzeyinde okunan sıcaklık değerine karşılık gelen doymuş buhar basıncı değerinden küçük ise yoğuşma olmamaktadır denir.

CSTB'nin yaptığı CLC 12-260039255 kodlu deney kapsamlı fiziksel sonuçlara ulaşabilmek ve üç farklı filtre modelleme yöntemini teyit etmek amacıyla bir CFD programı olan Solidworks Flow Simulation programında modellenmiştir. Modelleme sırasında toplam ağ sayısını azaltmak ve programın çalışma (işlem) süresini düşürebilmek amacıyla camlar, filtreler ve jaluzi modellenirken bazı basitleştirmeler

yapılmıştır. Deneyde kullanılan iç cam kombinasyonu aynı ısı iletkenlik değerine sahip tek katı olarak modellenmiş, jaluziler ise 0,30'luk gözeneklilik değerine sahip gözenekli ortam (porous media) olarak modellenmiştir. Filtreler ise “gözenekli ortamsız model”(model without porous media), “gözenekli ortamlı model” (model with porous media) ve “çizgisel kanal” (linear channel) olmak üzere üç farklı yöntem ile modellenmiş, sonuçlar bu yaklaşımlara göre karşılaştırılmıştır. Bu üç modelde hava geçiş alanının tam olarak aynı olması sağlanmıştır. Filtreler, “Model without porous media”da 775,5 mm² yüzey alanına sahip yüzey ile, “Model with porous media” de 1250,7 mm² alan ve % 63'lük geçirgenliğe sahip bir yüzey ile “çizgisel kanal”da ise yatay kesit boyunca 4.5 mm genişliğindeki çizgisel bir kanal olarak modellenmiştir. İç ortam ve dış ortam şartları CSTB’de yapılan deneyin 400. dakikasının şartları referans alınarak atanmıştır. Modellerdeki ağ sayıları 370000 ile 550000 arasında değişmektedir. CFD modeli sürekli halde (steady state) olarak çalıştırılmıştır.

CFD sonuçları hız, sıcaklık ve bağıl nem olmak üzere üç ana değişkenin değişimleri üzerinden yorumlanmıştır. CFD model sonuçları, deney sonuçları ile önemli oranda örtüşmektedir. Dış camın iç yüzeyinden, dış cam ile jaluzinin ortasından ve jaluzi ile iç camın ortasından üçer adet referans nokta seçilmiş; bu referans noktalar üç farklı model için ayrı ayrı karşılaştırılmıştır. CFD modelinden alınan sonuçlara göre cam yüzeyinde ve ara boşlukta yükseklik arttıkça sıcaklık artmakta, bağıl nem oranı ve akışkan hızı düşmektedir. Hız verileri jaluzi ile iç cam arasında üç farklı modelde önemli oranda örtüşmektedir. Üç farklı model sıcaklık dağılımı açısından önemli oranda örtüşmektedir. Ara boşluktaki sıcaklık dağılımının şekillenmesindeki en önemli etken baca etkisidir. Baca etkisi havanın kaldırma kuvveti sebebiyle oluşur. Havanın kaldırma kuvvetinin şiddeti ise hava yoğunluk farkına sebep olan sıcaklık farkı ve nem farkı nedeniyle oluşur. Ara boşluktaki hava hareketinde en temel etken doğal taşınım ile ısı transferidir. Hem doğal taşınım hem tek taraflı kısmi hava beslemesi yapılması tüm boşluktaki ortalama hız değerlerinin 0,1 m/s'nin altında kalmasına sebep olmuştur. “Çizgisel kanal” modelinde dar kanal etkisi ile görece yüksek hızlar, bağıl nemin ve yağışma noktasının görece düşük olmasına sebep olmuştur. August-Roche Magnus yöntemi sıcaklık ve bağıl nem değerleri kullanılarak ilgili noktanın yağışma noktasını bulmayı sağlayan bir yaklaşımdır. Bu yaklaşıma göre dış cam ile jaluzi arasındaki referans noktaların bağıl nem ve sıcaklık değerleri kullanılarak bulunmuş yağışma noktaları aynı hizadaki cam yüzeyindeki sıcaklık değerlerinden küçük olduğu için yağışma yoktur denir. Filtre pozisyonunun etkisi, filtrenin dış cama 25 mm, 38 mm ve 56 mm uzaklıkta olduğu model sonuçları ile karşılaştırılarak analiz edilmiştir. Filtreler dış camdan uzaklaştıkça dış cam civarındaki bağıl nem değerleri artmaktadır. Filtrenin dış cama olan mesafesi ara boşluk alt bölümündeki sıcaklık, bağıl nem ve hız dağılımlarını daha çok etkilemektedir. CFD sonuçlarına göre ara boşlukta ve cam yüzeyinde yağışma riski bulunmamaktadır. Sonuç olarak, filtre modelleme yaklaşımları ısı transferini ve akış davranışını modellemek için iyi bir alternatif olabilir.

Kapsamlı CFD analizi ile ulaşılan sonuçlar kullanılarak yeni bir Façade Respirante cephe modülü oluşturulmuştur. Oluşturulan modül, CSTB’de geliştirilmiş yağışma testi metodolojisi temel alınarak oluşturulan bir metodoloji kullanılarak FTI (Façade Testing Institute) laboratuvarlarında deneysel olarak analiz edilmiştir. İlk aşamada Jaluziler kaldırılmış, jaluziler tamamen kapatılmış ve jaluziler açılmış olarak üç adet deney yapılmıştır. Daha sonra kritik durum olan jaluzilerin indirilmiş ve kapatılmış olduğu durumda ayrı ayrı bir adet ve iki adet filtreyi de kapatılarak iki adet daha deney yapılmıştır. Toplamda beş farklı varyasyona göre beş farklı deney yapılmıştır. Bu

sayede Façade Respirante modülü ara boşluk içerisindeki havanın davranışına ve dış cam iç yüzey üzerindeki yoğuşma oluşumuna jaluzi ve filtrenin etkisini görmek amaçlanmıştır. Oluşturulan Façade Respirante modülü iç cam kombinasyonu 6/16/44.2 (6 mm cam + 16 mm hava boşluğu + 2 adet birbirlerine lamine edilmiş 4'er mm lik iç cam) dir. Yani cam boşluğu 16mm'dir ve iç camında laminasyon yapılmıştır. Ara boşluk mesafesi İç cam kombinasyonu ve dış cam dış yüzeyleri arasında 80.6 mm dir. Dış cam ise 6 mm kalınlıktadır.(Figure 7.9) Deney numunesinde kullanılacak cephe modülü 1260 mm x 2100 mm boyutlarındadır. Ara boşlukta dış cama 25 mm mesafede lamel genişliği 25 mm olan Hella marka Jaluzi yerleştirilmiştir. Alt kısma yoğuşma engelleme amaçlı hava girişini sağlamak amacıyla 500 µm lik ağ yapısına sahip 6 adet Sofabin marka filtre yerleştirilmiştir. Deneyde ortamı koşullandırmak amacıyla hava nemlendirme, nem alma, iklimlendirme ve basınçlandırma cihazı, nem ve sıcaklık ölçümü amacıyla ısı çiftler ve nem ölçerler ve ölçümleri değerlendirebilmek amacıyla veri kaydediciler kullanılmıştır. Alt yatay profile 200 mm, 400 mm, 1400 mm ve 1800 mm yükseklik mesafelerinde dış cam iç yüzeye dört adet, dış cam ve jaluzi arasına 4 adet jaluzi ve iç cam arasına dört adet olmak üzere ara boşluğa toplam 12 adet ısıçift yerleştirilmiştir. Jaluzi ile dış cam arasındaki bölgeye alt yatay profile 200 mm ve 1000 mm yükseklik mesafesinde sıcaklık ve nem ölçme yeteneğine sahip nem ölçerler yerleştirilmiştir. Ara boşluğa yerleştirilmiş nem ölçerler %0,8 belirsizlik oranı ile ısı çiftler ise $\pm 0,2$ °C belirsizlik değerleri ile kalibre edilmişlerdir.

Ölçüm sonuçlarında jaluziler kapalı, jaluziler açık ve jaluziler kaldırılmış durumları arasındaki yoğuşma riski açısından en kritik durumun jaluziler kapalı iken gerçekleştiği görülmüştür. En kritik durum olan jaluzilerin kapatıldığı durumda iken önce bir filtre kapatılmış, daha sonra iki filtre kapatılmıştır. Yoğuşmanın ilk kez iki filtrenin de kapatıldığı durumda başladığı görülmüştür.

Enerji performans analizi kapsamında önce oluşturulan Façade Respirante modülünün bütünsel ısı geçirgenlik katsayısı (U_{window}) ve profiller üzerindeki yoğuşma durumu bulunmuş sonrasında ise TS 825'e göre oluşturulmuş sınırdaki pencerenin iletim ve taşınım ile gerçekleşen ısı kaybı ve güneş enerjisi kazançları göz önünde bulundurularak aylık ve yıllık bazda sağlayacağı toplam tasarruf ve karbon ayak izi tespit edilmiştir.

EN 10077 standardına göre Bisco 2D sürekli hal (steady state) ısı transfer analizi programı aracılığıyla yapılan yoğuşma analizi sonucunda profiller üzerinde yoğuşma olmadığı sonucuna varılmıştır. "Vitrage Decision" programı ile yapılan model sonucu oluşturulmuş Façade Respirante modülü cam kombinasyonu ısı geçirgenlik katsayısı (U_g) değeri $0,79$ W/m²K, güneş enerjisi geçirme faktörü 0,39 (SHGC) olarak bulunmuştur. EN 10077-2 standardına göre ise tüm alüminyum çerçeve profillerinin ısı iletkenlik hesap değeri bulunmuştur. EN 10077-1 standardında tanımlanan "Component Assessment Method" a göre oluşturulmuş Façade Respirante cephe modülünün ısı geçirgenlik değeri (U_{window}) $1,56$ W/m²K olarak bulunmuştur. Bu değer TS 825 standardına göre sınır değer olan $2,40$ W/m²K değerine göre oldukça iyidir. TS 825'te tanımlanmış $2,40$ W/m²K değerine sahip cam kombinasyonunun solar faktör değeri "Guardian Glass Performance Calculator" programında yapılan modelde EN 410 standardına göre $0,418$ olarak bulunmuştur. TS 825'te tanımlanan değerler kullanılarak soğutma yükü, ısıtma yükü yıllık ve aylık bazda TS 825'te tanımlanan tüm iklim bölgeleri ve tüm yönler için hesaplanmıştır.

Yapılan analize göre soğutma yükünden en büyük tasarruf birinci iklim bölgesinde doğu-batı cephelerinde en düşük tasarruf ise dördüncü bölgede kuzey cephede olmuştur. Isıtma yükünden yapılan en büyük tasarruf değerine ise dördüncü bölgede

dođu ve batıya bakan cephelerde yapılan uygulamalarda ulařılmıştır. Enerji performans analizi göstermektedir ki; oluşturulan cephe sistemi ile sođutma yükünde aylık $6,4 \text{ W/m}^2$ ye kadar yıllık $17,8 \text{ W/m}^2$ 'ye kadar; ısıtma yükünde aylık $23,6 \text{ W/m}^2$ 'ye kadar ve yıllık $130,5 \text{ W/m}^2$ 'ye kadar tasarruf yapılması mümkündür. Günlük 10 saat ve haftalık 5 gün ısıtma ve iklimlendirme cihazlarının çalıştığı varsayılırsa yıllık toplam her bir m^2 'lik pencere için 339.3 kWh 'a kadar enerji tasarrufu imkanı sağlanmaktadır. 339.3 kWh 'lik tasarruf sayesinde bu miktar enerji üretiminde ortaya çıkan 234 kg CO_2 doğaya hiç salınmamış olacaktır. Bu sayede, 6 tane ağacın on yıllık yaşamı boyunca tolere edebileceđi miktardaki CO_2 doğaya hiç salınmamış olacaktır.

1. INTRODUCTION

Physical separators which separates conditioned environment and unconditioned environment is defined as building envelope. One of the most important task for energy performance of building envelope is minimizing air, light and sound transmission to inside and blocking water permeance to inside [1-3]. Façade is the most important element of building envelope. There are double skin façade applications in some high rise buildings in order to improve expected performance from façades.

As it is mentioned in the presentation of H.Blecker CTBUH 2012 , there are basically four different types of double skin façade systems in the literature [4]. These are;

Active Façade: The cavity is ventilated through HVAC equipment in this façade type. (Figure 1.1)

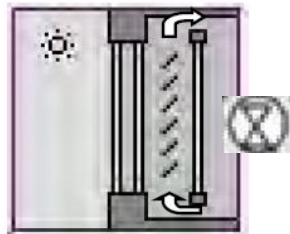


Figure 1.1 : Active façade [4].

Naturally Ventilated Façade: The cavity between façades is ventilated with natural convective flow of air in this façade type. (Figure 1.2)

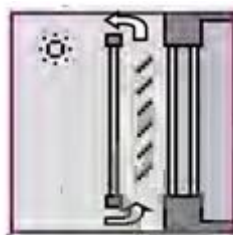


Figure 1.2 : Naturally ventilated façade [4].

Interactive Façade: The cavity between façades is ventilated both natural ventilation and mechanical (forced) ventilation in this façade type. (Figure 1.3)

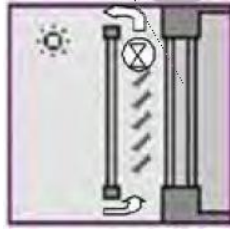


Figure 1.3 : Interactive façade [4].

Closed Cavity Façade: It is the double skin façade which does not allow air passage to inside of cavity in order to have better thermal performance. (Figure 1.4)

- **Closed Cavity Façade with minimal air supply:** This is another variation of Closed Cavity Façade, which allows minimal air passage to inside in order to prevent condensation by means of partial vapour pressure balance with outdoor. Façade Respirante systems belong to this class.

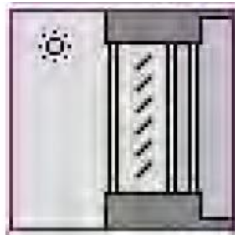


Figure 1.4 : Closed cavity façades [4].

The design parameters that has direct effect on Closed Cavity Façade performance are indicated below.

- Radiation performance (heat transfer via radiation) (specifically critical parameter for glazed buildings)
- Thermal performance
- Day lighting
- Condensation
- Maintenance and cleaning
- Earthquake resistance
- Ease of installation [4]

1.1 Purpose of Thesis

High energy efficiency without condensation risk in building envelopes is highly essential to supply thermal comfort conditions at indoor environment with lower cost. On the other hand, the application of double skin façades in Turkey conditions is quite untouched topic. There were supposed to be done a scientific study in this field to show decision makers probable risks and advantageous.

The purpose of thesis is configuration of new generation closed cavity façade which has maximum thermal performance without condensation risk.

2. FAÇADE RESPIRANTE

Façade Respirante is also called closed cavity façade (CCF) as it is mentioned in the first section. The main purpose of using the façade is to allow minimum air entrance to prevent condensation risk. Components of Façade Respirante is shown in Figure 2.1.

The main target of Façade Respirante system is achieving minimum heat transfer without condensation risk. The system is completely sealed from top and lateral sides, and it is ventilated by filters at bottom part of the frame system. The most important feature of the system is to minimize heat transfer without any condensation risk. Heat transfer through the system occurs by three different ways which are conduction, convection and radiation [5]. Reduction of the number of filters and filter mesh sizes minimize heat leakage by means of convection; helps to ensure hygiene by means of decrement of dust, dirt and volatile organic compounds (VOC) passage to cavity. However, insufficient air movement leads to condensation. Optimal number of filters is determined by the lowest filter number without condensation through condensation risk assessment experiments. The number of filters and filter mesh sizes varies with system sizes, project region where system is applied, hygroscopic features of system components.

Application of the façade mostly depends on the geographical and climatic conditions. That's why Façade Respirante is mostly applied at middle Europe zone countries like Germany, France, Belgium and Bulgaria where humid, mild climate without harsh winter conditions exist.

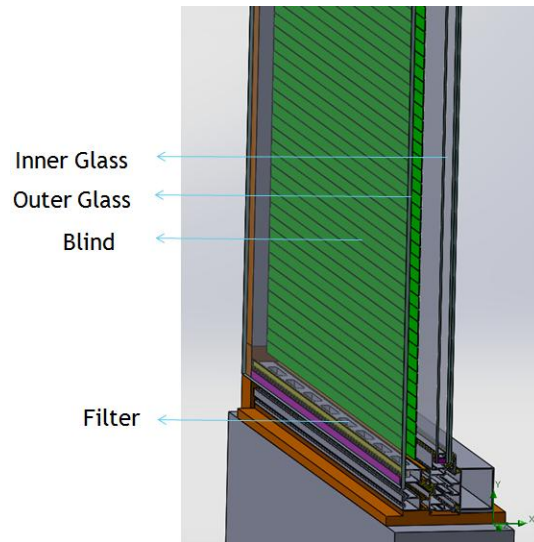


Figure 2.1 : Façade Respirante.

2.1 Literature Review

Various Façade Respirante details from several façade firms at different countries have been researched for Façade Respirante application based on appropriate climate conditions. Some façade companies like Schueco, Wicona, Rinalde, Goyeri Oustalu, Gartner GMBH, Reynaers are reviewed for this research. The specific details of Sopharma from Reynaers in Bulgaria, Hilti Innovation Center in Liechtenstein, Roche Diagnostics International AG in Rotkreuz, Leo in Frankfurt projects are identified in terms of thermal performance and condensation risk.

Innovations and energy efficiency in contemporary office buildings shows that closed cavity façade in Sopharma Towers reduced cycles of cavity cleaning, and constituted condense free façade under the local climatic conditions. 2,5 years after the façade has been installed, there was no dust at all compared to slightly ventilated façades. Energy efficiency is also increasing by means of slat angle and blind mode control [6].

Even though, façade of Sopharma and Litex towers are one of the most expensive façade built in Bulgaria, there is 30% cost cut from HVAC installed power , 40% less heating requirement by using sun energy in more efficient way and 20% potential savings in total [6].

“Double Skin Façades a Literature Review” is surveyed in order to see scope of double skin façade with all analysis criteria and all technical parameters [7]. This

report covers modelling issues in double skin façades in terms of thermal simulation and air flow. The buildings where double skin façade is applied are also presented with various technical features.

“M-Free S Closed Cavity Façade” [4] is presented by H. Blecker at CTBUH (Council on Tall Buildings and Urban Habitat) 2012. Conference proceeding of this presentation includes general review of double skin façade and evaluation of closed cavity façades in terms of energy, thermal comfort and acoustic aspect by modelling and testing.

“Condensation in a closed cavity double skin façade: A model for risk assessment” discusses the risk of condensation between the panes of façade in closed cavity façades. There are some assumptions regarding thermal, hygric and air flow behaviour. This paper claims that constituted model can be used for condensation risk modelling [8].

One of the objectives of this work is to take advantage of the other experimental works by use of the test results from highly reputable and independent test centres in order to provide reliable data. Therefore, Façade Respirante specimen with CLC 12-260039255 code from CSTB (Centre Scientifique et Technique du Bâtiment) data is used to have general idea about system behaviour in terms of thermal and condensation in this work. Condensation risk assessment methodology is based on 1°C temperature decrement in each 20 minutes with 80% relative humidity and 20°C initial condition at outdoor with total 400 minutes when the conditions of indoor being kept constant at 20°C and 50% relative humidity. The temperature and relative humidity values are followed at indoor, cavity and outdoor of test mock-up. If partial vapour pressure at cavity is lower than saturated vapour pressure at cavity at all records which are obtained in each 20 minutes, it is assessed that there is no condensation with respect to this methodology [9].

There are some researches related with this work. Before, CFD model is created, "Air Flow and Heat Transfer" is examined to simulate CFD model, compare and validate CFD results with experiment results. This paper illustrate the importance of the position of blinds and slat angles. Energy performance of double façade varies considerably with respect to position of blinds and angle of slat tilt. It also affects velocity distribution at cavity and total surface heat transmission coefficient.

Influence of blind position (outer, middle and inner) is higher compared to variation of slat angles ($\theta=0^\circ, 45^\circ, 90^\circ$) to distribution of temperature, velocity and SHTC's. "Air flow and heat transfer in double skin façades" also illustrates that there is 3°C difference at outer cavity, $1^\circ\text{C} - 1.5^\circ\text{C}$ difference at inner cavity and around 1°C difference on inner glass surface between CFD results and experiment results [10].

"Modelling Ventilation in naturally ventilated double-skin façade with a venetian blind" is examined in order to simplify blinds reliably. This paper proposes modelling venetian blinds as porous media instead of explicit slat model in order to decrease number of mesh and computing time as well as getting higher accuracy in CFD Model. All the results have been validated with performed field experiments [11].

"Double Skin Façade effects on heat loss of office buildings in Istanbul", " A new type of double-skin façade configuration for the hot and humid climate" and other similar articles which are at same field are examined to understand how to process data on CFD and how to validate CFD results with experiment results. "Double Skin Façade effects on heat loss of office buildings in Istanbul" shows that double skin façade decrease energy loss significantly minimize heat loss and improve U value compared to single skin façade in winter period. Cavity between façade acts like buffer zone in winter and glasses re-radiate solar radiation two times which decrease cooling load at summer [12].

August-Roche Magnus equations which calculate dew points by use of relative humidity and temperature data. This approach is used to determine dew points of specified points. This is another validation approach to investigate occurrence of condensation on glass surface [13].

All the documents above are used to inspire during preparation phase of this paper.

The equations which are used by Computational Fluid Dynamics simulation programs is stated at the lecture notes of The University of Iowa Mechanics of Fluids and Transport Processes by Stanley C. These equations which are computed at background are indicated in Equation 2.1 – 2.7. [14].

Navier Stokes Equation: (3D in Cartesian coordinates)

$$\rho \frac{\partial u}{\partial t} + \rho u \frac{\partial u}{\partial x} + \rho v \frac{\partial u}{\partial y} + \rho w \frac{\partial u}{\partial z} = -\frac{\partial \hat{p}}{\partial x} + \mu \left[\frac{\partial^2 u}{\partial x^2} + \frac{\partial^2 u}{\partial y^2} + \frac{\partial^2 u}{\partial z^2} \right] \quad (2.1)$$

$$\rho \frac{\partial v}{\partial t} + \rho u \frac{\partial v}{\partial x} + \rho v \frac{\partial v}{\partial y} + \rho w \frac{\partial v}{\partial z} = -\frac{\partial \hat{p}}{\partial y} + \mu \left[\frac{\partial^2 v}{\partial x^2} + \frac{\partial^2 v}{\partial y^2} + \frac{\partial^2 v}{\partial z^2} \right] \quad (2.2)$$

$$\rho \frac{\partial w}{\partial t} + \rho u \frac{\partial w}{\partial x} + \rho v \frac{\partial w}{\partial y} + \rho w \frac{\partial w}{\partial z} = -\frac{\partial \hat{p}}{\partial z} + \mu \left[\frac{\partial^2 w}{\partial x^2} + \frac{\partial^2 w}{\partial y^2} + \frac{\partial^2 w}{\partial z^2} \right] \quad (2.3)$$

Continuity equation;

$$\frac{\partial \rho}{\partial t} + \frac{\partial(\rho u)}{\partial x} + \frac{\partial(\rho v)}{\partial y} + \frac{\partial(\rho w)}{\partial z} = 0 \quad (2.4)$$

Newton's Second Law of Motion;

$$F = ma \quad (2.5)$$

Equation of state;

$$p = \rho RT \quad (2.6)$$

Rayleigh Equation;

$$R \frac{D^2 R}{Dt^2} + \frac{3}{2} \left(\frac{DR}{Dt} \right)^2 = \frac{p_v - p}{\rho_L} \quad (2.7)$$

André Bakker states in “Applied Computational Fluid Dynamics” Lecture-7 Meshing by Fluent Inc. that design quality of grid is highly significant. Grid has great influence on convergence, solution sensivity and required CPU time [15].

Accordingly, CFD model is created based on condensation risk test methodology from CSTB CLC 12-260039255 with taking result of 400th minute in order to have more comprehensive results than experiment results such as velocity, temperature, relative humidity and other related parameters throughout model.

“Air Pressure and the building envelope” states that the air pressure difference between interior and exterior of building envelope and between upper and lower levels of buildings. It also emphasize to stack effect which mostly occurs by air buoyancy. Intensity of air buoyancy is depended air density difference which varies with temperature difference and moisture difference [16].

TS 825 “Thermal Insulation Requirements in Buildings” is the Turkish standard which defines thermal comfort conditions, how to calculate solar heat gain for three different direction, calculation of heating and cooling load for specified 4 different regions and calculation of condensation situation [17].

EN ISO 10077 is mutual standard of “Euro Norm” and “International Standard Organization” which defines thermal performance of windows and the assessment of condensation risks. EN 10077-1 defines calculation of global thermal transmittance values (U_{cw}) for window modules. EN 10077-2 defines thermal performance calculation method for frames in windows [18,19].

3. CONFIGURATION METHODS OF FR TEST MOCK-UP

The methodology of this experimental work is developed based on characteristics of the façade. Accordingly, evaluation of CFD analysis method was decided.

3.1 Determination of Appropriate Façade Respirante Profile Detail

The most important parameters for designing façade respirante:

- Geometry of the cavity
- Opening principles of the cavity
- Type of glazing, shading and lighting devices
- Material choice for the panes and the shading devices
- Positioning of shading devices
- Number of filters
- Distance between inner pane and outer pane [7]

CSTB (Centre Scientifique et Technique du Bâtiment) condensation risk assessment experiment for the specified Façade Respirante (CLC 12-260039255) detail were used as the basis at the end of literature review. The data obtained by this experiment for the specified Façade Respirante model is used as reference values of CFD analysis.

3.2 Constitution of Façade Respirante Profile

Specified Façade Respirante model at experimental level is evaluated on CFD analysis with the results of experiment carried out by CSTB which is indicated in this research comparatively. As a result of this evaluation, the new Façade Respirante has been designed and its details are illustrated in Figures 3.1 and 3.2.

3.3 Test Model Constitution of Designed Façade Respirante Details

The design of the Façade Respirante is represented below.

Specific details of mock-up system is given in Figure 3.1.

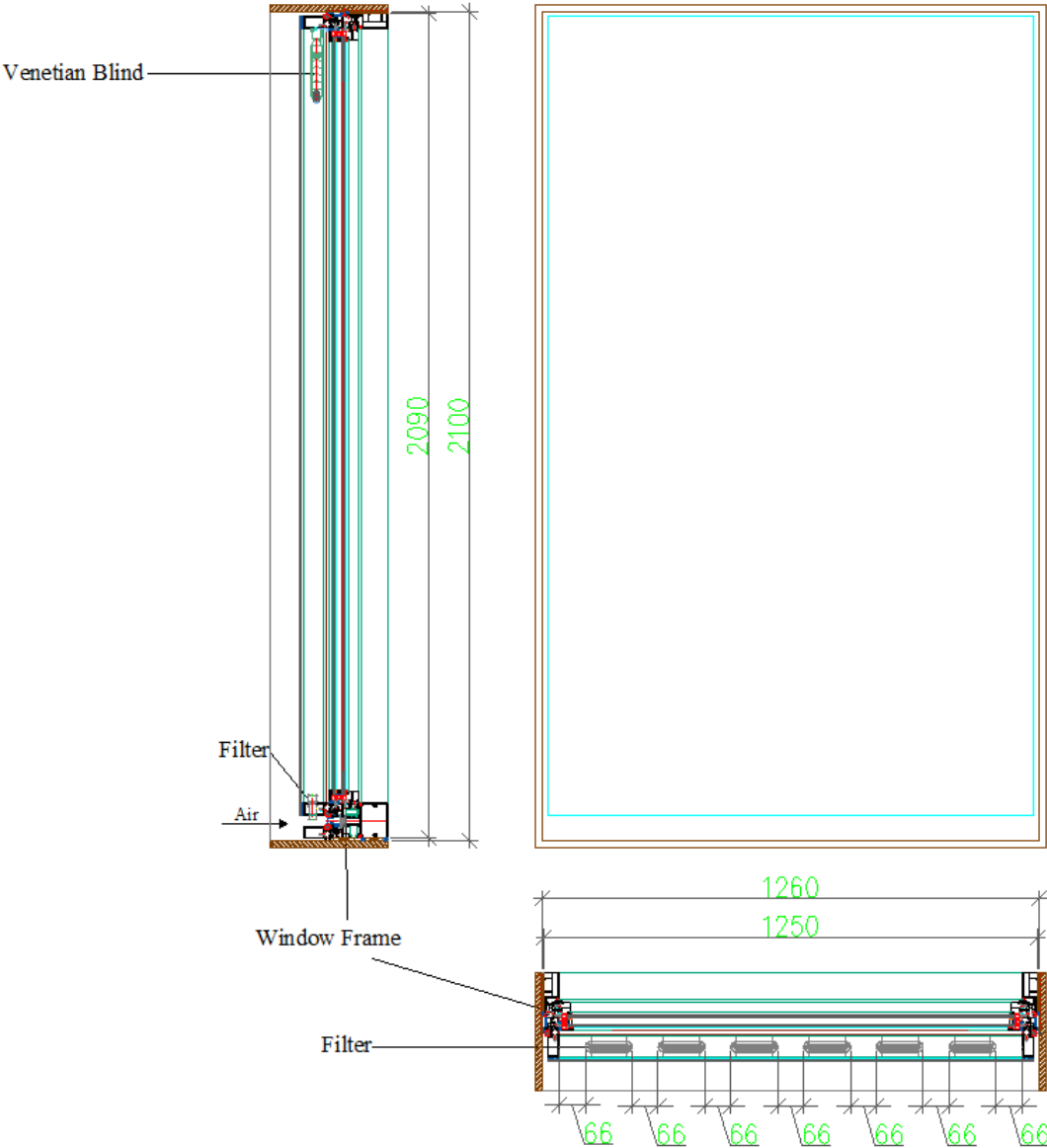


Figure 3.1 : General view of “Constituted Façade Respirante” test mock-up.

The filters which are used at experiment are illustrated in Figure 3.2.

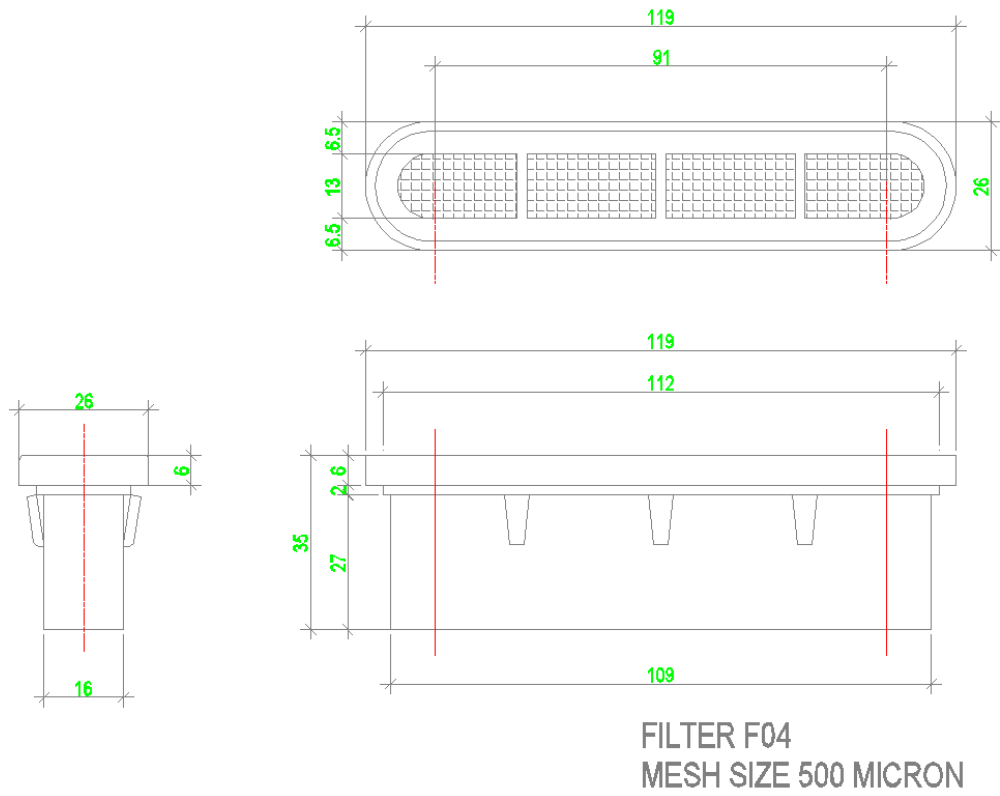


Figure 3.2 : Longitudinal section and cross section view of filters.

4. ANALYSIS METHODS

4.1 Analysis of FR in Laboratory Environment

Boundary conditions and initial conditions of condensation risk assessment test which is constituted by CSTB for Façade Respirante systems test methodology are presented in Section 4.1.1

Condensation test of Configured Façade Respirante is conducted in FTI (Façade Testing Institute) Labs based on the methodology of CSTB. This test is explained comprehensively in Section 6.

4.1.1 Setting the boundary conditions

The defined boundary conditions based on CSTB parameters are given below as indoor and outdoor conditions (Table 4.1).

Indoor Conditions: Temperature is kept at 20°C and relative humidity is kept at 50% and indoor is pressurized with an additional pressure of +50 Pa relatively.

Outdoor Conditions: Outdoor is conditioned to 20°C temperature and 80% relative humidity as an initial condition. Final temperature is 0°C at end of 400th minute thereby 1°C temperature reduction in each 20 minutes,

Humidity and temperature change at indoor, cavity and outdoor is tracked by means of hygrometers and thermocouples. The temperature value at interior side of exterior glass is measured. Corresponding saturation vapour pressure to related temperature (P_{sOe}) is identified from thermodynamic table. If vapour pressure at cavity is lower than corresponding saturation pressure to the temperature value at interior side of exterior glass, It is determined that there is no condensation.

Table 4.1 : Initial conditions and final situations data table.

Initial Conditions			
	Temperature (°C)	Humidity (%)	Pressure (Pa)
Indoor	20	50	50
Outdoor	20	80	0

1°C temperature reduction in each 20 minutes at outdoor.

Final Situation (At the end of 400th minute)			
	Temperature (°C)	Humidity (%)	Pressure (Pa)
Indoor	20	50	50
Outdoor	0	-	0

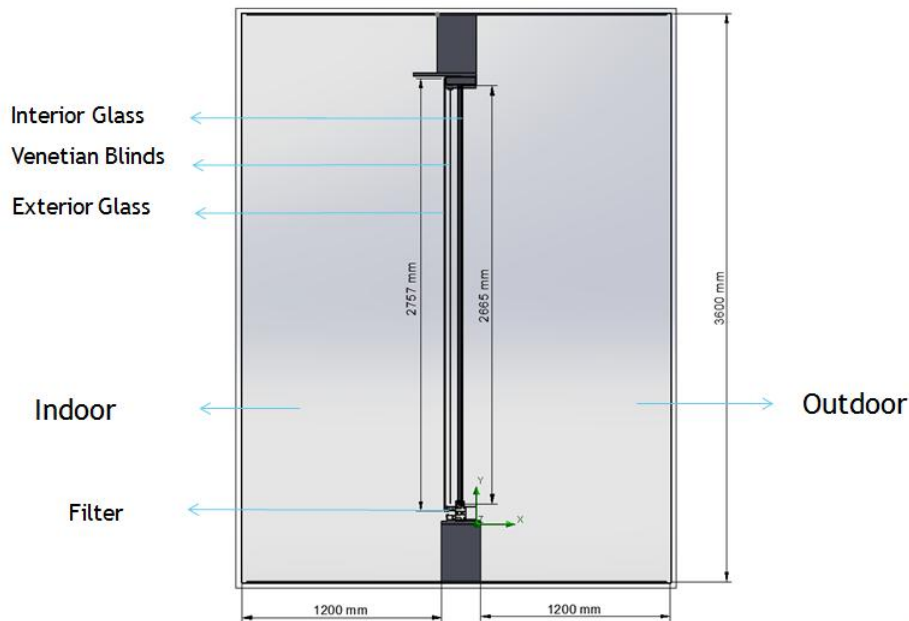


Figure 4.1 : The section view of experiment prototype based on Façade Respirante (CLC 12-260039255) detail from CSTB.

Figure 4.1 and Figure 4.2 illustrates experiment prototype and some experiment equipments in CLC 12-260039255 coded CSTB experiment. Table 4.2 shows the results of specified condensation risk assessment experiments with respect to time. There is no condensation at specified detail according to given results.

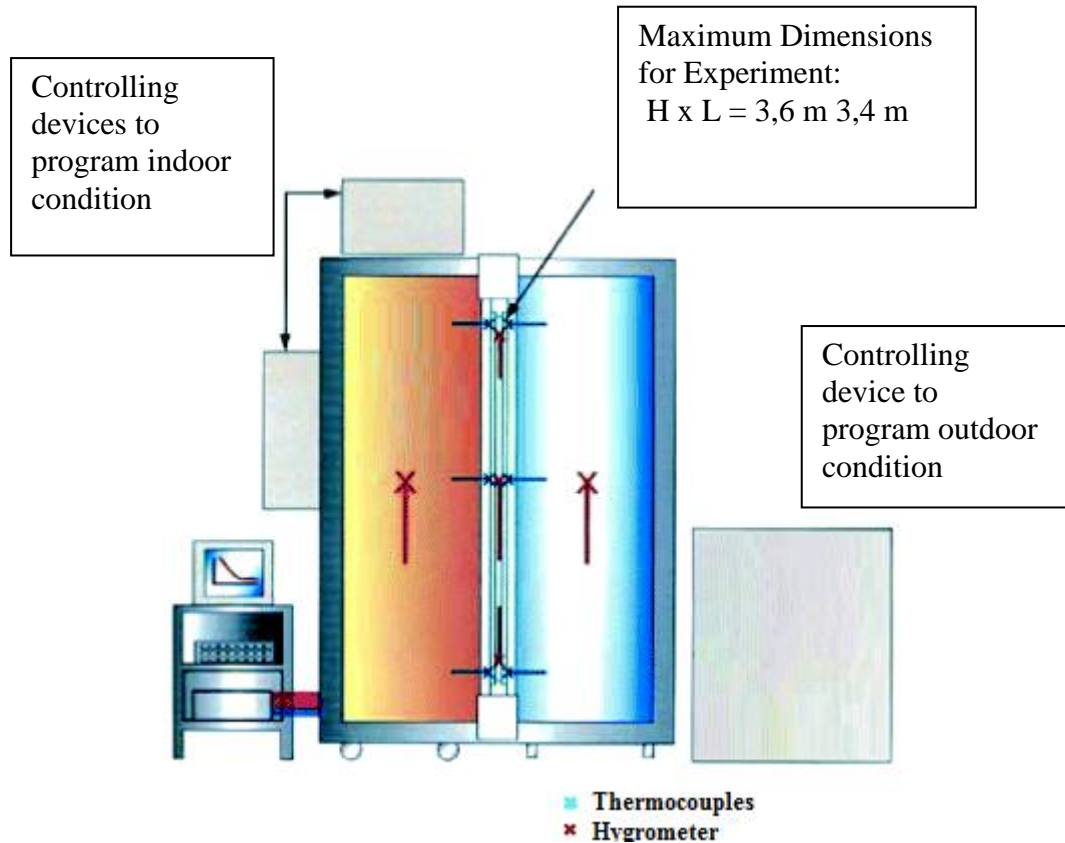


Figure 4.2 : Experimental Mock-up View of Façade Respirante [20]

4.1.2 Setting the boundary conditions of configured façade respirante condensation test

Condensation test of configured façade respirante based on comprehensive CFD results is carried out in FTI (Façade Testing Institute) Labs. Boundary conditions of this test is the same with methodology CSTB condensation test.

4.2 Analysis of FR with CFD Model

The conditions at the end of 400th minute CSTB test which is shown with red rectangle in Table 4.2 is modelled with CFD in order to have comprehensive results in various points of model. CFD results are validated with experimental results given in Table 4.2, as well. CFD results are the base for the configuration of façade respirante module.

4.2.1 Setting boundary conditions of CFD Model

The conditions at the end of 400th minute which is shown with red rectangle in Table 4.2 are used for CFD analysis. According to August-Roche Magnus method which is indicated in Section 5.3.5 “Validation with August-Roche Magnus Approach”,

Table 4.2 : Results of condensation risk assessment experiment results at the specified Façade Respirante system [9].

Time	T indoor (°C)	RH of indoor (%)	T cavity (°C)	RH of Cavity (%)	T_{ext glass} (°C)	T_{ext} (°C)	RH of outdoor (%)	Indoor Vapour Pressure (mmHg)	Cavity Vapour Pressure (mmHg)	Corresponding VP to T int side of ext glass (mmHg)	Outdoor Vapour Pressure (mmHg)
0	20.7	50.5	19.9	82.1	19.8	20.2	80.8	9.222	13.553	17.313	14.313
0 h 20 min	20.5	50.8	19.5	82	19.1	19.2	81.8	9.197	13.238	16.576	13.637
0 h 40 min	20.5	51	18.8	81.1	18.1	18.2	81.3	9.241	12.624	15.57	12.758
1 h 00 min	20.5	50.8	17.9	80.2	17.1	17.2	81.2	9.199	11.747	14.619	11.949
1 h 20 min	20.6	50.9	17	79.2	16.2	16.2	80.9	9.233	10.996	13.806	11.182
1 h 40 min	20.6	50.7	16.1	78.6	15.1	15.2	81	9.215	10.302	12.867	10.515
2 h 00 min	20.5	50.6	15.1	78	14.2	14.2	81.1	9.168	9.599	12.141	9.865
2 h 20 min	20.6	50.7	14.2	77.4	13.2	13.3	80.3	9.238	8.972	11.376	9.214
2 h 40 min	20.5	50.9	13.2	76.9	12.2	12.3	80.5	9.218	8.361	10.654	8.619
3 h 00 min	20.5	50.8	12.3	76.4	11.3	11.3	80.4	9.198	7.829	10.039	8.052
3 h 20 min	20.5	50.8	11.4	75.7	10.4	10.3	80	9.196	7.317	9.455	7.494
3 h 40 min	20.6	50.8	10.4	75.2	9.3	9.2	80.5	9.249	6.789	8.783	7.009
4 h 00 min	20.5	50.7	9.3	79	7.9	7.9	86.9	9.181	6.385	7.988	6.915
4 h 20 min	20.5	50.8	8.5	82.3	7.4	7.3	90.5	9.203	6.44	7.72	6.918
4 h 40 min	20.5	50.7	7.4	84.3	6.3	6.1	90.1	9.17	6.037	7.157	6.369
5 h 00 min	20.6	50.6	6.5	85.2	5.3	5.2	91	9.216	5.675	6.678	6.049
5 h 20 min	20.5	50.9	5.5	85.3	4.4	4.2	90.4	9.194	5.268	6.271	5.602
5 h 40 min	20.5	50.7	4.5	85.4	3.4	3.2	91	9.178	4.9	5.844	5.231
6 h 00 min	20.6	50.8	3.6	85	2.4	2.1	91.2	9.192	4.582	5.444	4.871
6 h 20 min	20.5	50.8	2.6	84.3	1.3	1.2	91.8	9.198	4.263	5.031	4.589
6 h 40 min	20.5	50.7	1.6	83.8	0.3	0.2	91.7	9.181	3.943	4.68	4.271

dew point of the specified condition at 400th minute is -0.8°C for cavity and -1.0°C for exterior side. These are the values when condensation start under indicated temperature and vapor pressure values as it is shown in Table 4.3.

Table 4.3 : Dew points of experimental values.

Point	Temperature (Fluid) [°C]	Relative Humidity [%]	Dew Points (°C)
Cavity	1.6	83.8	-0.8
Exterior Side	0.2	91.7	-1.0

4.3 Analysis of FR in terms of Energy Performance

Energy performance analysis is composed of condensation risk analysis of frames, thermal transmittance of window and energy performance analysis based on heat transfer due to temperature difference and solar radiation intensity from different directions aspect.

4.3.1 Setting boundary conditions of energy performance analysis

Boundary conditions and initial conditions of energy performance analysis section are given in terms of condensation, thermal transmittance and energy performance separately.

4.3.2 Condensation risk analysis of frames

Boundary conditions in condensation risk analysis is given below. These values are based on the specified standarts which are given section 7.1.1.

Glass Combination	: 6/80.6/6/10/16/44.2 (Fig. 6.2)
Outdoor temperature	: -3 °C
Indoor temperature	: 20 °C
Relative humidity (RH)	: 50 %
Dew point	: 9.3°C (Table 7.2)
U value of the inner glass combination (U_g)	: 1.1 W/m ² K
Thermal conductivity of inner glass air gap (λ)	: 0.022 W/m ² K (Table 7.3)

[18,19,21-25]

4.3.3 Thermal transmittance analysis of frames

Boundary conditions in thermal transmittance analysis is given below. These values are based on the specified standards which are given section 7.1.1.

Dimensions	: 1260mm x 2100mm
Glass Combination	: 6/80.6/6/10/16/44.2 (Fig. 6.2)
Indoor temperature	: 20 °C
Temperature Difference for U_f Calculation	: 20 °C [19,21]]
Thermal Conductivity of the insulation panel(λ)	:0,035 W/m ² K
Thermal Conductivity of the Spacer (λ)	:0.11W/mK “Aluminum spacer”

EN 10077-2 defines that to glass part of the profiles has to replace with insulation panel to determine thermal transmittance value.

4.3.4 Energy performance

Energy performance analysis based on below boundary conditions. All the values are specified at TS 825 (Thermal Insulation Requirements in Buildings).

Indoor: Temperature:	19°C (Heating season assumption) [17] 23°C (Cooling season assumption) [26]
Outdoor Temperature:	Obtained from Table 4.4
Thermal Transmittance of CCF:	1.56 W/m ² K (section 7.1.6.5)
Solar Radiation Intensity:	Obtained from Table 4.5
Solar factor (SHGC):	0.39 (CCF) 0.42 (RW)
Shading Factor:	0.5

Table 4.4 : Monthly average ambient air temperatures [17].

	1. Region (°C)	2. Region (°C)	3. Region (°C)	4. Region (°C)
January	8.4	2.9	-0.3	-5.4
February	9.0	4.4	0.1	-4.7
March	11.6	7.3	4.1	0.3
April	15.8	12.8	10.1	7.9
May	21.2	18.0	14.4	12.8
June	26.3	22.5	18.5	17.3
July	28.7	24.9	21.7	21.4
August	27.6	24.3	21.2	21.1
September	23.5	19.9	17.2	16.5
October	18.5	14.1	11.6	10.3
November	13.0	8.5	5.6	3.1
December	9.3	3.8	1.3	-2.8

23°C indoor temperature complies ASHRAE Standard 55-2013 with 25°C mean radiant temperature, 0.1 m/s air speed, 50% humidity, 1.1 metabolic rate and 0.5 clothing level. [26]

The assumption of heating and air conditioning hours for daily office occupancy is 10 hours and the office is occupied 5 days in a week. There is 52 weeks in total. Corresponding monthly working time is 216.7 hour.

Table 4.5 : Solar radiation values from different directions [17].

	Solar Radiation (South) (W/m ²)	Solar Radiation (North) (W/m ²)	Solar Radiation (West-East) (W/m ²)
January	72.0	26.0	43.0
February	84.0	37.0	57.0
March	87.0	52.0	77.0
April	90.0	66.0	90.0
May	92.0	79.0	114.0
June	95.0	83.0	122.0
July	93.0	81.0	118.0
August	93.0	73.0	106.0
September	89.0	57.0	81.0
October	82.0	40.0	59.0
November	67.0	27.0	41.0
December	64.0	22.0	37.0

5. DETERMINATION OF FR MODELLING BY CFD (COMPUTATIONAL FLUID DYNAMICS)

5.1 General Features of CFD Model

Experimental model is simulated by the aid of Solidworks Flow Simulation a CFD (Computational Fluid Dynamics) program in order to support experiment results through computer simulation [14,27,28].

5.1.1 Specific system definitions for CFD model

CFD model was developed based on Laboratory Test Mock-up which is described at section 4.1 and section 4.2 .

5.1.1.1 Glass combination

Exterior glass is 6 mm thickness single glass and interior glass combination is 4/16/55.2. 4/16/55.2 means 4 mm glass, 16 mm gap and two laminated glass which has 5 mm thickness from outer to inner side. Height of glass is 2757 mm and horizontal axis of glass is 1400 mm. 160mm /1400mm horizontal axis length of glass is modeled in order to simulate one filter air flow behavior. U_g value of interior glass is $1.1 \text{ W/m}^2\text{K}$.

5.1.1.2 Support of specimen

Support, which has 200 mm thickness, is placed to bottom and top of the experiment specimen to simulate airflow in a realistic way. Insulation panel is chosen as support material in order to minimize effect of heat transfer.

5.1.1.3 Filters

The most important purpose of the experiments is determining the number of filters in order to control the amount of air entering to FR. In the beginning, the number of filters has been chosen as 8 filters in total. All of these filters are placed with 46 mm

intervals. Surface area of each filters are 1250.7 mm² and air passage area on filter surface is 775.45 mm². (Figure 3.2)

5.1.1.4 Venetian blinds

The width of each venetian blind piece is 25 mm. Venetian blinds are modeled with porous media approach at open position with an angle of 45° to vertical axis and at closed position. The position of venetian blinds can change in order to increase energy performance with respect to summer and winter conditions [10].

5.1.2 Simplifications

When the number of mesh increase, running time of CFD analysis might take days, maybe weeks. CFD model should be as simple as possible in order to reduce running time to reasonable amount of time. Therefore, there is glass simplification, filter simplification and blind simplification at CFD model in this study.

5.1.2.1 Glass simplifications

4/16/55.2 glass combination which has $U_g=1.1$ W/m²K value is modeled as the glass with $\lambda=0.021$ W/mK thermal conductivity and 15.52 mm thickness in order to decrease mesh crowd due to modeling silicone, aluminum spacer, argon in glass combination. Simplification approach is indicated below.

$$R_{total} = \frac{1}{h_{(in)A}} + \frac{d}{\lambda A} + \frac{1}{h_{(out)A}} \text{ [K/W]} \quad (5.1)$$

$$R = \frac{1}{U} = \frac{1}{h_{(in)}} + \frac{d}{\lambda} + \frac{1}{h_{(out)}} \text{ [m}^2\text{K/W]}$$

$$\frac{1}{1.1} = 0.13 + \frac{0.01552}{\lambda} + 0.04$$

$$\lambda=0,021 \text{ W/mK}$$

5.1.2.2 Filter simplification

There are various filter simplifications in order to reduce total time of CFD run.

Filter Area=1250.73 mm²

Filter surface area where allows air passage: 775.45 mm²

Porous Media: Function which arranges fluid permeability ratio of a region with respect to various directions.

Isotropic Porous Media: Independency of permeability from direction of airflow.

Filters are modelled with three different simplification approach

- Identifying filter as isotropic porous media with 0.63 permeability ratio at CFD model.
- Identifying filter model as large as surface area of filter where air passes.
- Identifying filter model as linear channel with the assumption of total filter surface area distributed uniformly, continuously all horizontal section long.

5.1.2.3 Blind simplification

To be able to simplify the blind for the best possible results, four different details were compared based on accuracy of results. The CFD models which are simulated in a correct simplified way leads to reach more accurate results with less running time.

Blinds are modelled with 4 different method. Modelling methods are indicated below:

- Modelling blinds as vertical continuous solid
- Modelling blinds as vertical discrete solid (Figure 5.1)
- Modelling blinds as a solid which consists horizontal pieces.
- Modelling as porous media with 0.30 permeability ratio. [11]

0.30 corresponds to porosity ratio of blinds which is 45° angle to vertical axis.

5.2 General Settings of CFD Models

5.2.1 Determination of the initial conditions

Gravity is defined to (-y) direction with 9.81 m/s^2 . Heat transfer and fluid distribution is simulated without radiation effect for both transient and steady state separately.

5.2.2 Boundary conditions

5.2.2.1 Indoor conditions

Measured relative humidity and temperature values of indoor at CSTB experiment are entered exactly the same with 0.1 precision to CFD model. (Table 4.2)

5.2.2.2 Outdoor conditions

Measured relative humidity and temperature values of outdoor at CSTB experiment are entered exactly the same with 0.1 precision to CFD model. (Table 4.2)

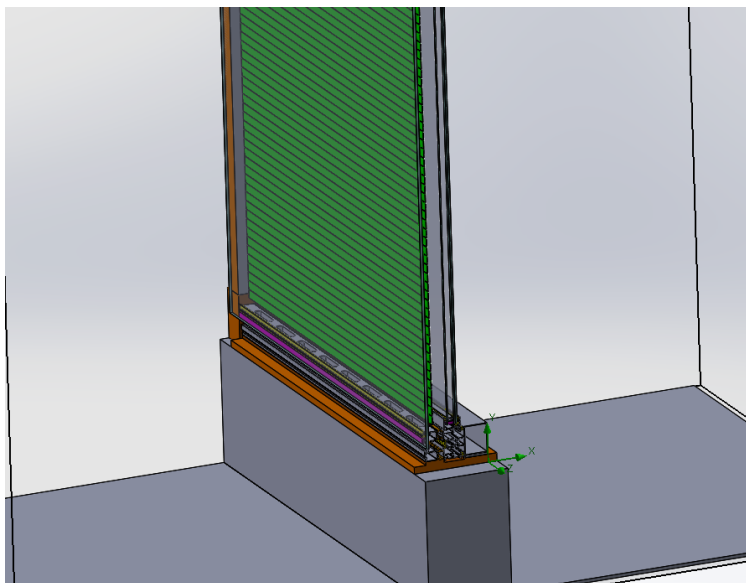


Figure 5.1 : 3D view of CFD model with discrete blinds.

5.2.2.3 Turbulence model

Flow is modelled both laminar and turbulent. Turbulent model is modelled with 2% turbulent intensity and 1.7 mm turbulent length. Standard k- ϵ turbulence model is applied to model. Turbulence model is set based on indoor and outdoor conditions as it is mentioned above.

5.2.2.4 Other settings

Wind

There is no defined wind as boundary condition.

Window

Aluminum frame profiles around glass is simplified at the first models and they are removed due to being lead to meaningless results at CFD model.

Distance

Distance between glasses can be various lengths in terms of convenience to climate condition. The distance between glasses is 75 mm.

5.2.3 Mesh settings

Meshing strategy identifies where to solve flow. Mesh has considerable influence on convergence rate, accuracy of solution and needed running time. Mesh distribution and mesh numbers of all CFD model in this paper is illustrated in Table 5.1 and Figure 5.2 [15].

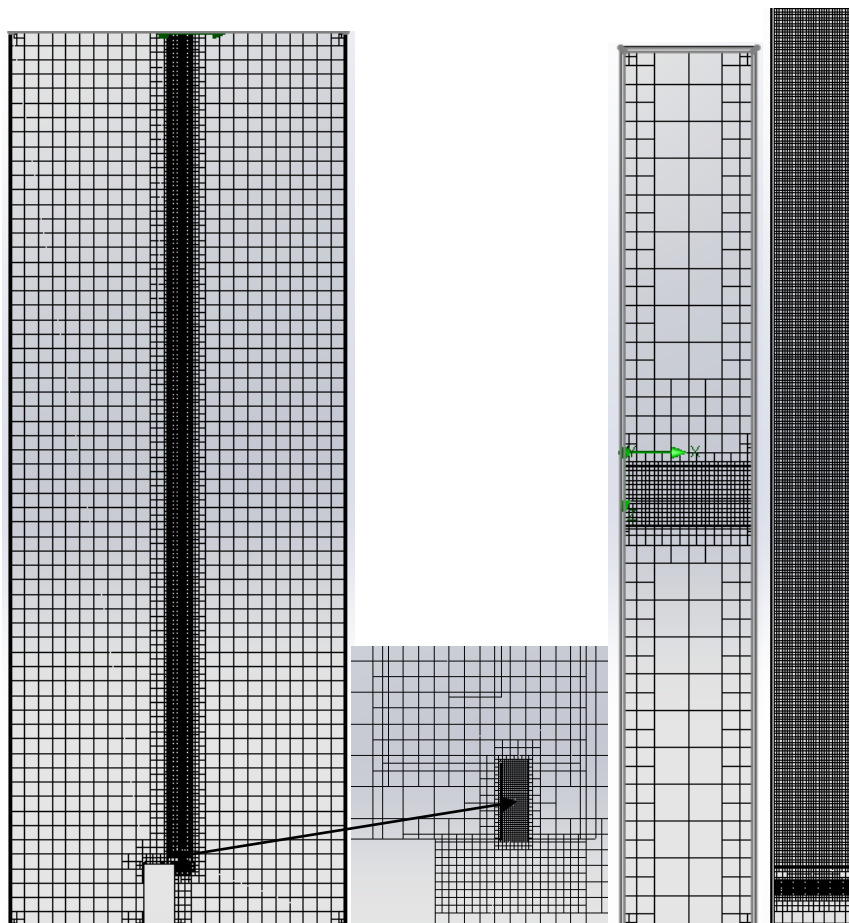


Figure 5.2 : Mesh distribution of CFD model (from left to right Y-Z axis view, filter mesh, X-Z axis view, X-Y view).

Table 5.1 : Total iteration number and total mesh number.

	CFD Model without Porous Media	CFD Model with Porous Media	CFD Model with Linear Channel
Iteration	1362	1250	5426
Cells	370820	452032	551404
Fluid Cells	263486	296016	360082
Solid Cells	14262	42112	59770
Partial Cells	93072	113904	131552

5.3 Results

The results of the research are focused the effect of three major variations. These are velocity, temperature, and relative humidity. According to August-Roche Magnus method which is indicated at section 5.3.5 “Validation with August-Roche Magnus Approach”, dew point of the specified conditions at 400 th minute is **-0.8 °C** for cavity and **-1.0 °C** for exterior side in experimental results and dew point in specified conditions at Ca.1 is 0.24°C (Model without porous media), 0.24°C (model with porous media), -0.24°C (model with linear channel) in CFD analysis and dew point in specified conditions at Ca.2 is 0.10°C (Model without porous media), 0.22°C (model with porous media), -0.47°C (model with linear channel) in CFD analysis . These are the values when condensation start.

Results are based on specified boundary conditions. Indoor is 20 °C and 50% relative humidity, outdoor is 0°C.

5.3.1 Specified points

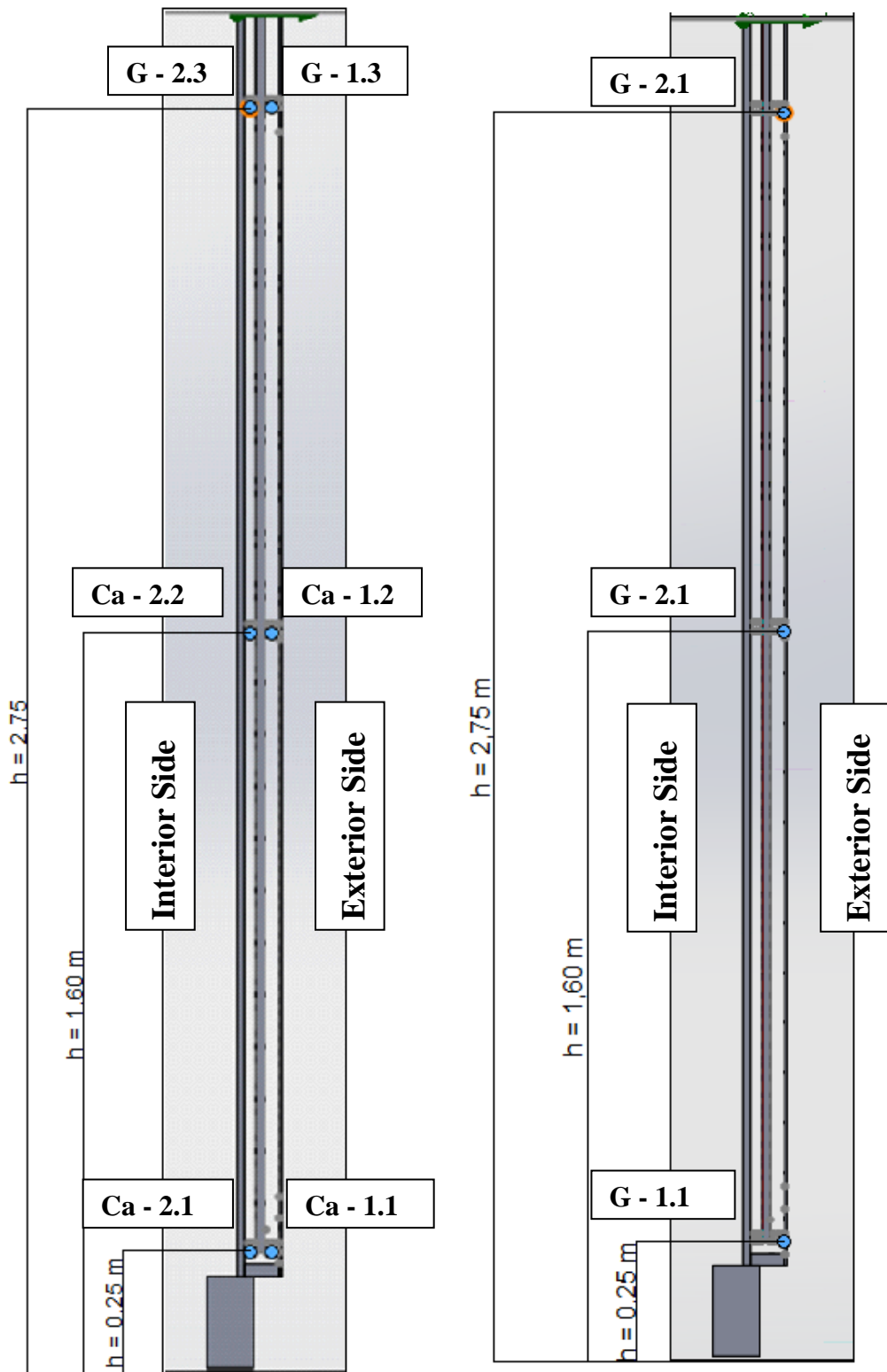


Figure 5.3 : Specified points.

Table 5.2 : Explanation of specified points.

Point	Explanation
G - 1.1	Interior surface bottom point of exterior glass
G - 1.2	Interior surface mid point of exterior glass
G - 1.3	Interior surface top point of exterior glass
Ca 1.1	Bottom part middle point between exterior glass and blind
Ca 2.1	Bottom part middle point between blind and interior glass
Ca 1.2	Mid part middle point between exterior glass and blind
Ca 2.2	Mid part middle point between blind and interior glass
Ca 1.3	Top part middle point between exterior glass and blind
Ca 2.3	Mid part middle point between blind and interior glass

5.3.2 Velocity, temperature and RH values from specified points

All measurements are taken from specific points which are indicated with respect to velocity, temperature and RH levels based on three different modeling approach. These parameters are from cavity and glass surfaces of points which are shown on from Table 5.3 until Table 5.8.

Various results of “Model without Porous Media” from specified points in cavity and on exterior glass interior surface are indicated in Table 5.3 and Table 5.4.

Table 5.3 : “Model without Porous Media” results from specified points in cavity.

Point	x [m]	y [m]	z [m]	Velocity [m/s]	Temperature (Fluid) [°C]	Relative Humidity [%]
Ca 1.1	0.08	-2.70	0.08	0.039	0.98	94.46
Ca 2.1	0.08	-2.70	0.03	0.037	0.86	92.85
Ca 1.2	0.08	-1.35	0.08	0.011	4.97	71.53
Ca 2.2	0.08	-1.35	0.03	0.028	11.95	44.35
Ca 1.3	0.08	-0.20	0.08	0.025	6.32	65.26
Ca 2.3	0.08	-0.20	0.03	0.001	15.81	34.73

Table 5.4 : “Model without Porous Media” results from specified points on exterior glass surface.

Point	x [m]	y [m]	z [m]	Velocity [m/s]	Temperature (Fluid) [°C]	Relative Humidity [%]
G - 1.1	0.08	-2.70	0.09	0.00	0.46	98.01
G - 1.2	0.08	-1.35	0.09	0.00	1.47	91.43
G - 1.3	0.08	-0.20	0.09	0.00	2.52	84.93

Various results of “Model with Porous Media” from specified points in cavity and on exterior glass interior surface are indicated in Table 5.5 and Table 5.6.

Table 5.5 : “Model with Porous Media” results from specified points in cavity.

Point	x [m]	y [m]	z [m]	Velocity [m/s]	Temperature (Fluid) [°C]	Relative Humidity [%]
Ca 1.1	0.08	-2.70	0.08	0.052	0.96	94.70
Ca 2.1	0.08	-2.70	0.03	0.050	1.05	93.90
Ca 1.2	0.08	-1.35	0.08	0.008	4.36	74.60
Ca 2.2	0.08	-1.35	0.03	0.028	11.84	44.77
Ca 1.3	0.08	-0.20	0.08	0.048	4.17	75.69
Ca 2.3	0.08	-0.20	0.03	0.001	15.51	35.38

Table 5.6 : “Model with Porous Media” results from specified points on exterior glass surface.

Point	x [m]	y [m]	z [m]	Velocity [m/s]	Temperature (Fluid) [°C]	Relative Humidity [%]
G - 1.1	0.08	-2.70	0.09	0.00	0.48	97.95
G - 1.2	0.08	-1.35	0.09	0.00	1.55	90.85
G - 1.3	0.08	-0.20	0.09	0.00	1.60	90.60

Various results of “Model with linear channel” from specified points in cavity and on exterior glass interior surface are indicated in Table 5.7 and Table 5.8.

Table 5.7 : “Model with linear channel” results from specified points in cavity.

Point	x [m]	y [m]	z [m]	Velocity [m/s]	Temperature (Fluid) [°C]	Relative Humidity [%]
Ca 1.1	0.08	-2.70	0.08	0.047	0.90	91.19
Ca 2.1	0.08	-2.70	0.03	0.053	0.74	89.16
Ca 1.2	0.08	-1.35	0.08	0.043	3.74	75.29
Ca 2.2	0.08	-1.35	0.03	0.030	11.70	43.32
Ca 1.3	0.08	-0.20	0.08	0.031	6.45	62.77
Ca 2.3	0.08	-0.20	0.03	0.004	15.94	33.25

Table 5.8 : “Model with linear channel” results from specified points on exterior glass surface.

Point	x [m]	y [m]	z [m]	Velocity [m/s]	Temperature (Fluid) [°C]	Relative Humidity [%]
G - 1.1	0.08	-2.70	0.09	0.00	0.37	95.02
G - 1.2	0.08	-1.35	0.09	0.00	1.68	86.99
G - 1.3	0.08	-0.20	0.09	0.00	2.01	85.47

The tables above indicates that the fluid temperature in cavity and on glass surface gets higher as long as the height of measured points gets higher in three different model. Relative humidity values in cavity and on glass surface gets lower as long as the height of measured points gets higher in three different model. Velocity values in cavity between blind and interior glass gets lower as long as the height of points gets higher. These tables illustrate how chimney effect reacts in the cavity in three different models.

5.3.3 Value comparison charts between three different models

CFD results from specified points are arranged as charts in order to compare the values in terms of relative humidity, temperature and velocity as it is shown at Figure 5.4, Figure 5.5 and Figure 5.6.

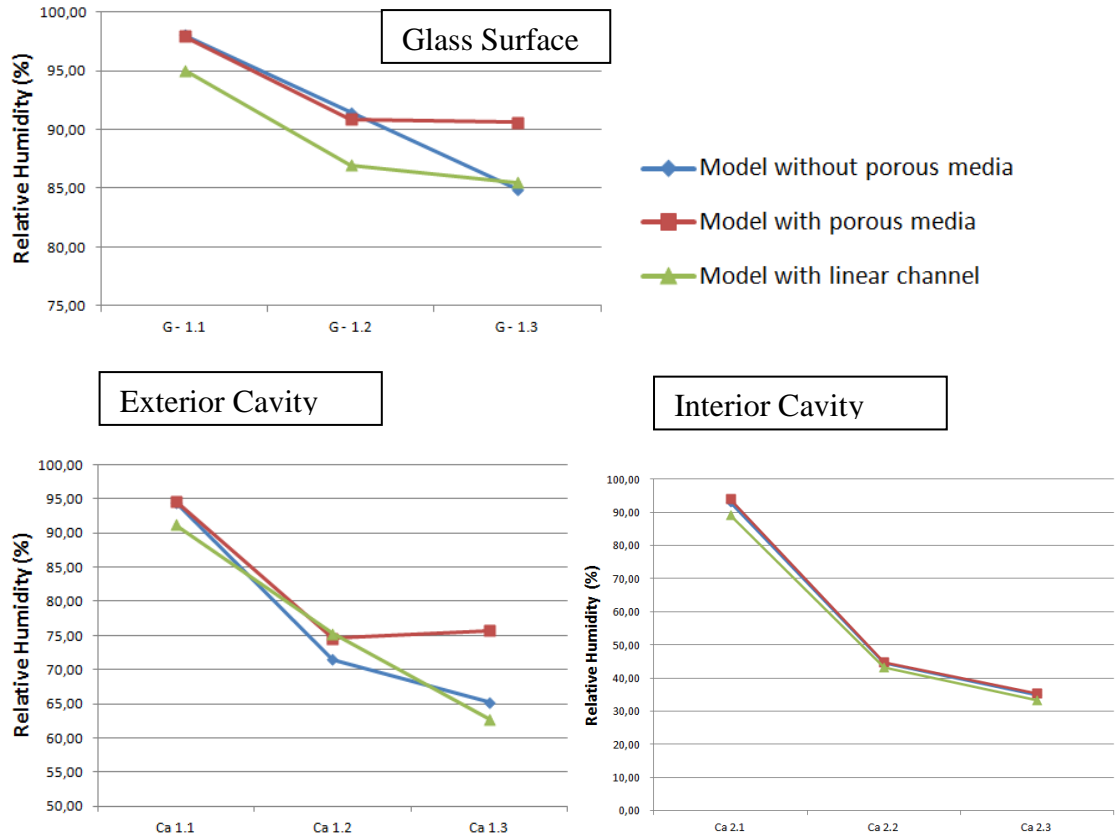


Figure 5.4 : Relative humidity values at glass surface (above), cavity between exterior glass and blind (bottom left), cavity between blind and interior glass (bottom right).

The values obtained from interior cavity match up with each others in quite high level in terms of relative humidity, temperature and velocity.

Specified tables and charts in “5.3 Result” section indicates that there is no condensation at measured points. It is also illustrated in specified table and charts that there is highly convenience with experimental results.

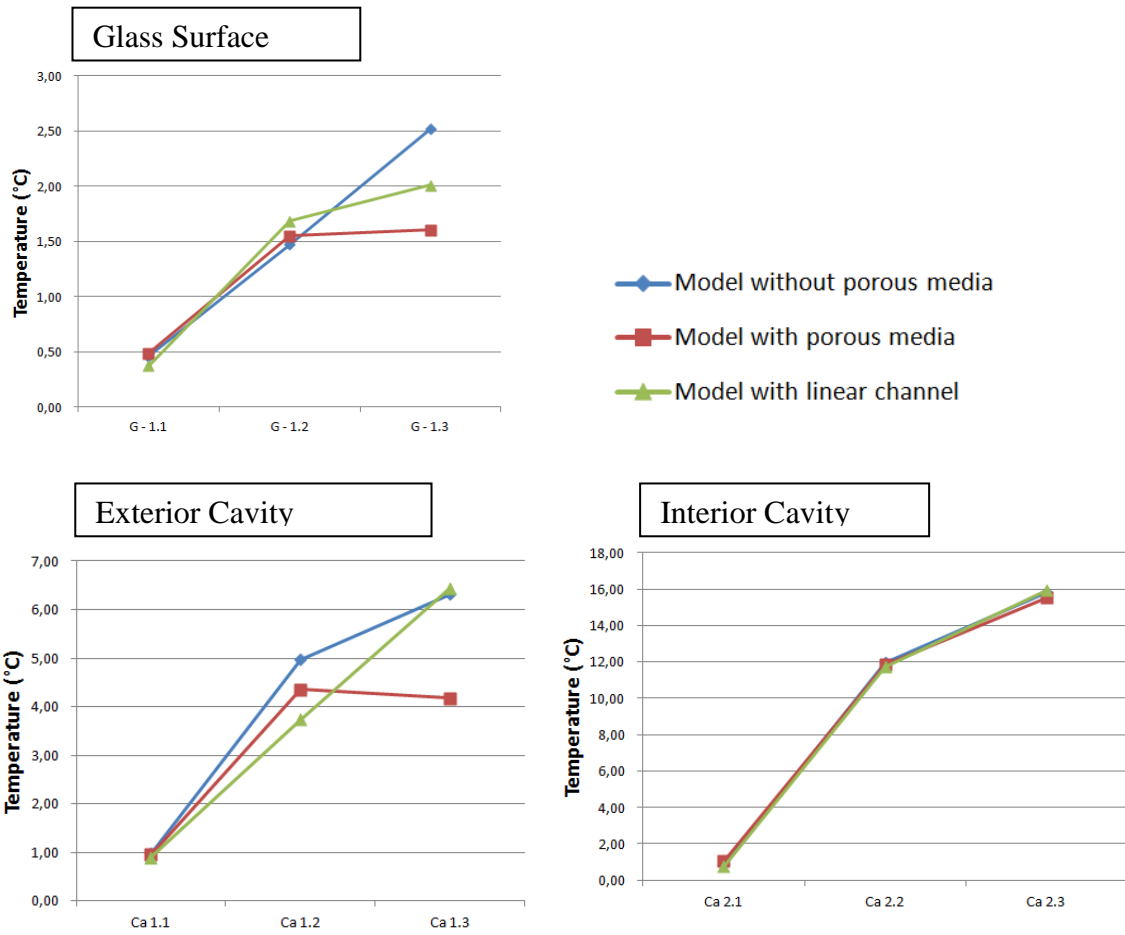


Figure 5.5 : Temperature values at glass surface (above), cavity between exterior glass and blind (bottom left), cavity between blind and interior glass (bottom right).

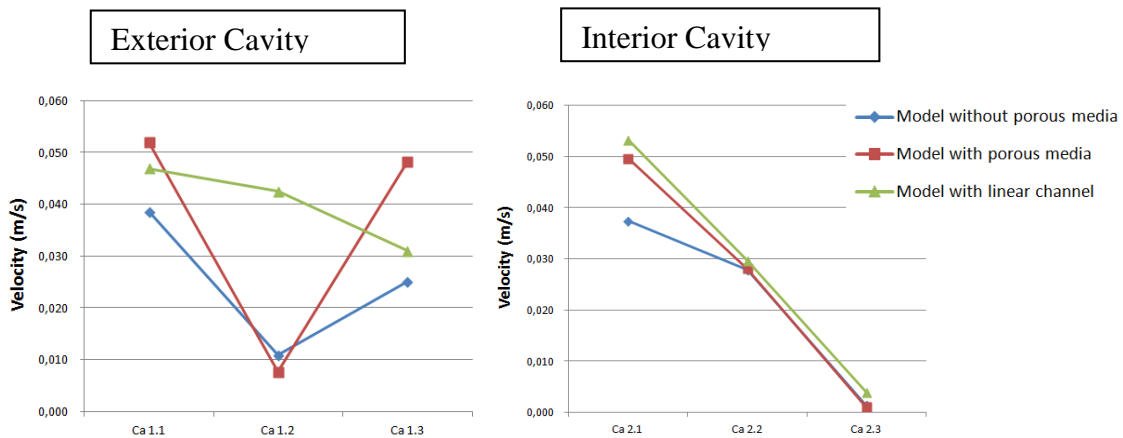


Figure 5.6 : Velocity values at glass surface (above), cavity between exterior glass and blind (bottom left), cavity between blind and interior glass (bottom right).

5.3.4 Cut plots from the middle of right plane

Cut plots from middle of right plane is taken in order to compare all of models in terms of velocity, temperature and relative humidity in Figure 5.7, Figure 5.8 and Figure 5.9.

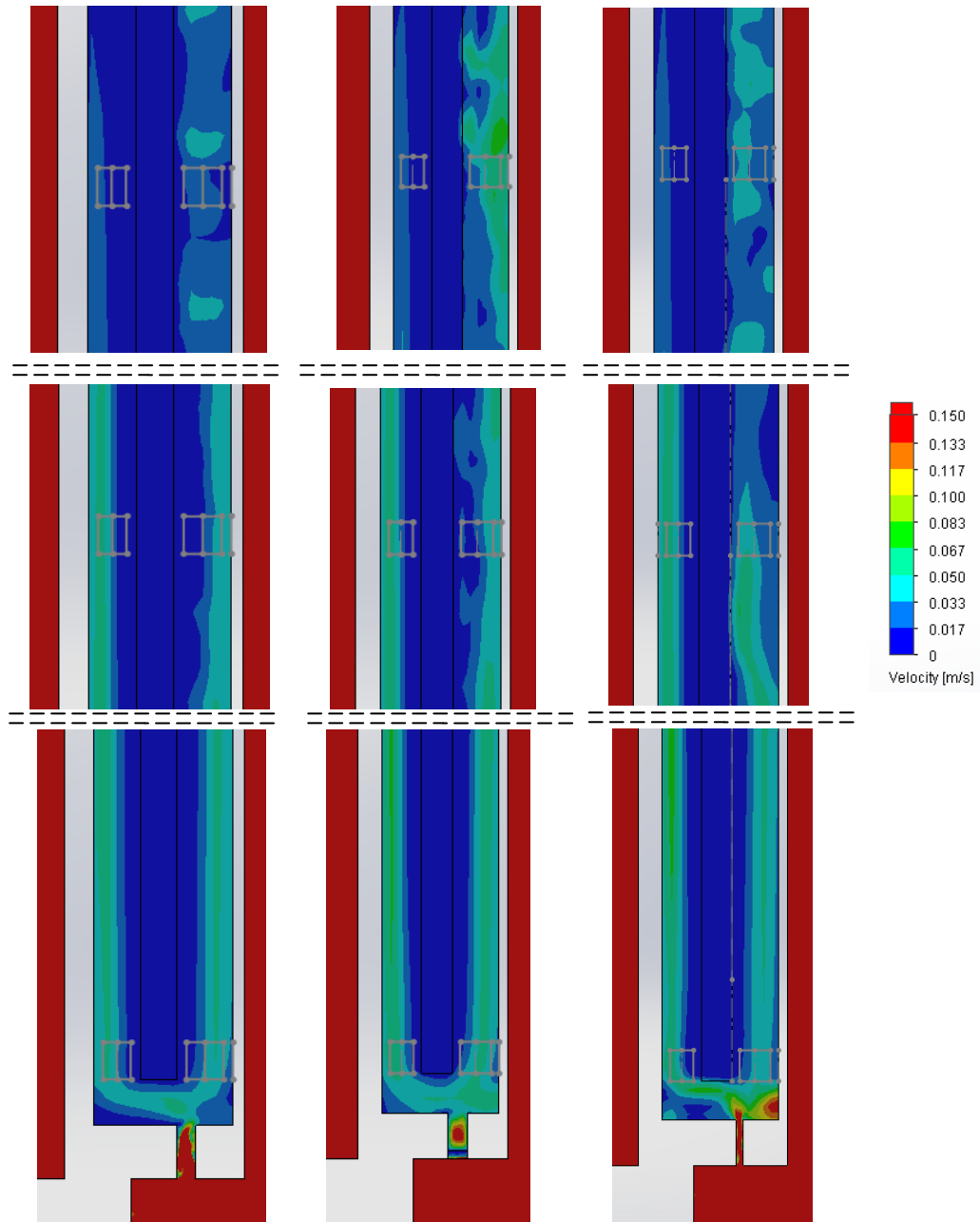


Figure 5.7 : Model without porous Media (left), model with porous media (middle), model with linear channel (right) velocity distributions.

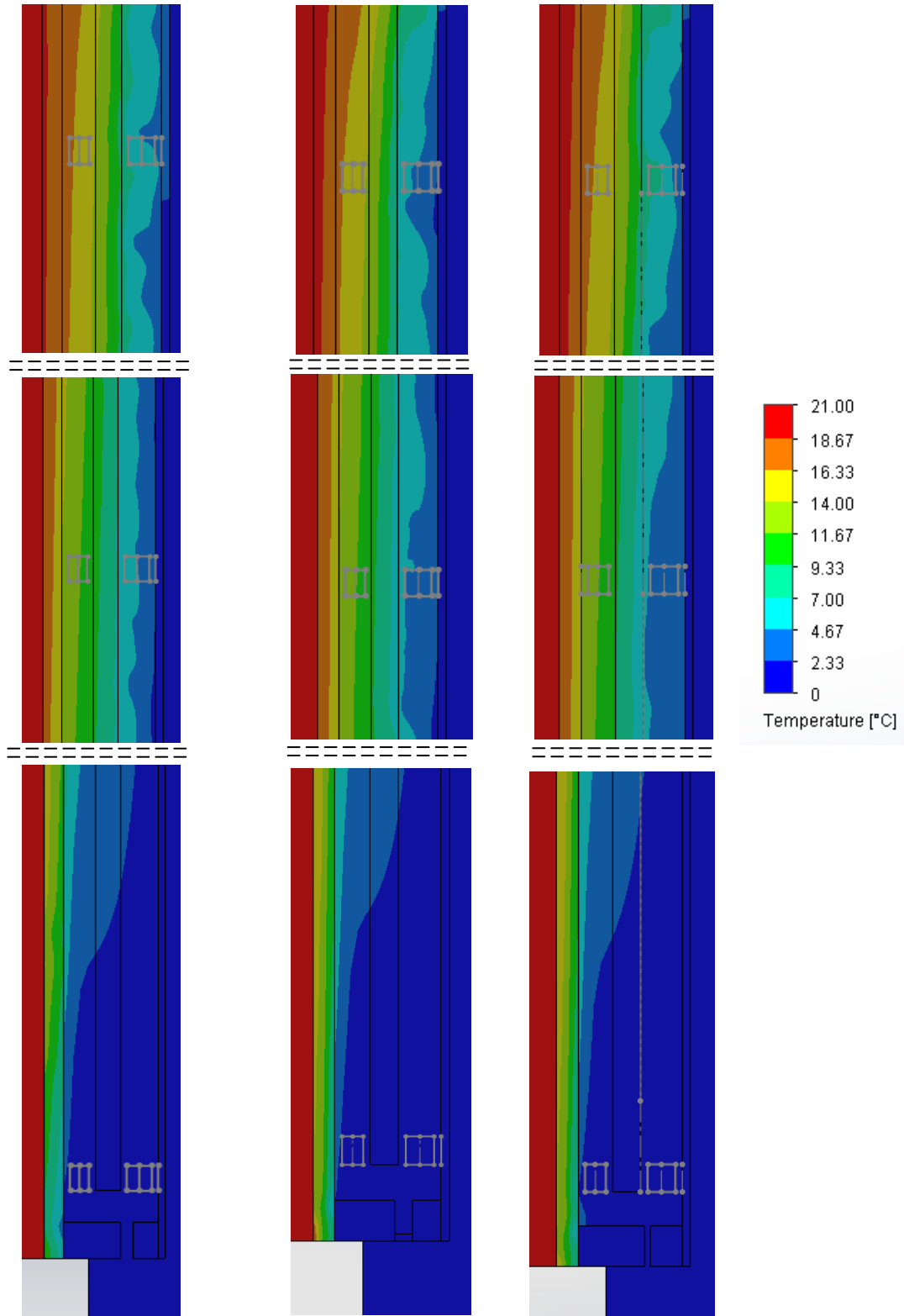


Figure 5.8 : Model without porous Media (left), model with porous media (middle), model with linear channel (right) temperature distribution.

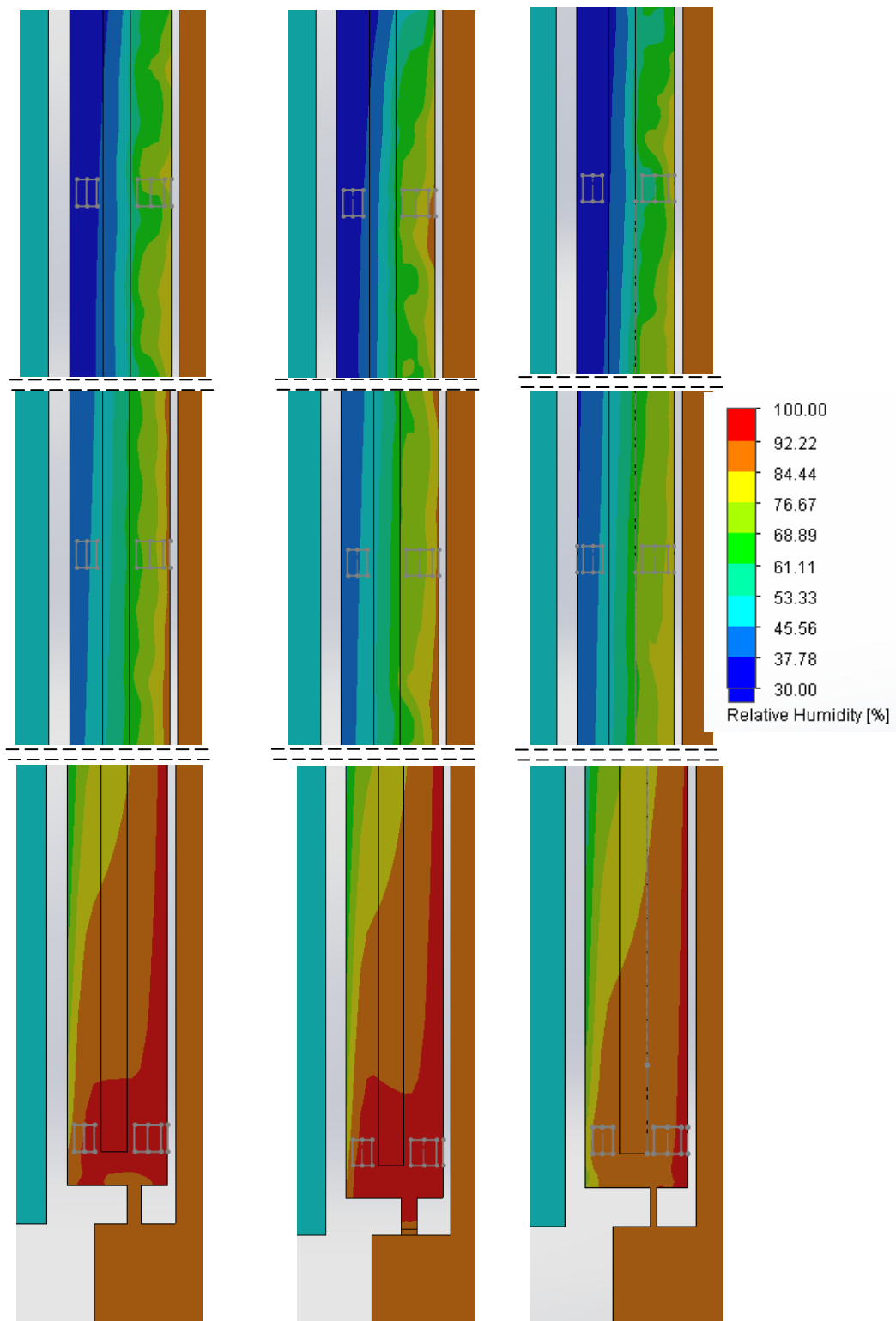


Figure 5.9 : Model without porous media (left), Model with porous media (middle), model with linear channel (right) relative humidity distributions.

CSTB condensation assessment risk test results at 400th minute is given below.(Table 5.9) (Comprehensive test results are given in Table 4.2)

Table 5.9 : Experiment results at 400th minute.

Region	Temperature (°C)	Relative Humidity (%)
Cavity	1.6	83.8
Exterior Glass Interior Surface	0.3	n/a

Even though there are some mismatches in velocity cut plots between three different models (Figure 5.7), trend of velocity distribution is highly matched with each other's. Similarity ratio decreases as long as height increase.

There is high similarity between three different models in terms of temperature distribution. Temperature values obtained from test are also validate CFD output as it is clearly shown with Table 4.2 and Figure 5.8.

On the ground of observing higher velocities due to narrow channel effect of linear channel, relative humidity values are relatively lower with respect to other models which is shown at Figure 5.9.

“Air flow and heat transfer in double skin façades” illustrates that there is 3°C difference at outer cavity, 1°C – 1.5 °C difference at inner cavity and around 1°C difference on inner glass surface in 20°C and 30°C interval between CFD results and experiment results. As it is obviously seen from Table 5.9 and Figure 5.8 and Figure 5.9, there is significantly less difference between model results and experimental results.

5.3.5 Validation with August-Roche Magnus Approach

Table 5.10 indicates corresponded dew points with respect to relative humidity and temperature values according to August-Roche Magnus approach. If temperature of any surface which contact with indoor is lower than dew point of indoor environment, there is condensation occurrence at specified surface. Minimum temperature on surface is mostly seen on aluminium profile surface or glass surface.

August-Roche Magnus Formula;

The Magnus-Tetens formula for the vapour pressure is given by [13]

$$p_w = 0.6105 \cdot e^{(aT/(b+T))} \quad [\text{kPa}] \quad (5.2)$$

with $a=17.27$

$$b=237.7 \text{ } ^\circ\text{C}$$

and T_d is in $^\circ\text{C}$.

$$a=6.105 \text{ millibar}; \quad b=17.27; \quad c=237.7^\circ\text{C}; \quad 0^\circ\text{C} \leq T \leq +60^\circ\text{C} \quad (\pm 0.4^\circ\text{C})$$

The relative humidity and vapour saturation pressure has direct relation with the vapor pressure by

$$p_w = RH \cdot p_{ws} \quad (5.3)$$

Saturated air means the air which has 100% relative humidity and the temperature equals to dew point temperature

$$\begin{aligned} p_w &= RH \cdot p_{ws} \\ \Rightarrow 0.6105 \cdot \exp\left[\frac{a \cdot T_d}{b + T_d}\right] &= 0.6105 \cdot RH \cdot \exp\left[\frac{a \cdot T}{b + T}\right] \\ \Rightarrow T_d(T, RH) &= \frac{b \cdot \alpha(T, RH)}{a - \alpha(T, RH)} \end{aligned} \quad (5.4)$$

where

$$\alpha(T, RH) = \ln(RH) + \frac{a \cdot T}{b + T} \quad (5.5)$$

[13].

Table 5.10 : Dew point value changes with respect to relative humidity and temperature.

INDOOR TEMP. °C	RELATIVE HUMIDITY (RH. %)													
	30	35	40	45	50	55	60	65	70	75	80	85	90	95
30.0	10.5	12.8	14.9	16.8	18.4	20.0	21.4	22.7	23.9	25.1	26.2	27.2	28.2	29.1
29.0	9.7	12.0	14.0	15.8	17.5	19.0	20.4	21.7	23.0	24.1	25.2	26.2	27.2	28.1
28.0	8.8	11.1	13.1	14.9	16.6	18.1	19.5	20.8	22.0	23.1	24.2	25.2	26.2	27.1
27.0	7.9	10.2	12.2	14.0	15.7	17.2	18.6	19.8	21.0	22.2	23.2	24.3	25.2	26.1
26.0	7.1	9.3	11.3	13.1	14.8	16.2	17.6	18.9	20.1	21.2	22.3	23.3	24.2	25.1
25.0	6.2	8.5	10.5	12.2	13.8	15.3	16.7	18.0	19.1	20.3	21.3	22.3	23.2	24.1
24.0	5.3	7.6	9.6	11.3	12.9	14.4	15.7	17.0	18.2	19.3	20.3	21.3	22.3	23.1
23.0	4.5	6.7	8.7	10.4	12.0	13.5	14.8	16.1	17.2	18.3	19.4	20.3	21.3	22.2
22.0	3.6	5.8	7.8	9.5	11.1	12.5	13.9	15.1	16.3	17.4	18.4	19.4	20.3	21.2
21.0	2.8	4.9	6.9	8.6	10.2	11.6	12.9	14.2	15.3	16.4	17.4	18.4	19.3	20.2
20.0	1.9	4.1	6.0	7.7	9.3	10.7	12.0	13.2	14.4	15.4	16.4	17.4	18.3	19.2
19.0	1.0	3.2	5.1	6.8	8.3	9.7	11.1	12.3	13.4	14.5	15.5	16.4	17.3	18.2
18.0	0.2	2.3	4.2	5.9	7.4	8.8	10.1	11.3	12.4	13.5	14.5	15.4	16.3	17.2
17.0	-0.7	1.4	3.3	5.0	6.5	7.9	9.2	10.4	11.5	12.5	13.5	14.5	15.3	16.2
16.0	-1.6	0.5	2.4	4.1	5.6	7.0	8.2	9.4	10.5	11.6	12.5	13.5	14.4	15.2
15.0	-2.4	-0.3	1.5	3.2	4.7	6.0	7.3	8.5	9.6	10.6	11.6	12.5	13.4	14.2
14.0	-3.3	-1.2	0.6	2.3	3.7	5.1	6.4	7.5	8.6	9.6	10.6	11.5	12.4	13.2
13.0	-4.2	-2.1	-0.3	1.3	2.8	4.2	5.4	6.6	7.7	8.7	9.6	10.5	11.4	12.2
12.0	-5.0	-3.0	-1.2	0.4	1.9	3.2	4.5	5.6	6.7	7.7	8.7	9.6	10.4	11.2
11.0	-5.9	-3.9	-2.1	-0.5	1.0	2.3	3.5	4.7	5.7	6.7	7.7	8.6	9.4	10.2
10.0	-6.8	-4.8	-3.0	-1.4	0.1	1.4	2.6	3.7	4.8	5.8	6.7	7.6	8.4	9.2

Condensation risk on exterior glass interior surface is assessed at Table 5.11, Table 5.12 and Table 5.13 with respect to dew points of cavity temperature and cavity relative humidity from same height according to August-Roche Magnus formula with on specified points, which are indicated at 5.3.1 specified points section. (G and Ca 1 points)

Table 5.11 : Condensation risk assessment in “Model without porous media”.

Point	Velocity [m/s]	Temperature (Fluid) [°C]	Relative Humidity [%]	Dew Points (°C)	γ	Point	Temperature (Fluid) [°C]	Condensation Sit.
Ca 1.1	0.039	0.98	94.46	0.19	0.014	G - 1.1	0.46	No Condensation
Ca 1.2	0.011	4.97	71.53	0.26	0.019	G - 1.2	1.47	No Condensation
Ca 1.3	0.025	6.32	65.26	0.28	0.020	G - 1.3	2.52	No Condensation

Table 5.12 : Condensation risk assessment in “Model with porous media”.

Point	Velocity [m/s]	Temperature (Fluid) [°C]	Relative Humidity [%]	Dew Points (°C)	γ	Point	Temperature (Fluid) [°C]	Condensation Sit.
Ca 1.1	0.052	0.96	94.70	0.20	0.015	G - 1.1	0,48	No Condensation
Ca 1.2	0.008	4,36	74.60	0.24	0.018	G - 1.2	1,55	No Condensation
Ca 1.3	0.048	4,17	75.69	0.26	0.019	G - 1.3	1,60	No Condensation

Table 5.13 : Condensation risk assessment in “Model with linear channel”.

Point	Velocity [m/s]	Temperature (Fluid) [°C]	Relative Humidity [%]	Dew Points (°C)	γ	Point	Temperature (Fluid) [°C]	Condensation Sit.
Ca 1.1	0.047	0.90	91.19	-0.37	-0.027	G - 1.1	0,37	No Condensation
Ca 1.2	0.043	3,74	75.29	-0.23	-0.016	G - 1.2	1,68	No Condensation
Ca 1.3	0.031	6,45	62.77	-0.13	-0.010	G - 1.3	2,01	No Condensation

The dew points in the middle of cavity between blind and exterior glass are considerably lower than temperature on glass surface with same height. Therefore, there is no condensation.

5.3.6 Effect of different filter distance to exterior glass

This part evaluates effects of the filter distance to exterior glass in “Model without porous media”.

Table 5.14 : Effect of “25 mm distance to exterior glass” in cavity.

Point	x [m]	y [m]	z [m]	Velocity [m/s]	Temperature (Fluid) [°C]	Relative Humidity [%]
Ca 1.1	0.08	-2.70	0.08	0.039	0.98	94.46
Ca 2.1	0.08	-2.70	0.03	0.037	0.86	92.85
Ca 1.2	0.08	-1.35	0.08	0.011	4.97	71.53
Ca 2.2	0.08	-1.35	0.03	0.028	11.95	44.35
Ca 1.3	0.08	-0.20	0.08	0.025	6.32	65.26
Ca 2.3	0.08	-0.20	0.03	0.001	15.81	34.73

Table 5.15 : Effect of “25 mm distance to exterior glass” on exterior glass surface.

Point	x [m]	y [m]	z [m]	Velocity [m/s]	Temperature (Fluid) [°C]	Relative Humidity [%]
G - 1.1	0.08	-2.70	0.09	0.00	0.46	98.01
G - 1.2	0.08	-1.35	0.09	0.00	1.47	91.43
G - 1.3	0.08	-0.20	0.09	0.00	2.52	84.93

Table 5.16 : Effect of “38 mm distance to exterior glass” in cavity.

Point	x [m]	y [m]	z [m]	Velocity [m/s]	Temperature (Fluid) [°C]	Relative Humidity [%]
Ca 1.1	0.08	-2.70	0.08	0.040	0.97	94.54
Ca 2.1	0.08	-2.70	0.03	0.039	0.86	93.69
Ca 1.2	0.08	-1.35	0.08	0.012	4.98	71.49
Ca 2.2	0.08	-1.35	0.03	0.028	11.98	44.33
Ca 1.3	0.08	-0.20	0.08	0.035	4.98	71.53
Ca 2.3	0.08	-0.20	0.03	0.001	15.99	34.30

Table 5.17 : Effect of “38 mm distance to exterior glass” on exterior glass surface.

Point	x [m]	y [m]	z [m]	Velocity [m/s]	Temperature (Fluid) [°C]	Relative Humidity [%]
G - 1.1	0.08	-2.70	0.09	0.00	0.46	98.03
G - 1.2	0.08	-1.35	0.09	0.00	1.42	91.70
G - 1.3	0.08	-0.20	0.09	0.00	2.05	87.78

Table 5.18 : Effect of “56 mm distance to exterior glass” in cavity.

Point	x [m]	y [m]	z [m]	Velocity [m/s]	Temperature (Fluid) [°C]	Relative Humidity [%]
Ca 1.1	0.08	-2.70	0.08	0.040	1.03	94.31
Ca 2.1	0.08	-2.70	0.03	0.042	0.93	94.38
Ca 1.2	0.08	-1.35	0.08	0.012	4.48	74.01
Ca 2.2	0.08	-1.35	0.03	0.028	11.98	44.42
Ca 1.3	0.08	-0.20	0.08	0.010	5.40	69.45
Ca 2.3	0.08	-0.20	0.03	0.001	15.68	35.02

Table 5.19 : Effect of “56 mm distance to exterior glass” on exterior glass surface.

Point	x [m]	y [m]	z [m]	Velocity [m/s]	Temperature (Fluid) [°C]	Relative Humidity [%]
G - 1.1	0.08	-2.70	0.09	0.00	0.46	98.23
G - 1.2	0.08	-1.35	0.09	0.00	1.41	91.86
G - 1.3	0.08	-0.20	0.09	0.00	1.95	88.40

All the above data taken from the models with different filter positions shows the outputs indicated below.

When filter gets closer to interior side, relative humidity next outer glass becomes higher.

The filter position has no considerable effect on to velocity distribution.

Filter position influence more below part of cavity from temperature, velocity and relative humidity aspect.

5.4 Next Step

The report based on CLC 12-260039255 numbered lab experiment by CSTB is modeled and simulated at Solidworks Flow Simulation CFD program in order to have comprehensive results in this work. Façade Respirante is constituted by using comprehensive results of CFD analysis which is validated with CSTB lab report. Accordingly, a new Façade Respirante mock-up was developed. There will be new experiment with currently developed Façade Respirante. The lab results of this experiment will be also compared with validated CFD model which is revised with respect to dimensions of currently constituted model in order to reach Façade Respirante which has maximum thermal performance without condensation. Moreover, the Façade Respirante configuration will be developed under different climatic conditions, as well. This study will be also presented as master thesis at Istanbul Technical University Energy Institute.

6. TESTING THE FR FOR CONDENSATION RISK

This chapter includes condensation risk assessment of previously constituted closed cavity façade at FTI (Façade Testing Institute) Labs in İstanbul Çatalca district.

The purpose is to assess the risk of condensation on exterior glazing surface and aluminum surface which contact with cavity air. Hygrometers and thermocouples, which are placed to critical points, also help us to determine by tracking relative humidity and temperature variations inside of the cavity.

Thermocouples (Thermal sensors) and hygrometers are placed to various zones in order to measure temperature values with 0.1 °C and 0.1% precision and from 0.5% to 1.6% uncertainty for hygrometer and 0.1°C temperature uncertainty for thermocouples.

All the measurements are collected by means of data logger. Thermal and hygric measurements are recorded with 30 seconds intervals. Experiment is carried out between 06 -15 May 2015 dates. Experiment is carried out according to five different variation.

Please see below mock-up variation with respect to blind and filter situation for each day respectively.

- Venetian blind is removed
- Adjusting venetian blind with vertically positioned (closed)
- Adjusting venetian blind with 90° vertical angle (open)

When blinds are vertically positioned which is the most critical among the others:

- Sealing one filter out of six filters
- Sealing two filters on right and left side out of six filters

6.1 Methodology of Experiment

Boundary conditions and initial conditions of condensation risk assessment experiment which is constituted by CSTB for Façade Respirante systems test methodology is indicated below. [9]

6.1.1 Setting the boundary conditions

The defined boundary conditions based on CSTB parameters are given below as indoor and outdoor conditions (Table 6.1).

Indoor Conditions: Temperature is kept at 20°C and relative humidity is kept at 50% and indoor is pressurized with an additional pressure of +50 Pa relatively.

Outdoor Conditions: Outdoor is conditioned to 20°C temperature and 80% relative humidity as an initial condition. Final temperature is 0°C at end of 400th minute thereby 1°C temperature reduction in each 20 minutes.

Humidity and temperature change at indoor, cavity and outdoor is tracked by means of hygrometers and thermocouples. The temperature value at interior side of exterior glass is measured. Corresponding saturation vapour pressure to related temperature is identified from thermodynamic table. If vapour pressure at cavity is lower than corresponding saturation pressure to the temperature value at interior side of exterior glass, It is determined that there is no condensation.

Table 6.1 : Initial conditions and final situations data table.

Initial Conditions			
	Temperature (°C)	Humidity (%)	Pressure (Pa)
Indoor	20	50	50
Outdoor	20	80	0

1°C temperature reduction in each 20 minutes at outdoor.

Final Situation (At the end of 400th minute)			
	Temperature (°C)	Humidity (%)	Pressure (Pa)
Indoor	20	50	50
Outdoor	0	-	0

6.2 Description of Mock-Up

Components of test mock-up is explained in terms of technical features in this section.

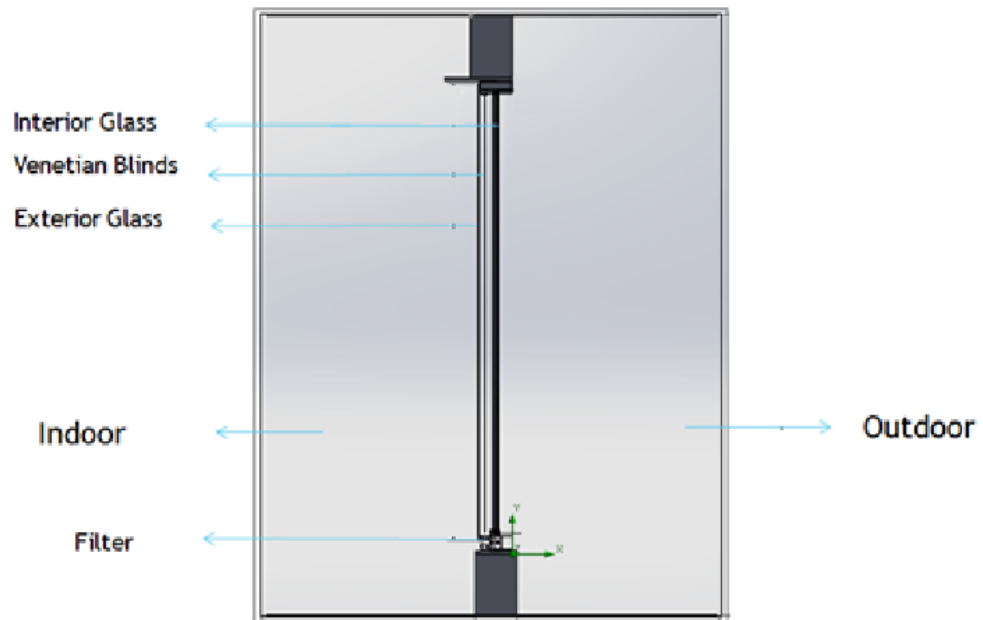


Figure 6.1 : Section view of experiment stand.

6.2.1 General features of glazing combination

Glass combination of mock up is shown below.

Dimensions: 1260 mm x 2100 mm

Glazing Combination: Clear Float Glass 6 mm + 81 mm Respired Cavity Gap including blind) + Clear Float Glass 6 mm + Sun-Guard HS Superneutral 70 (low-e layer) + 16 mm Cavity (90% Argon) + Clear Laminated Glass 8mm 44.2 8

Total volume of cavity between inner glass combination and outer glass is 0.18 m^3 .

6.2.1.1 Inner glass combination

Inner glazing combination is calculated through Guardian Glass Performance Calculator program. The output of the program is illustrated below.

6.2.1.2 Outer glass

Clear Float Glass with 6 mm thickness is used as outer glass.

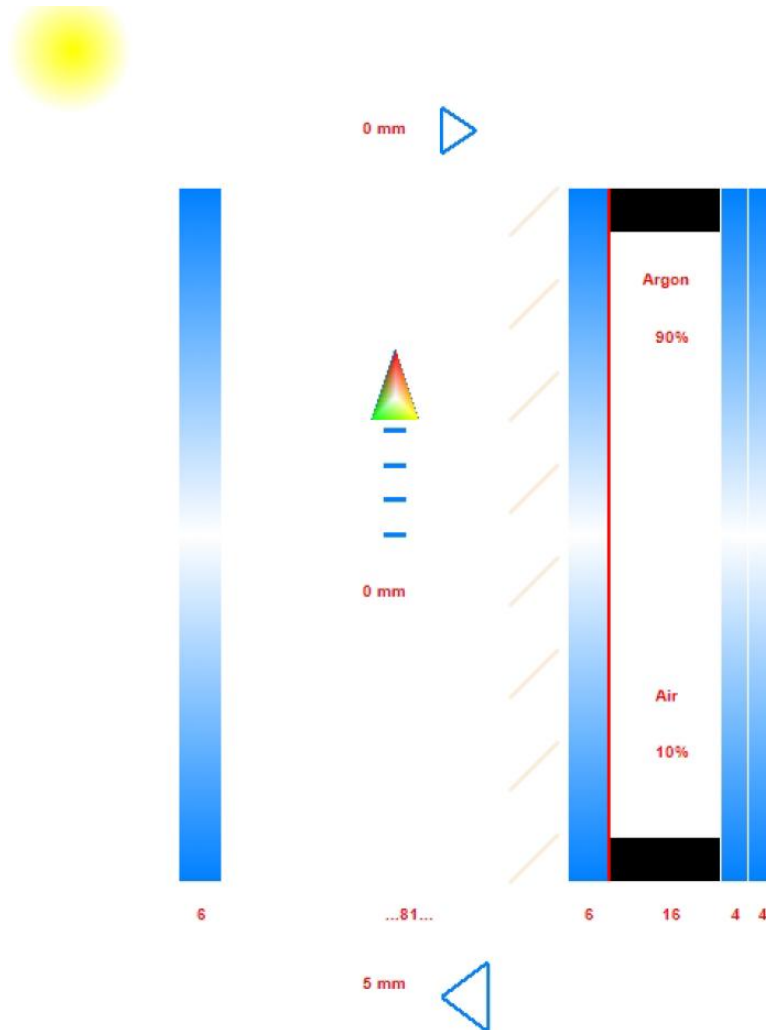
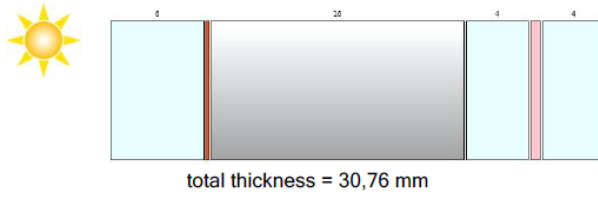


Figure 6.2 : Glazing combinations of Façade Respirante.

6.2.2 Venetian blinds

The Venetian blinds which are used in this experiment is the product of Hella. Blinds is made of aluminum and It is electrically controlled. Slat width of the blind is 25 mm.



Glazing from external to internal:

<p>Pane 1</p> <p>6 mm Float Glass ExtraClear SunGuard SN 70/41</p> <p>Spacer 1 - 16 mm</p> <p>10% Air 90% Argon</p>	<p>Pane 2</p> <p>4 mm Float Glass Clear 0,76 mm PVB Clear 4 mm Float Glass Clear</p>
--	---

Results

Visible light (EN 410 - 2011)		Solar energy (EN 410 - 2011)	
transmittance [%]	$\tau_v = 67,6$	solar factor [%]	$g = 40,5$
reflectance external [%]	$\rho_v = 10,4$	shading coefficient [g/0.87]	$sc = 0,47$
reflectance internal [%]	$\rho_v = 11,0$	direct transmittance [%]	$\tau_e = 34,6$
general colour rendering index [%]	$R_a = 94,8$	direct reflectance external [%]	$\rho_e = 33,3$
		direct reflectance internal [%]	$\rho_e = 25,0$
Thermal properties (EN 673 - 2011)		direct absorption [%]	$a = 32,1$
U-value [W/(m ² K)]	$U_g = 1,1$	UV transmittance [%]	$\tau_{uv} = 0,5$
slope $\alpha = 90^\circ$		secondary internal heat transfer factor [%]	$q_i = 5,9$
		Other data	
		estimated sound reduction index [dB]	$R_w = \text{NPD}$
		(EN 717-1)	$C = \text{NPD}$
			$C_{tr} = \text{NPD}$

Figure 6.3 : Technical features of inner glass combination [Guardian Glass Configurator].

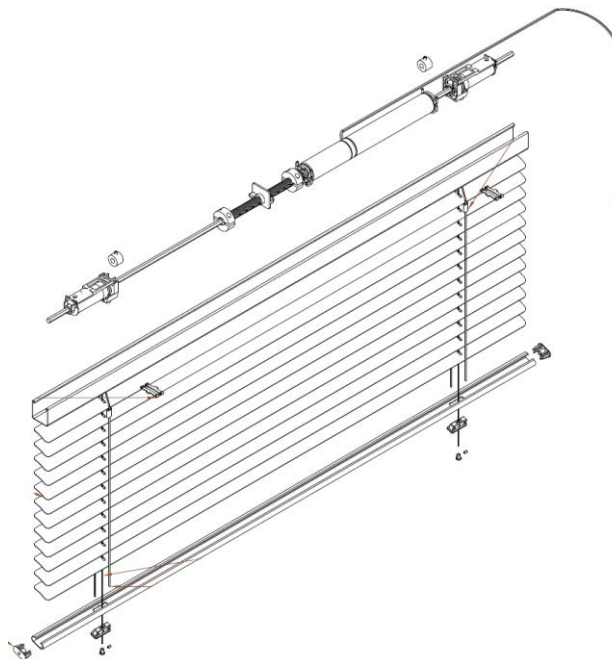


Figure 6.4 : Hella blind [29].

6.2.3 Filters

There are 6 pieces filters to supply slightly ventilation in order to prevent condensation. The number of filter can be decreased in accordance with condensation situation. SOFABIN FILTRE04 500G model (Figure 6.5) is used in this experiment. Filter mesh size is 500 micron. Mesh size directly affect air passage behaviour inside to cavity, as well as dust and dirt accumulation. Some feature of specified filter is shown below.

- Filter Dimension:** $\Phi 19\text{mm} \times 111.5 \text{ mm}$
- Filter Surface area:** 1250.73 mm^2
- Mesh Size:** $500\mu\text{m}$
- Air Passage area:** 800.47 mm^2
- Number of Filter:** 6
- Total Filter Surface Area:** 75.1 cm^2
- Total Air Passage Area:** 48.0 cm

Section and plan view of specified filter is illustrated in Figure 6.5.

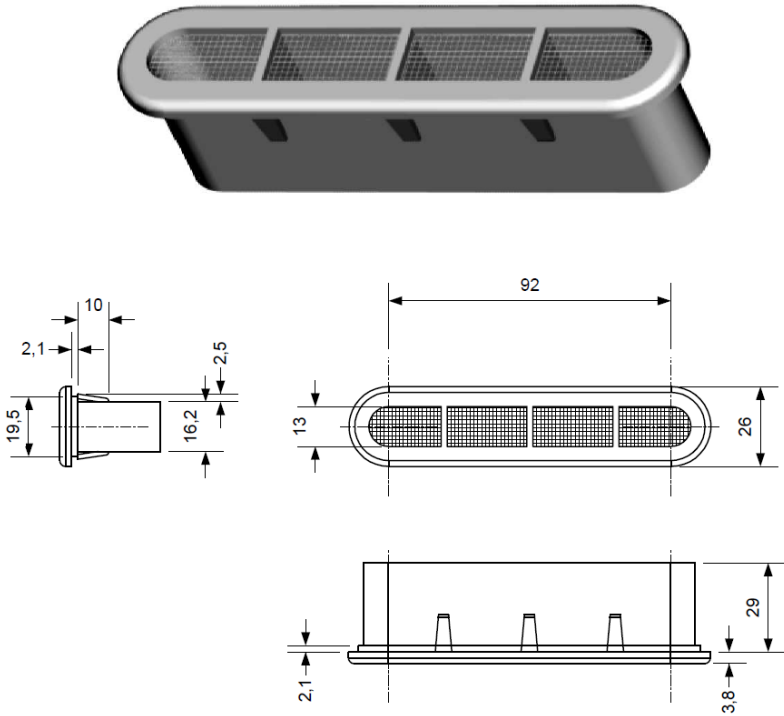


Figure 6.5 : Plan and section and view of filters [30].

6.2.4 General views of façade respirante details

The design of the Façade Respirante is represented below.

1) Specific detailing of mock-up system is given in Figure 6.6.

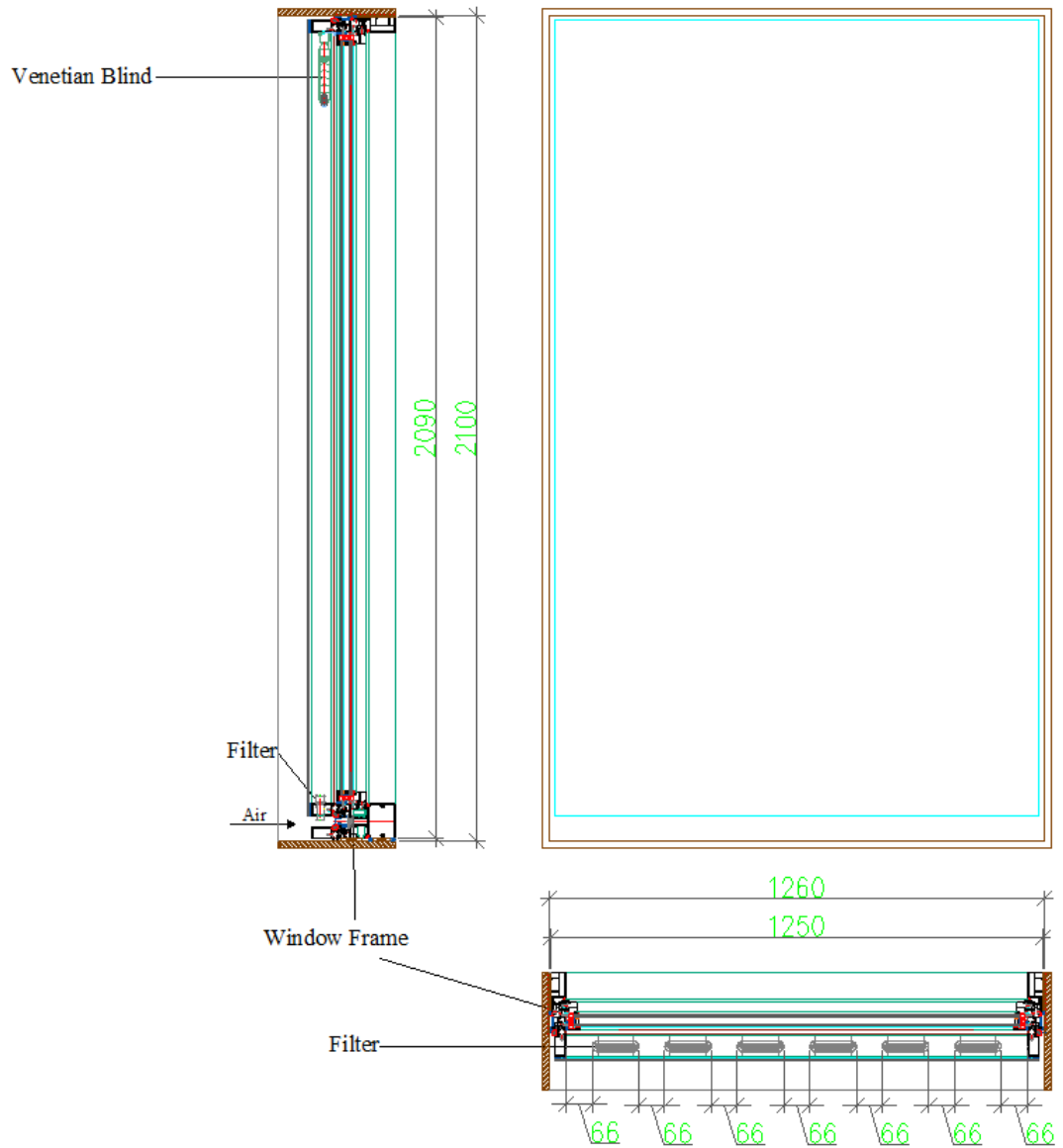


Figure 6.6 : General view of constituted façade respirante test mock-up after analysis.

2.)Frame details of closed cavity façade system is shown in Figure 6.7, Figure 6.8 and Figure 6.9.

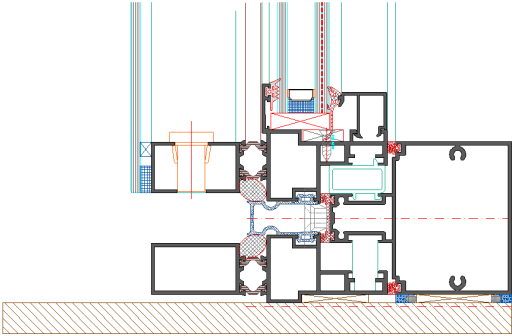


Figure 6.7 : Horizontal frame-1 (Bottom).

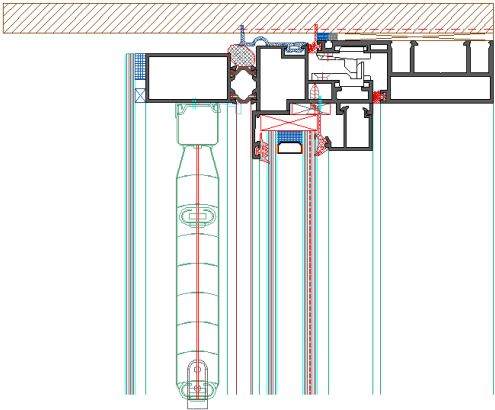


Figure 6.8 : Horizontal frame-2 (Top).

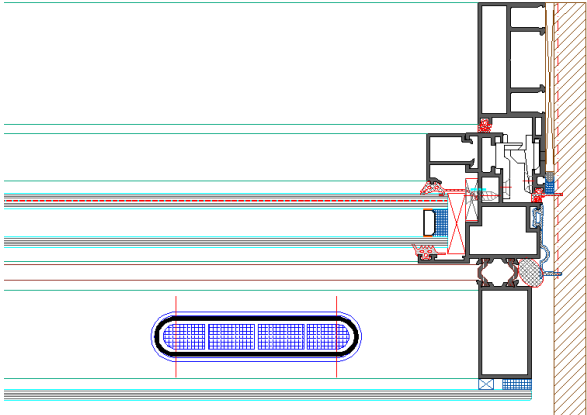


Figure 6.9 : Vertical frame

6.3 Selection of Experiment Equipments

Various equipments are used for the purpose of measuring easy, sensible and reliable. Used equipments are hygrometers, data logger, thermal sensor (thermocouple), humidifier, dehumidifier and air conditioner (Figure 6.10).

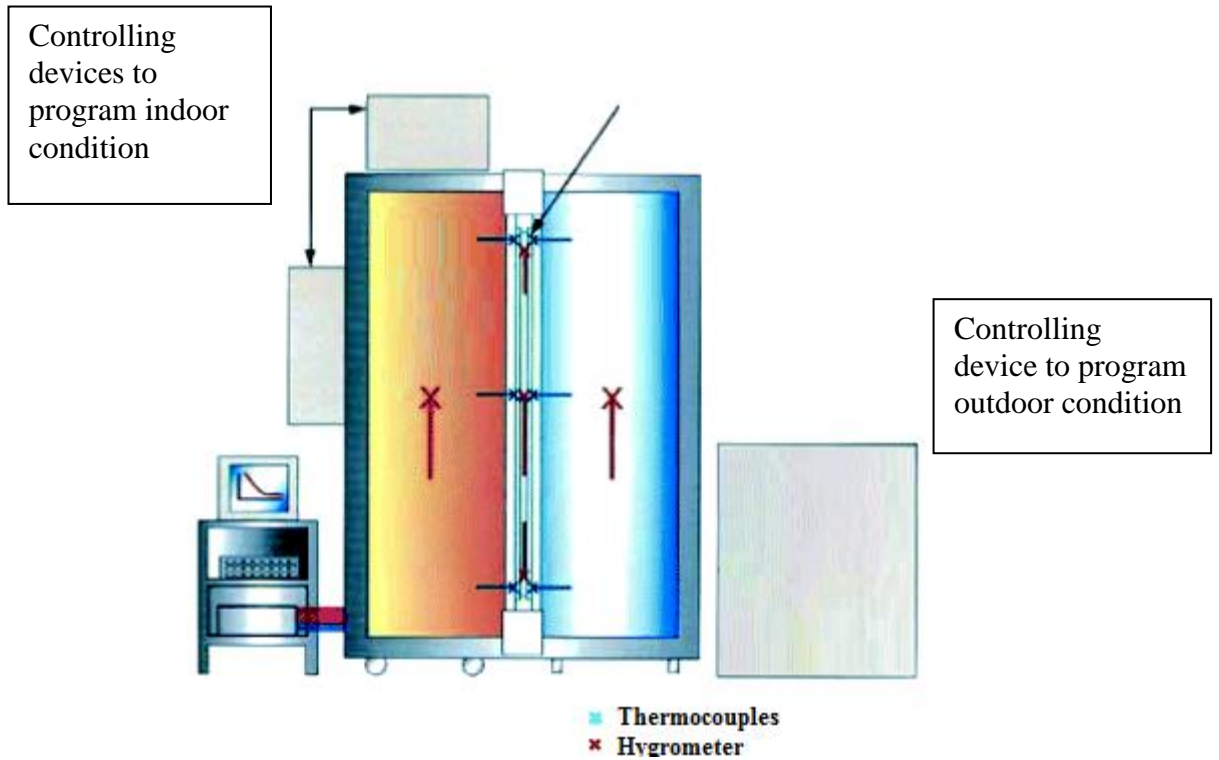


Figure 6.10 : Experimental mock-up view of Façade Respirante [20].

6.3.1 Identification of experiment equipments

The positions of experiment equipments are identified in Figure 6.11.

6.3.1.1 Thermocouple (Thermal Sensor)

Thermal Sensors (Thermocouple) are used in order to measure temperature values sensitively in various zones. Used thermocouples used in this experiment are T type product of Omega brand. Measurement sensibility of the product is $0,1\text{ }^{\circ}\text{C}$. The product is made of copper-constantan. It is suited for measurements in the -200 to $350\text{ }^{\circ}\text{C}$ range. T thermocouples have a sensitivity of about $43\text{ }\mu\text{V}/^{\circ}\text{C}$. It has $\pm 0,5\text{ }^{\circ}\text{C}$ tolerance between $-40\text{ }^{\circ}\text{C}$ - $125\text{ }^{\circ}\text{C}$.

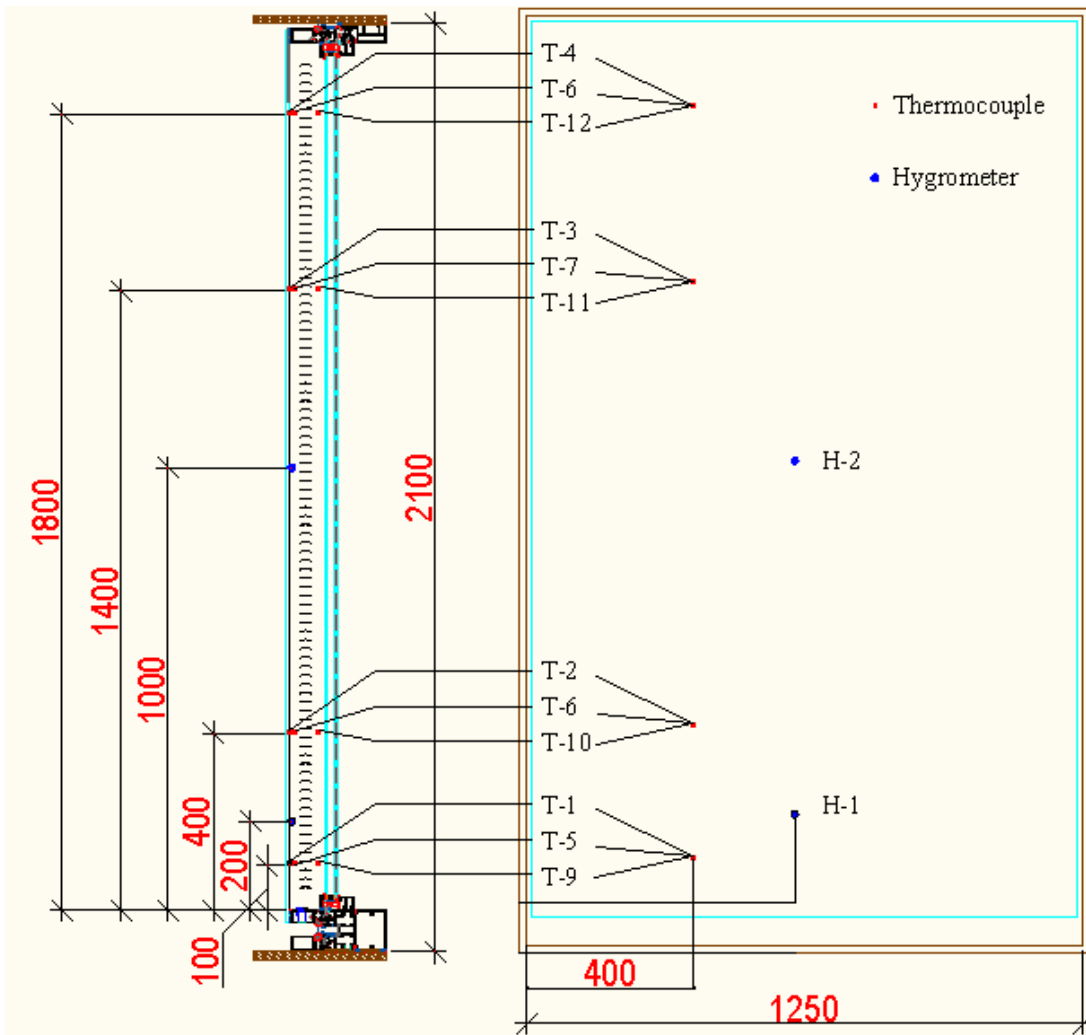


Figure 6.11 : Section detail (left) and plan detail (right) placement of thermocouples and hygrometers.



Figure 6.12 : Omega T type thermocouple.

Locating thermal sensors (Thermocouple)

There are four thermocouples on glazing surface with various heights, four thermocouples in between blind and exterior glass and four thermocouples in between blind and interior glass. There are additionally 2 more thermal sensors at

indoor and outdoor. Overall, 14 thermal sensors are used for this experiment. Positions and heights of thermocouples are identified as it is illustrated in Table 6.2.

Table 6.2 : The zones where thermal sensors (Thermocouple) are located and height of them .

Symbol	Name	Position	Height (mm)
T-1	Thermocouple-1	Exterior Glass Interior Surface	100
T-2	Thermocouple-2	Exterior Glass Interior Surface	400
T-3	Thermocouple-3	Exterior Glass Interior Surface	1400
T-4	Thermocouple-4	Exterior Glass Interior Surface	1800
T-5	Thermocouple-5	Cavity Between Exterior Glass and Blind	100
T-6	Thermocouple-6	Cavity Between Exterior Glass and Blind	400
T-7	Thermocouple-7	Cavity Between Exterior Glass and Blind	1400
T-8	Thermocouple-8	Cavity Between Exterior Glass and Blind	1800
T-9	Thermocouple-9	Cavity Between Interior Glass and Blind	100
T-10	Thermocouple-10	Cavity Between Interior Glass and Blind	400
T-11	Thermocouple-11	Cavity Between Interior Glass and Blind	1400
T-12	Thermocouple-12	Cavity Between Interior Glass and Blind	1800

6.3.1.2 Hygrometers (Humidity Sensors)

Hygrometer (Humidity Sensor) is the instrument which measures moisture content in air. There are various types of hygrometers which are based on three different technology such as resistive sensors, capacitive sensors and thermal conductivity sensing technology. Resistive sensors can be used for remote locations, capacity sensors are able to indicate wide RH range and thermal conductivity sensors are highly resistant against corrosive conditions at high temperatures. [31]

Two different type of hygrometers are used in this experiment. These are Dixell XH20P (Figure 6.13) and OMET T3111P (Figure 6.14). Dixell XH20P can cover from 0% to 99% relative humidity range with 1,7% uncertainty in accordance with the calibration indicated 6.3.2.1 section. Omet T3111P product can measure humidity from 0%to 100% relative humidity with maximum 0.7% uncertainty with the calibration indicated 6.3.2.1 section.

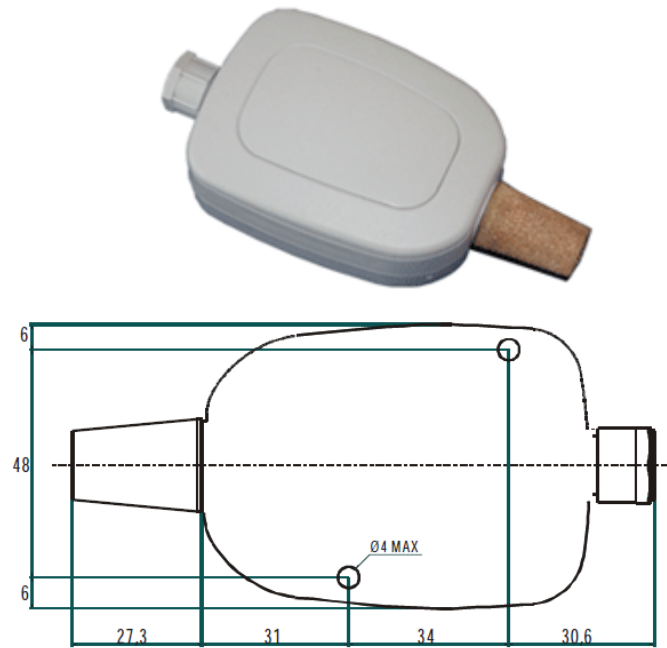


Figure 6.13 : Dixell XH20P hygrometer [32].



Figure 6.14 : OMET T3111P hygrometer [33].

Locating hygrometers in experiment

Hygrometers in cavity are also capable of measuring temperature values. The humidity probe locations will give the temperature values of the specified points. Position of hygrometers are illustrated in Table 6.3.

Table 6.3 : Hygrometer positions in experiment.

Symbol	Name	Position	Height (mm)
H-1	Hygrometer-1	Cavity Between Exterior Glass and Blind	200
H-2	Hygrometer-2	Cavity Between Exterior Glass and Blind	1000
H-3	Hygrometer-3	Indoor	1050
H-4	Hygrometer-4	Outdoor	1050

6.3.1.3 Data logger

Data logger is the device which records measured data obtained by sensors according to time intervals. The data logger which is used in this experiment is HP Agilent data logger 34972A model. The data logger is located interior side in this experiment. The image of the product is given in Figure 15.



Figure 6.15 : HP Agilent 34972A data logger [34].

6.3.1.4 Humidity control

Humidity control is supposed to be exist in order to keep indoor in 50% relative humidity and to start outdoor in 80% relative humidity.

Humidifier: Sinbo Ultrasonic Humidifier is used to humidify indoor and outdoor in this experiment.

Dehumidifier: Olefini OLE-12 NA (Figure 6.16) is used to dehumidify excessive humidity from indoor.



Figure 6.16 : Olefini-12 NA dehumidifier [35].

6.3.2 Calibration

Experiment instruments such as COMET T3111P, COMET T3111, DIXELL XH20P Omega T Type thermocouples are calibrated in “Penta Otomasyon” labs which is accredited by Turkish Accreditation Agency.

6.3.2.1 Hygric sensors

COMET T3111P, COMET T3111 and DIXELL XH20P are calibrated in terms of hygric measurements. There is 0.1% precision and from 0.5% to 1.6% uncertainty depending on measurement instrument. Hygric calibration details are illustrated in Table 6.4.

Table 6.4 : Hygric calibrations.

	Reference Humidity (%)	Error (%)		Reference Humidity (%)	Error (%)		Reference Humidity (%)	Error (%)
	21.6	0.7		21.6	-0.8		22.3	-1.4
COMET T3111P	52.9	0.5	COMET T3111	52.9	-0.7	DIXELL XH20P	49.8	-1.6
	83.4	0.7		83.4	-0.8		82.6	-1.7

6.3.2.2 Thermal sensors

COMET T3111P, COMET T3111 and all thermocouples are calibrated in terms of thermal measurements. There is 0.01°C precision and from 0.5% to 1.6% uncertainty (Table 6.5) depending on measurement instrument.

Table 6.5 : Thermal calibrations.

COMET T3111		COMET T3111P		Thermocouple	
Reference Temperature (°C)	Error (%)	Reference Temperature (°C)	Error (%)	Reference Temperature (°C)	Meas. Uncertainty (°C)
-5.2	-0.1	-5.2	-0.2	-10.0	±0.2
5.4	-0.2	5.6	0.2	0.0	±0.2
20.3	-0.2	20.5	0.2	10.0	±0.2
				20.0	±0.2

6.4 Set Cases

All the measurements are collected by means of data logger. Thermal and hygric measurements are recorded with 30 seconds intervals.

Experiment is carried out between 06th May - 15th May 2015 dates in order to confirm measurement accuracy. Experiment is carried out according to five different variation.

Please see below mock-up variation with respect to blind and filter situation for each day respectively.

- Venetian blind is removed
- Adjusting venetian blind with vertically positioned (closed)
- Adjusting venetian blind with 90° vertical angle (open)

When blinds are vertically positioned which is the most critical among the others

- Sealing one filter out of six filters
- Sealing two filters on right and left side out of six filters

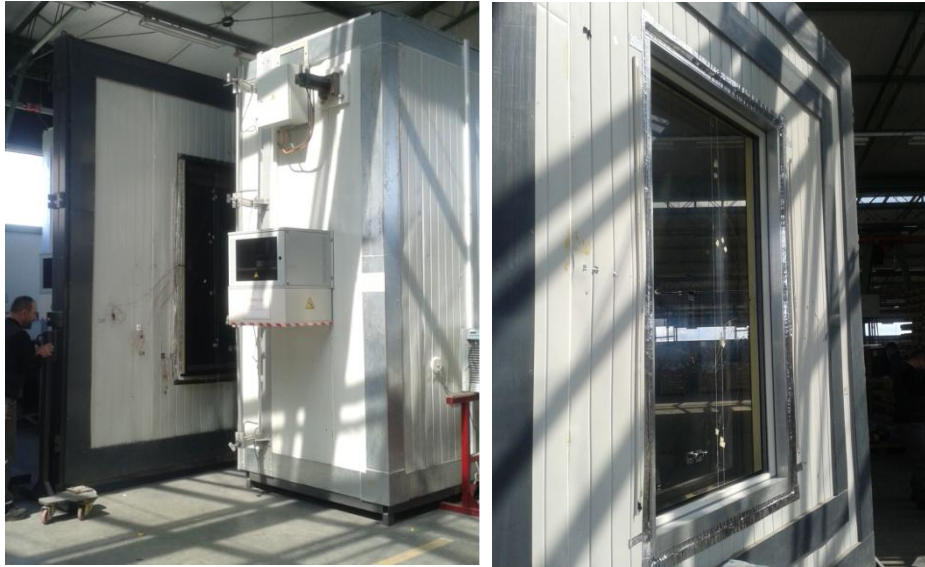


Figure 6.17 : General view of experiment stand.

6.5 Results

Experiment results are evaluated with respect to 3 different criteria which are indicated below.

- Effect of blind onto temperature and relative humidity variation
- Effect of slat angle onto temperature and relative humidity variation
- Effect of the number of filter decrement temperature and relative humidity variation

T_{indoor}	Indoor Temperature
RH_{indoor}	Indoor Relative Humidity
$T_{\text{ext glass}}$	Inner side temperature of exterior glass
$T_{\text{outer cavity}}$	Temperature of the cavity between outer glass and blind
$T_{\text{inner cavity}}$	Temperature of the cavity between blind and inner glass
RH_{cavity}	Cavity Relative Humidity
T_{ext}	Outdoor temperature
RH_{outdoor}	Outdoor relative humidity
P_{ivp}	Indoor Vapour Pressure
P_{cvp}	Cavity Vapour Pressure
P_{svp}	Corresponded Saturated Vapour Pressure to inner side temperature of exterior glass
P_{ovp}	Outdoor Vapour Pressure

6.5.1 Venetian blind with vertically positioned (Slats are closed)

Experiment result table and experiment result chart of venetian blind with vertically position is presented at Table 6.6 and Figure 6.18 respectively.

Partial vapour pressure of cavity is lower than corresponded saturated partial vapour pressure to $T_{\text{exterior glass}}$ throughout experiment. Therefore, there is no condensation.

The mean pressure difference value between P_{cvp} and P_{svp} is 13 Pa in last 100 minute.

Table 6.6 : Condensation risk experiment result table of venetian blind with vertically positioned.

Time	T _(indoor) (°C)	RH _{indoor} (%)	T _{ext} glass (°C)	T _{outer cavity} (°C)	T _{inner cavity} (°C)	RH _{cavity} (%)	T _{ext} (°C)	RH outdoor (%)	P _{ivp} (kPa)	P _{cvp} (kPa)	P _{svp} (kPa)	P _{ovp} (kPa)	P _{svp} - P _{cvp} (ΔP) (Pa)
0	22.6	50.2	21.0	21.4	21.7	61.6	20.1	78.0	1.374	1.570	2.474	1.827	904
0 h 20 min	22.6	50.2	20.5	21.0	21.4	61.3	19.2	74.8	1.374	1.524	2.407	1.656	882
0 h 40 min	22.6	50.0	19.9	20.6	21.1	61.2	18.2	72.4	1.368	1.480	2.316	1.506	837
1 h 00 min	22.6	50.0	19.1	19.9	20.5	62.1	17.1	70.7	1.368	1.436	2.211	1.371	774
1 h 20 min	22.6	50.0	18.3	19.1	20.0	63.6	15.8	69.4	1.368	1.407	2.101	1.247	694
1 h 40 min	22.6	50.0	17.6	18.5	19.4	65.3	15.0	69.4	1.368	1.390	2.011	1.184	621
2 h 00 min	22.6	50.0	16.9	17.9	18.8	67.4	14.1	69.0	1.368	1.375	1.916	1.110	541
2 h 20 min	22.6	50.0	16.1	17.2	18.2	69.7	13.2	68.8	1.368	1.361	1.828	1.043	467
2 h 40 min	22.5	50.0	15.1	16.3	17.5	72.8	12.0	69.0	1.360	1.346	1.717	0.967	372
3 h 00 min	22.5	50.0	14.4	15.6	16.9	75.5	11.1	69.7	1.359	1.336	1.634	0.919	298
3 h 20 min	22.4	50.0	13.4	14.7	16.0	79.2	9.9	70.5	1.350	1.319	1.529	0.859	211
3 h 40 min	22.3	50.2	12.5	13.9	15.3	82.5	9.0	71.2	1.349	1.306	1.451	0.816	146
4 h 00 min	22.2	50.5	11.6	13.0	14.6	85.4	8.0	72.2	1.346	1.280	1.363	0.774	83
4 h 20 min	22.0	50.7	10.7	12.2	13.8	86.5	7.1	73.3	1.335	1.227	1.283	0.739	56
4 h 40 min	21.9	50.9	9.9	11.4	13.1	86.8	6.2	74.2	1.333	1.172	1.216	0.702	44
5 h 00 min	21.7	50.9	8.9	10.5	12.2	87.0	5.1	74.8	1.317	1.102	1.137	0.656	34
5 h 20 min	21.4	50.0	7.9	9.6	11.4	87.1	4.1	76.1	1.271	1.039	1.062	0.622	23
5 h 40 min	21.2	50.9	6.9	8.7	10.6	87.2	3.1	77.0	1.277	0.977	0.996	0.586	19
6 h 00 min	21.0	50.2	6.1	7.9	9.8	87.3	2.3	78.7	1.246	0.928	0.941	0.566	13
6 h 20 min	20.5	50.0	4.8	6.9	8.8	87.9	1.7	80.9	1.202	0.872	0.875	0.559	3
6 h 40 min	20.3	49.6	4.2	6.6	8.5	88.0	1.0	80.2	1.178	0.855	0.861	0.528	6

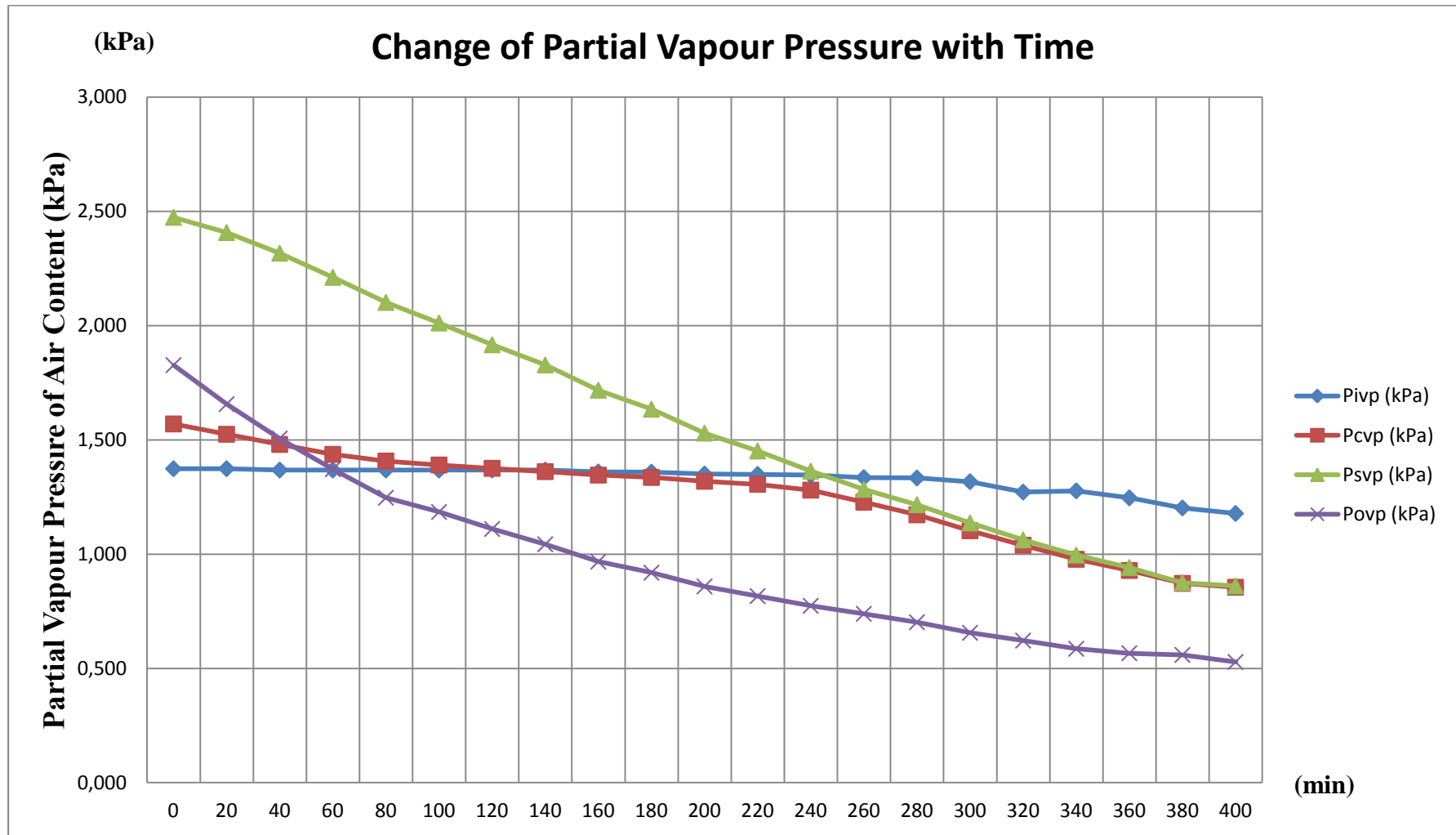


Figure 6.18 : Condensation risk experiment result chart of venetian blind with vertically positioned

6.5.2 Venetian blind with horizontally positioned (Slats are open)

Experiment result table and experiment result chart of venetian blind with vertically position is presented at Table 6.7 and Figure 6.19 respectively.

Partial vapour pressure of cavity is lower than corresponded saturated partial vapour pressure to $T_{\text{exterior glass}}$ throughout experiment. Therefore, there is no condensation.

The mean pressure difference value between P_{cvp} and P_{svp} is 17 Pa in last 100 minute.

Table 6.7 : Condensation risk experiment result table of venetian blind with horizontally positioned (slats are opened).

Time	T _(indoor) (°C)	RH _{indoor} (%)	T _{ext glass} (°C)	T _{outer cavity} (°C)	T _{inner cavity} (°C)	RH _{cavity} (%)	T _{ext} (°C)	RH _{outdoor} (%)	P _{ivp} (kPa)	P _{cvp} (kPa)	P _{svp} (kPa)	P _{ovp} (kPa)	P _{svp} - P _{cvp} (ΔP) (Pa)
0	20.4	50.0	19.6	20.0	19.9	66.9	19.9	80.6	1.195	1.556	2.282	1.863	726
0 h 20 min	20.4	50.0	19.4	19.8	19.8	65.5	19.0	80.0	1.195	1.507	2.244	1.748	738
0 h 40 min	20.4	50.0	19.1	19.5	19.6	64.0	17.9	80.4	1.195	1.446	2.201	1.649	755
1 h 00 min	20.4	50.0	18.5	19.1	19.3	63.4	17.0	78.9	1.195	1.394	2.120	1.529	726
1 h 20 min	20.5	50.0	18.0	18.6	18.8	63.6	16.0	77.0	1.202	1.356	2.054	1.399	697
1 h 40 min	20.5	50.0	17.3	18.0	18.4	64.5	15.1	75.9	1.202	1.332	1.973	1.302	641
2 h 00 min	20.5	50.2	16.7	17.5	17.9	65.8	14.2	75.5	1.207	1.311	1.899	1.221	587
2 h 20 min	20.5	50.4	16.1	16.9	17.4	67.3	13.4	75.3	1.213	1.296	1.829	1.156	533
2 h 40 min	20.4	50.7	15.2	16.1	16.6	70.0	12.2	74.8	1.210	1.275	1.719	1.061	444
3 h 00 min	20.4	50.9	14.2	15.2	15.8	72.9	11.0	74.8	1.215	1.257	1.619	0.980	362
3 h 20 min	20.3	50.0	13.5	14.5	15.2	75.4	10.2	75.3	1.188	1.246	1.545	0.935	299
3 h 40 min	20.3	50.4	13.0	14.1	14.9	76.6	9.6	75.5	1.198	1.230	1.498	0.901	268
4 h 00 min	20.3	50.4	11.8	12.9	13.7	81.0	8.2	76.4	1.198	1.202	1.378	0.829	176
4 h 20 min	20.2	50.2	10.9	12.1	12.9	84.1	7.3	77.2	1.185	1.184	1.298	0.788	114
4 h 40 min	20.1	50.7	9.9	11.2	12.2	87.1	6.3	78.1	1.188	1.158	1.221	0.743	63
5 h 00 min	20.0	50.2	8.8	10.2	11.3	88.2	5.1	79.2	1.171	1.098	1.134	0.694	37
5 h 20 min	20.0	50.7	8.1	9.5	10.6	88.4	4.3	79.6	1.181	1.051	1.082	0.659	30
5 h 40 min	20.0	50.2	7.0	8.5	9.5	88.5	3.1	80.7	1.171	0.978	1.002	0.614	24
6 h 00 min	20.0	50.9	6.2	7.7	8.9	88.6	2.4	80.0	1.186	0.931	0.949	0.579	18
6 h 20 min	20.0	49.6	5.5	7.0	8.2	88.9	1.6	81.3	1.156	0.890	0.902	0.556	12
6 h 40 min	20.0	50.9	4.8	6.3	7.6	89.6	0.8	80.7	1.186	0.857	0.861	0.521	4

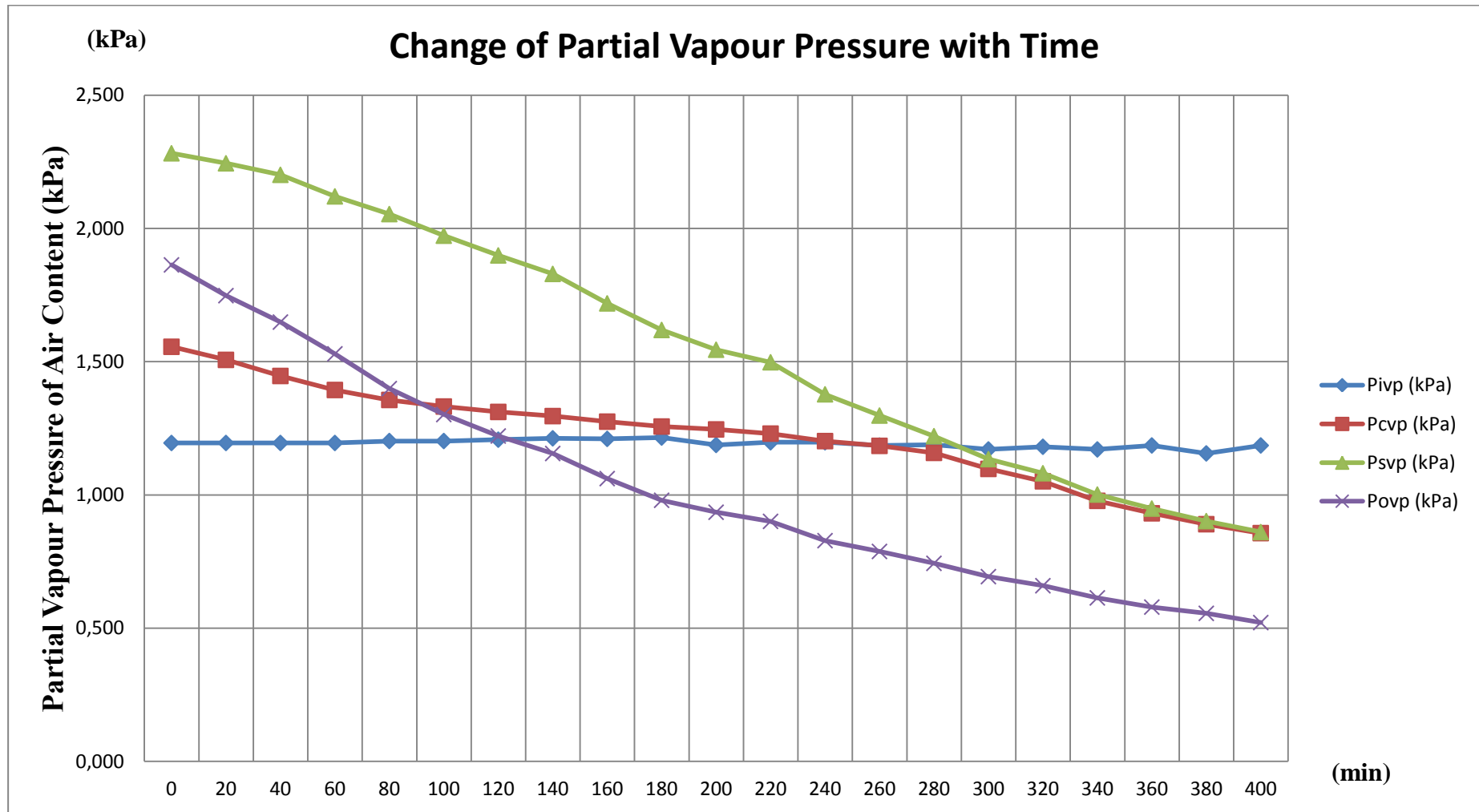


Figure 6.19 : Condensation risk experiment result chart of venetian blind with horizontally positioned (slats are opened).

6.5.3 Venetian blinds are removed

Experiment result table and experiment result chart of the venetian blinds are removed case is presented at Table 6.8 and Figure 6.20 respectively.

Partial vapour pressure of cavity is lower than corresponded saturated partial vapour pressure to $T_{\text{exterior glass}}$ throughout experiment. Therefore, there is no condensation.

The mean pressure difference value between P_{cvp} and P_{svp} is 18 Pa in last 100 minute.

Table 6.8 : Venetian blinds are removed.

Time	$T_{\text{(indoor)}}$ (°C)	RH_{indoor} (%)	$T_{\text{ext glass}}$ (°C)	$T_{\text{outer cavity}}$ (°C)	$T_{\text{inner cavity}}$ (°C)	RH_{cavity} (%)	T_{ext} (°C)	RH_{outdoor} (%)	P_{ivp} (kPa)	P_{cvp} (kPa)	P_{svp} (kPa)	P_{ovp} (kPa)	$P_{\text{svp}} - P_{\text{cvp}}$ (ΔP) (Pa)
0	20.0	50.7	19.2	19.4	19.2	80.6	19.9	80.0	1.181	1.817	2.226	1.849	409
0 h 20 min	20.1	50.9	19.2	19.5	19.4	75.1	19.1	79.8	1.193	1.697	2.213	1.754	516
0 h 40 min	20.1	50.9	18.9	19.3	19.3	71.5	18.2	79.1	1.193	1.597	2.174	1.654	577
1 h 00 min	20.1	50.7	18.4	18.9	19.0	69.1	17.1	80.2	1.188	1.508	2.109	1.563	601
1 h 20 min	20.1	50.7	18.1	18.6	18.7	68.5	16.4	79.4	1.188	1.466	2.067	1.479	601
1 h 40 min	20.1	50.4	17.1	17.9	18.0	68.9	15.0	77.0	1.183	1.405	1.949	1.313	544
2 h 00 min	20.1	50.2	16.6	17.4	17.6	69.5	14.1	75.9	1.178	1.376	1.890	1.221	514
2 h 20 min	20.1	50.2	16.0	16.8	17.1	70.2	13.3	75.7	1.178	1.338	1.811	1.154	473
2 h 40 min	20.1	50.0	15.0	15.9	16.3	71.7	12.0	75.3	1.173	1.294	1.705	1.054	410
3 h 00 min	20.1	50.0	14.5	15.4	15.8	72.9	11.3	75.3	1.173	1.272	1.643	1.006	371
3 h 20 min	20.0	50.0	13.4	14.5	14.9	75.2	10.1	75.3	1.166	1.236	1.538	0.929	303
3 h 40 min	20.0	50.0	13.0	14.0	14.5	76.6	9.5	75.7	1.166	1.221	1.491	0.897	270
4 h 00 min	20.0	50.0	11.9	13.0	13.7	79.7	8.3	77.2	1.166	1.191	1.389	0.843	198
4 h 20 min	20.0	50.0	11.4	12.5	13.1	81.3	7.8	77.4	1.167	1.179	1.345	0.817	165
4 h 40 min	20.0	50.0	10.2	11.5	12.2	84.9	6.5	78.5	1.166	1.153	1.246	0.758	93
5 h 00 min	20.1	50.0	9.1	10.4	11.1	87.8	5.2	79.6	1.173	1.104	1.154	0.702	50
5 h 20 min	20.0	50.0	8.1	9.5	10.2	88.5	4.2	80.5	1.166	1.046	1.078	0.661	32
5 h 40 min	20.0	50.0	7.4	8.8	9.7	88.7	3.4	79.2	1.167	1.004	1.026	0.615	22
6 h 00 min	20.0	50.0	6.3	7.8	8.7	89.0	2.3	79.6	1.166	0.939	0.954	0.572	15
6 h 20 min	20.0	50.0	6.0	7.5	8.5	89.0	1.9	80.5	1.167	0.922	0.937	0.562	15
6 h 40 min	20.0	50.0	5.2	6.7	7.7	89.6	0.9	80.9	1.166	0.878	0.882	0.527	4

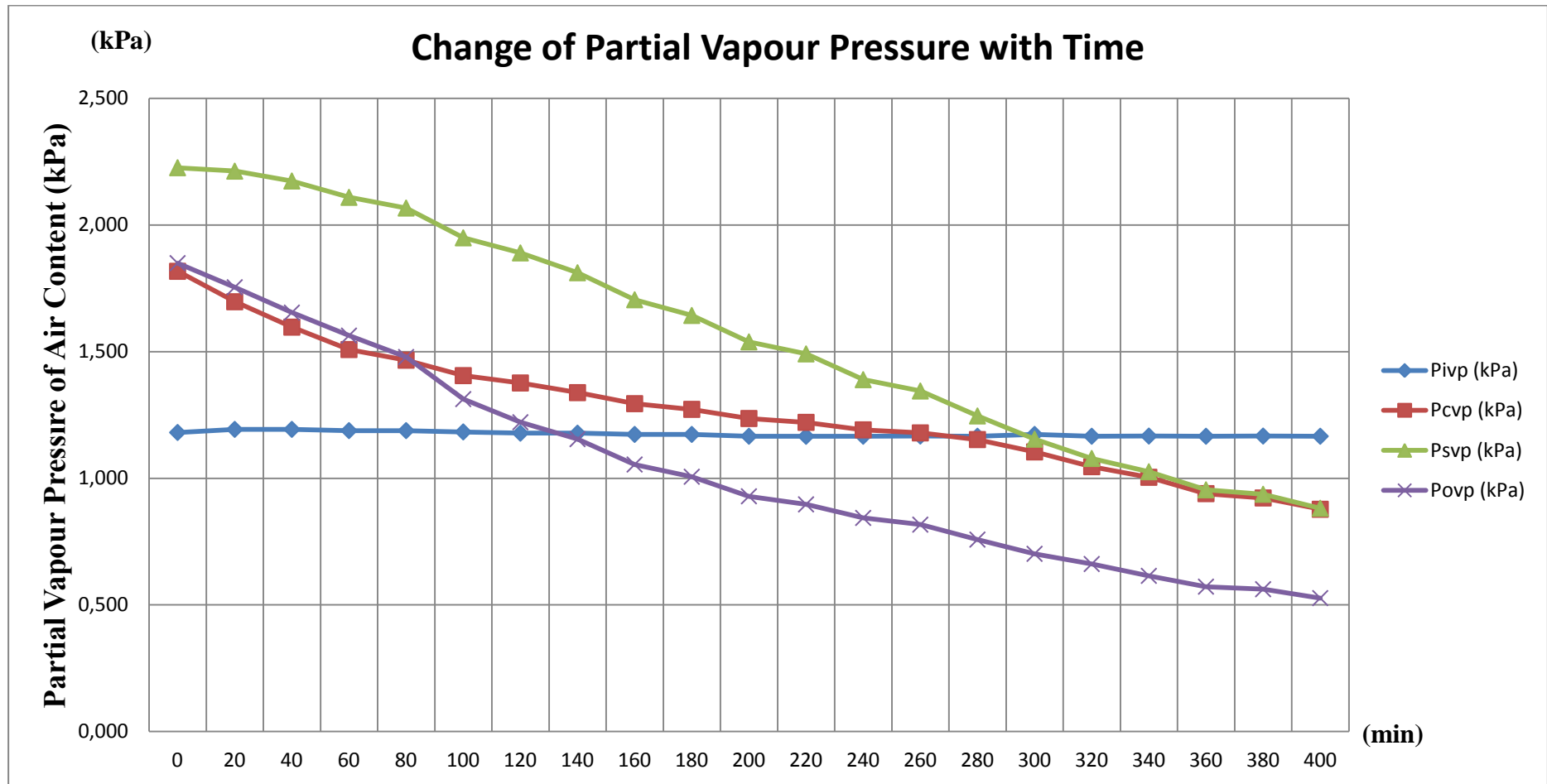


Figure 6.20 : Venetian blinds are removed

The result of three different case indicates that the most critical case is venetian blinds with vertically positioned (slats are closed) among the others.

Table 6.9 : Mean pressure difference value between P_{cvp} and P_{svp} in last 100 minute.

Cases	(ΔP) in $T_{300-400}$ (Pa)
Slats are closed	13
Slats are open	17
Venetian blinds are removed	18

6.5.4 One filter is sealed

The venetian blind inside of Façade Respirante system is arranged as vertically positioned which is the most critical case in terms of condensation risk. (Table 6.9) After one filter is sealed, the experiment is started.

Experiment result table and experiment result chart of sealing one filter case is presented at Table 6.10 and Figure 6.21 respectively.

Partial vapour pressure of cavity is lower than corresponded saturated partial vapour pressure to $T_{\text{exterior glass}}$ throughout experiment. Therefore, there is no condensation.

The mean pressure difference value between P_{cvp} and P_{svp} is 10 Pa in last 100 minute.

Table 6.10 : One filter is sealed.

Time	T _(indoor) (°C)	RH _{indoor} (%)	T _{ext glass} (°C)	T _{outer cavity} (°C)	T _{inner cavity} (°C)	RH _{cavity} (%)	T _{ext} (°C)	RH _{outdoor} (%)	P _{ivp} (kPa)	P _{cvp} (kPa)	P _{svp} (kPa)	P _{ovp} (kPa)	P _{svp} - P _{cvp} (ΔP) (Pa)
0	20.1	49.8	19.5	19.8	19.6	61.3	20.0	79.3	1.168	1.410	2.261	1.849	851
0 h 20 min	20.1	49.8	19.4	19.7	19.7	61.7	19.2	79.6	1.168	1.412	2.241	1.762	829
0 h 40 min	20.2	50.0	18.9	19.4	19.5	62.1	18.1	78.7	1.180	1.395	2.184	1.634	789
1 h 00 min	20.2	49.8	18.5	19.1	19.3	61.9	17.4	76.8	1.175	1.363	2.130	1.518	766
1 h 20 min	20.2	50.0	17.9	18.6	18.9	62.1	16.3	73.3	1.180	1.325	2.048	1.351	724
1 h 40 min	20.3	49.8	17.2	17.9	18.3	63.1	15.2	70.9	1.182	1.288	1.953	1.219	665
2 h 00 min	20.3	50.0	16.7	17.6	18.2	63.8	14.6	70.1	1.188	1.277	1.902	1.165	625
2 h 20 min	20.3	50.2	16.1	17.0	17.7	65.4	13.8	69.2	1.193	1.261	1.826	1.086	565
2 h 40 min	20.3	49.8	15.4	16.4	17.3	67.0	12.9	68.8	1.182	1.248	1.751	1.024	503
3 h 00 min	20.3	50.0	14.5	15.6	16.5	69.9	11.8	68.4	1.187	1.236	1.649	0.946	413
3 h 20 min	20.3	50.2	13.4	14.5	15.6	73.7	10.4	68.4	1.193	1.218	1.530	0.862	312
3 h 40 min	20.3	50.0	12.9	14.1	15.2	75.5	9.9	68.6	1.188	1.209	1.483	0.836	274
4 h 00 min	20.2	50.0	12.0	13.3	14.5	78.5	8.9	68.8	1.180	1.198	1.403	0.784	205
4 h 20 min	20.2	50.0	11.2	12.6	13.8	81.6	8.1	69.4	1.180	1.185	1.330	0.749	144
4 h 40 min	20.1	50.0	10.7	12.1	13.4	83.7	7.5	69.9	1.173	1.176	1.282	0.724	106
5 h 00 min	20.1	50.0	10.1	11.5	12.9	86.0	6.8	70.5	1.173	1.165	1.231	0.696	66
5 h 20 min	20.0	50.0	9.1	10.6	12.0	88.3	5.8	71.2	1.166	1.127	1.153	0.656	25
5 h 40 min	20.0	50.2	8.2	9.8	11.4	88.8	4.9	72.0	1.171	1.076	1.089	0.623	13
6 h 00 min	20.0	50.4	7.3	8.9	10.5	88.9	3.8	72.7	1.176	1.011	1.018	0.582	8
6 h 20 min	20.0	50.7	6.1	7.8	9.5	88.8	2.6	74.4	1.181	0.940	0.942	0.548	2
6 h 40 min	20.0	50.9	5.5	7.3	9.0	88.7	1.9	75.1	1.186	0.903	0.904	0.526	1

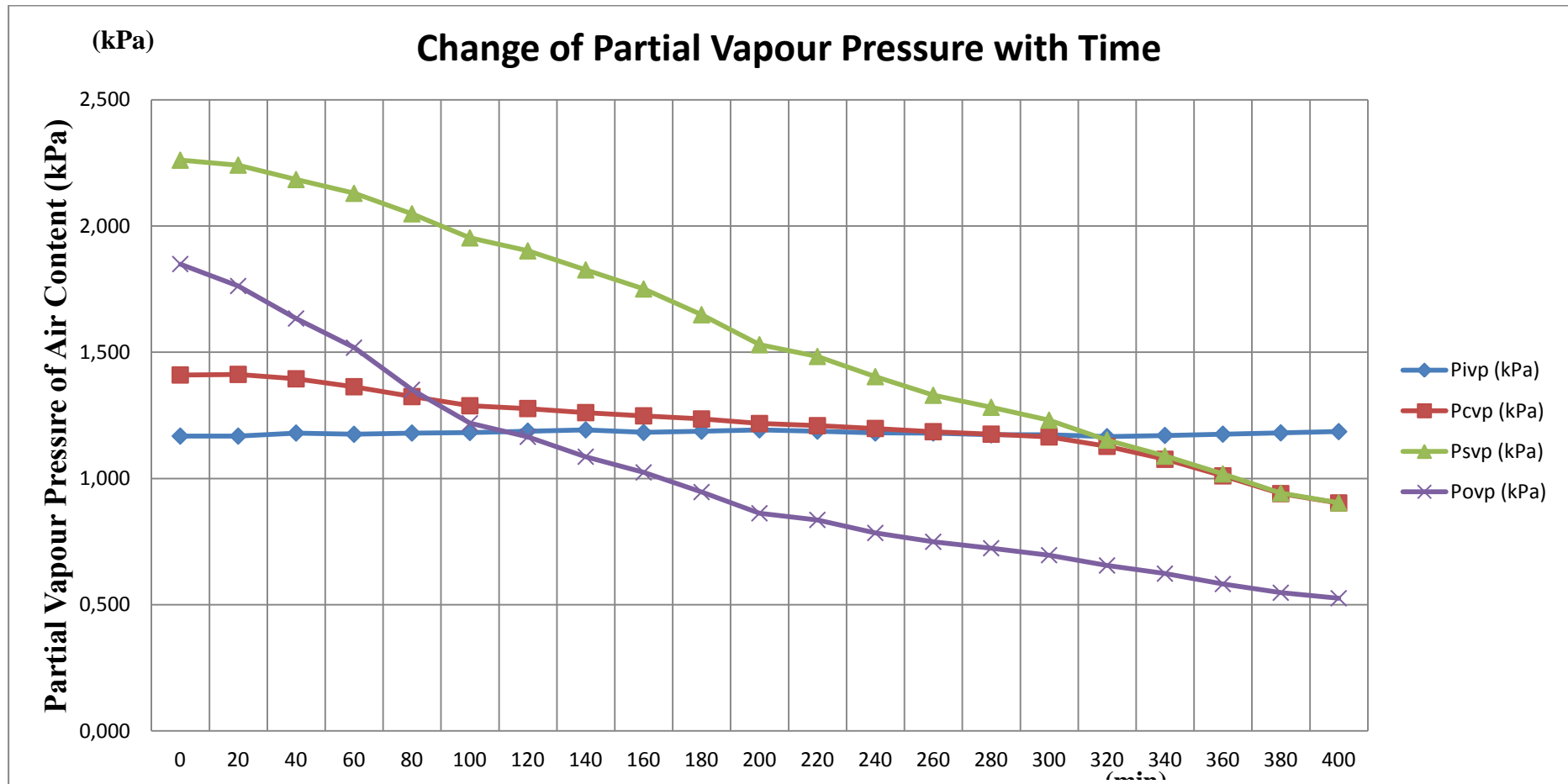


Figure 6.21 : One filter is sealed.

6.5.5 Two filters are sealed

The venetian blind inside of Façade Respirante system is arranged as vertically positioned which is the most critical case in terms of condensation risk. (Table 6.9) After one filter is sealed, the experiment is started.

Experiment result table and experiment result chart of sealing two filters case is presented at Table 6.11 and Figure 6.22 respectively.

Partial vapour pressure of cavity is higher than corresponded saturated partial vapour pressure to $T_{\text{exterior glass}}$ in some moments. Therefore, this case leads to condensation formation on interior surface of exterior glass.

The mean pressure difference value between P_{cvp} and P_{svp} is -5 Pa in last 100 minute.

Table 6.11 : Two filters are sealed.

Time	T _(indoor) (°C)	RH _{indoor} (%)	T _{ext glass} (°C)	T _{outer cavity} (°C)	T _{inner cavity} (°C)	RH _{cavity} (%)	T _{ext} (°C)	RH _{outdoor} (%)	P _{ivp} (kPa)	P _{cvp} (kPa)	P _{svp} (kPa)	P _{ovp} (kPa)	P _{svp} - P _{cvp} (ΔP) (Pa)
0	22.8	49.8	19.8	20.3	20.7	79.9	19.9	84.7	1.377	1.902	2.306	1.962	404
0 h 20 min	23.0	49.4	19.8	20.3	20.6	76.0	19.1	81.1	1.382	1.803	2.301	1.785	497
0 h 40 min	23.0	49.2	19.4	20.0	20.5	74.5	18.2	78.1	1.376	1.740	2.248	1.624	508
1 h 00 min	23.1	51.1	19.0	19.7	20.2	73.7	17.5	75.5	1.439	1.689	2.192	1.502	503
1 h 20 min	23.1	50.4	18.6	19.4	20.1	73.4	16.7	72.9	1.421	1.651	2.140	1.379	489
1 h 40 min	23.2	50.4	17.8	18.7	19.5	73.7	15.4	70.1	1.429	1.587	2.030	1.219	444
2 h 00 min	23.2	50.2	16.9	18.0	18.9	75.3	14.2	68.3	1.423	1.549	1.925	1.101	376
2 h 20 min	23.2	50.9	16.3	17.4	18.5	76.9	13.5	67.5	1.441	1.528	1.852	1.039	323
2 h 40 min	23.2	50.4	15.2	16.5	17.6	79.9	12.1	67.3	1.429	1.495	1.728	0.950	233
3 h 00 min	23.1	50.9	14.3	15.7	16.9	83.0	11.0	67.5	1.433	1.475	1.631	0.887	155
3 h 20 min	23.0	49.4	13.8	15.2	16.5	84.7	10.5	67.7	1.384	1.458	1.575	0.861	117
3 h 40 min	23.0	50.2	13.1	14.6	16.0	86.6	9.7	68.1	1.406	1.435	1.508	0.820	72
4 h 00 min	22.9	50.4	12.3	13.8	15.3	88.2	8.8	68.8	1.403	1.391	1.428	0.780	38
4 h 20 min	22.7	50.4	11.2	12.8	14.3	88.9	7.7	69.2	1.387	1.309	1.326	0.728	17
4 h 40 min	22.6	50.7	10.6	12.1	13.7	88.9	6.9	69.7	1.384	1.256	1.273	0.693	17
5 h 00 min	22.3	50.7	9.7	11.3	13.0	89.0	6.0	70.7	1.359	1.192	1.199	0.661	7
5 h 20 min	22.1	51.0	9.0	10.7	12.4	89.0	5.4	72.0	1.351	1.143	1.147	0.646	4
5 h 40 min	22.0	50.4	8.4	10.2	11.9	89.0	4.8	71.6	1.329	1.106	1.103	0.615	-3
6 h 00 min	21.7	50.4	7.4	9.2	11.0	88.8	3.6	73.1	1.305	1.031	1.025	0.578	-6
6 h 20 min	21.4	51.5	6.5	8.3	10.2	88.8	2.7	74.6	1.308	0.972	0.965	0.554	-7
6 h 40 min	21.0	49.8	5.2	7.1	8.9	88.9	1.6	77.4	1.234	0.893	0.881	0.529	-12

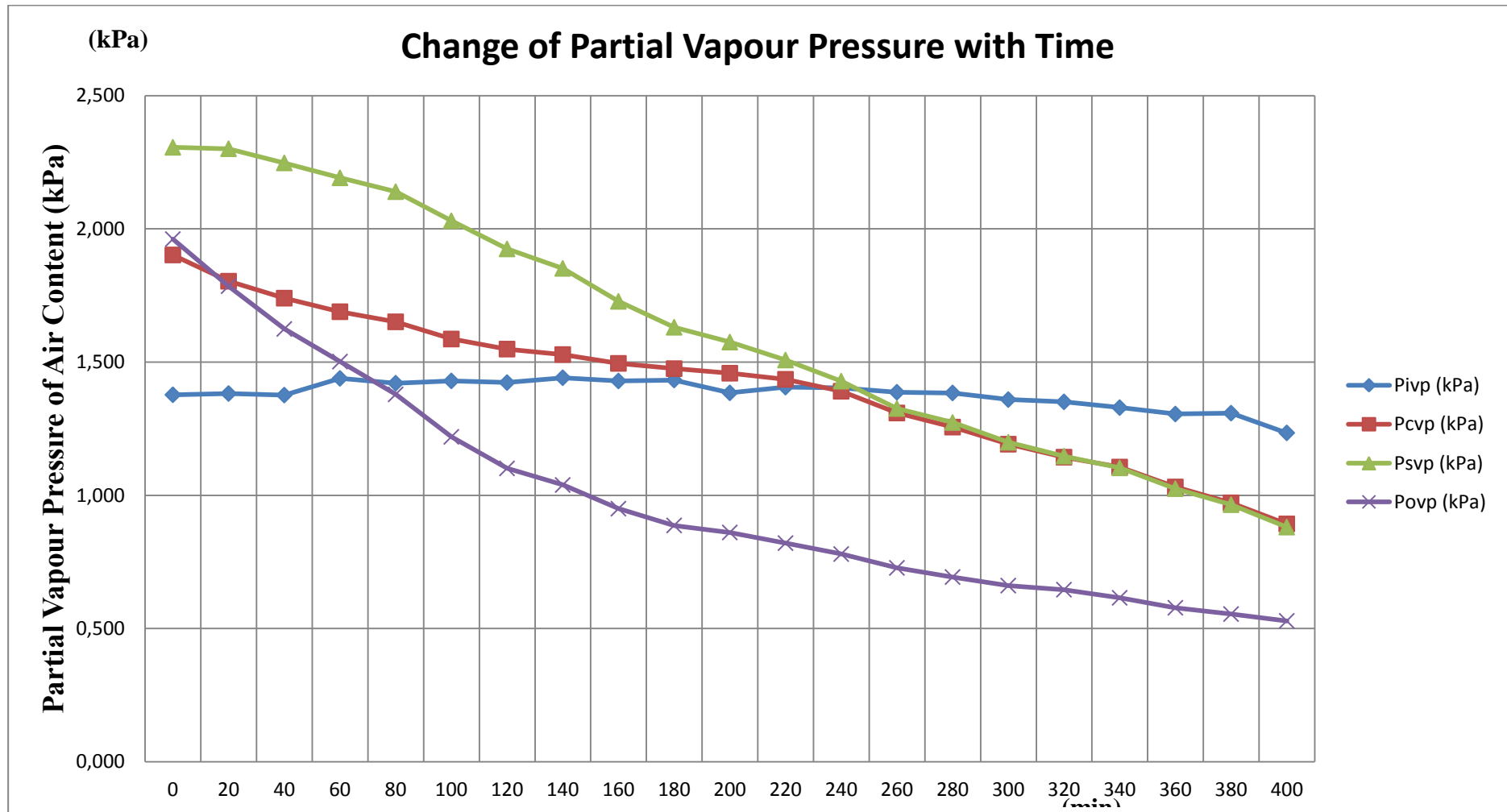


Figure 6.22 : Two filters are sealed.

As it is illustrated at Figure 6.21, Figure 6.22 and indicated at Table 6.10 and Table 6.11 that there is no condensation, if one filter is sealed and there is condensation formation on interior surface of exterior glass, if two filters are sealed.

Table 6.12 : Mean pressure difference value between P_{cvp} and P_{svp} in last 100 minute.

Cases	(ΔP) in $T_{300-400}$ (Pa)
One filter is sealed	10
Two filters are sealed	-5

Experiment results indicates that there is high tendency to condensation formation at venetian blinds vertically positioned case. On the other hand, when the blinds are removed, there is less probability to form condensation on outer glass surface. Moreover, as long as number of filter decrease, there is higher condensation risk. There is no condensation on glass surfaces, if there is at least 5 filters at below side of configured façade respirante system.

7. ANALYZING THE FR BASED ON ITS ENERGY PERFORMANCE

Energy performance analysis section determines thermal transmission value for windows (U_{window}) and its effect on heating load and cooling load with respect to the reference window which is defined in TS 825 (Thermal Insulation Requirements for Buildings)

7.1 Thermal Analysis

Thermal Analysis section presents condensation risk assessment and U Value analysis of closed cavity façade (Façade Respirante) frame details.

7.1.1 Referenced standards and norms

Condensation risk assessment and U Value analysis of constituted closed cavity façade system is based on the standards, which are given below.

EN ISO 10077-1	Thermal Performance of Windows
EN ISO 10077-2	Thermal Performance of Windows
Method	Component assessment method
EN 12631	Thermal Performance of Curtain Walling
EN 12524	Building Materials and Products
EN 10456	Building Materials and Products
EN ISO 6946	Building Components and Building Elements
TS 2164	Principles for the preparation of the projects of the central heating system

7.1.2 Technical features in terms of building physics

Thermal conductivity values of the frame components are presented below according to EN 10077 standard.

Table 7. 1 Thermal conductivity values of various materials [18,19].

Materials	Thermal Conductivity (W/mK)
Aluminum	160
EPDM Gasket	0.25
Silicone	0.35
Backing Rod	0.035
Glass Soda Lime	1.00
Polyamide Reinf.	0.30
Butyl Hot Melt	0.24
PVB	0.20
PVC	0.17
Insulation	0.035

7.1.3 Boundary conditions and initial conditions

Boundary conditions and initial conditions of the condensation risk assessment and U value analysis is indicated below.

Dimensions	: 1260mm x 2100mm
Glass Combination	: 6/80.6/6/10/16/44.2 (Figure 6.2)
Outdoor temperature	: -3 °C [25]
Indoor temperature	: +20 °C
Relative humidity (RH)	: 50 %
Dew point	: 9.3°C (Table 7.2)
U value of the inner glass combination (U_g)	: 1,1 W/m ² K
Thermal conductivity of inner glass air gap (λ)	: 0,022 W/m ² K (Table 7.3)
Temperature Difference for U_f Calculation	: 20 °C [18,19]
Thermal Conductivity of the insulation panel (λ):	0,035 W/m ² K
Thermal Conductivity of the Spacer (λ)	:0.11W/mK “Aluminum spacer”

Table 7.2 indicates corresponded dew points with respect to relative humidity and temperature values according to August-Magnus approach (Section 5.3.5). If temperature of any surface which contact with indoor is lower than dew point of indoor environment, there is condensation occurrence at specified surface. Minimum temperature on surface is mostly seen on aluminium profile surface or glass surface.

Table 7. 2 Dew point table respect to RH vs. indoor temperature.

INDOOR TEMP. °C	RELATIVE HUMIDITY (RH. %)													
	30	35	40	45	50	55	60	65	70	75	80	85	90	95
30.0	10.5	12.8	14.9	16.8	18.4	20.0	21.4	22.7	23.9	25.1	26.2	27.2	28.2	29.1
29.0	9.7	12.0	14.0	15.8	17.5	19.0	20.4	21.7	23.0	24.1	25.2	26.2	27.2	28.1
28.0	8.8	11.1	13.1	14.9	16.6	18.1	19.5	20.8	22.0	23.1	24.2	25.2	26.2	27.1
27.0	7.9	10.2	12.2	14.0	15.7	17.2	18.6	19.8	21.0	22.2	23.2	24.3	25.2	26.1
26.0	7.1	9.3	11.3	13.1	14.8	16.2	17.6	18.9	20.1	21.2	22.3	23.3	24.2	25.1
25.0	6.2	8.5	10.5	12.2	13.8	15.3	16.7	18.0	19.1	20.3	21.3	22.3	23.2	24.1
24.0	5.3	7.6	9.6	11.3	12.9	14.4	15.7	17.0	18.2	19.3	20.3	21.3	22.3	23.1
23.0	4.5	6.7	8.7	10.4	12.0	13.5	14.8	16.1	17.2	18.3	19.4	20.3	21.3	22.2
22.0	3.6	5.8	7.8	9.5	11.1	12.5	13.9	15.1	16.3	17.4	18.4	19.4	20.3	21.2
21.0	2.8	4.9	6.9	8.6	10.2	11.6	12.9	14.2	15.3	16.4	17.4	18.4	19.3	20.2
20.0	1.9	4.1	6.0	7.7	9.3	10.7	12.0	13.2	14.4	15.4	16.4	17.4	18.3	19.2
19.0	1.0	3.2	5.1	6.8	8.3	9.7	11.1	12.3	13.4	14.5	15.5	16.4	17.3	18.2
18.0	0.2	2.3	4.2	5.9	7.4	8.8	10.1	11.3	12.4	13.5	14.5	15.4	16.3	17.2
17.0	-0.7	1.4	3.3	5.0	6.5	7.9	9.2	10.4	11.5	12.5	13.5	14.5	15.3	16.2
16.0	-1.6	0.5	2.4	4.1	5.6	7.0	8.2	9.4	10.5	11.6	12.5	13.5	14.4	15.2
15.0	-2.4	-0.3	1.5	3.2	4.7	6.0	7.3	8.5	9.6	10.6	11.6	12.5	13.4	14.2
14.0	-3.3	-1.2	0.6	2.3	3.7	5.1	6.4	7.5	8.6	9.6	10.6	11.5	12.4	13.2
13.0	-4.2	-2.1	-0.3	1.3	2.8	4.2	5.4	6.6	7.7	8.7	9.6	10.5	11.4	12.2
12.0	-5.0	-3.0	-1.2	0.4	1.9	3.2	4.5	5.6	6.7	7.7	8.7	9.6	10.4	11.2
11.0	-5.9	-3.9	-2.1	-0.5	1.0	2.3	3.5	4.7	5.7	6.7	7.7	8.6	9.4	10.2
10.0	-6.8	-4.8	-3.0	-1.4	0.1	1.4	2.6	3.7	4.8	5.8	6.7	7.6	8.4	9.2

Overlapped zone of both red rectangular at Table 7.2 represents frequently used dew-points in condensation risk analysis. There is dew point value change according to various temperature and various relative humidity as it is shown at Table 7.2.

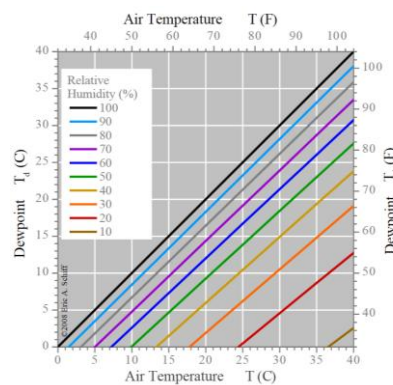


Figure 7. 1 The change of dew point value according air temperature vs. dew point temperature.

7.1.4 General views of constituted closed cavity façade details

The design of the closed cavity façade (façade respirante) is illustrated at below from Figure 7.2 to Figure 7.5.

1.) Specific detailing of mock-up system is given in Figure 7.2.

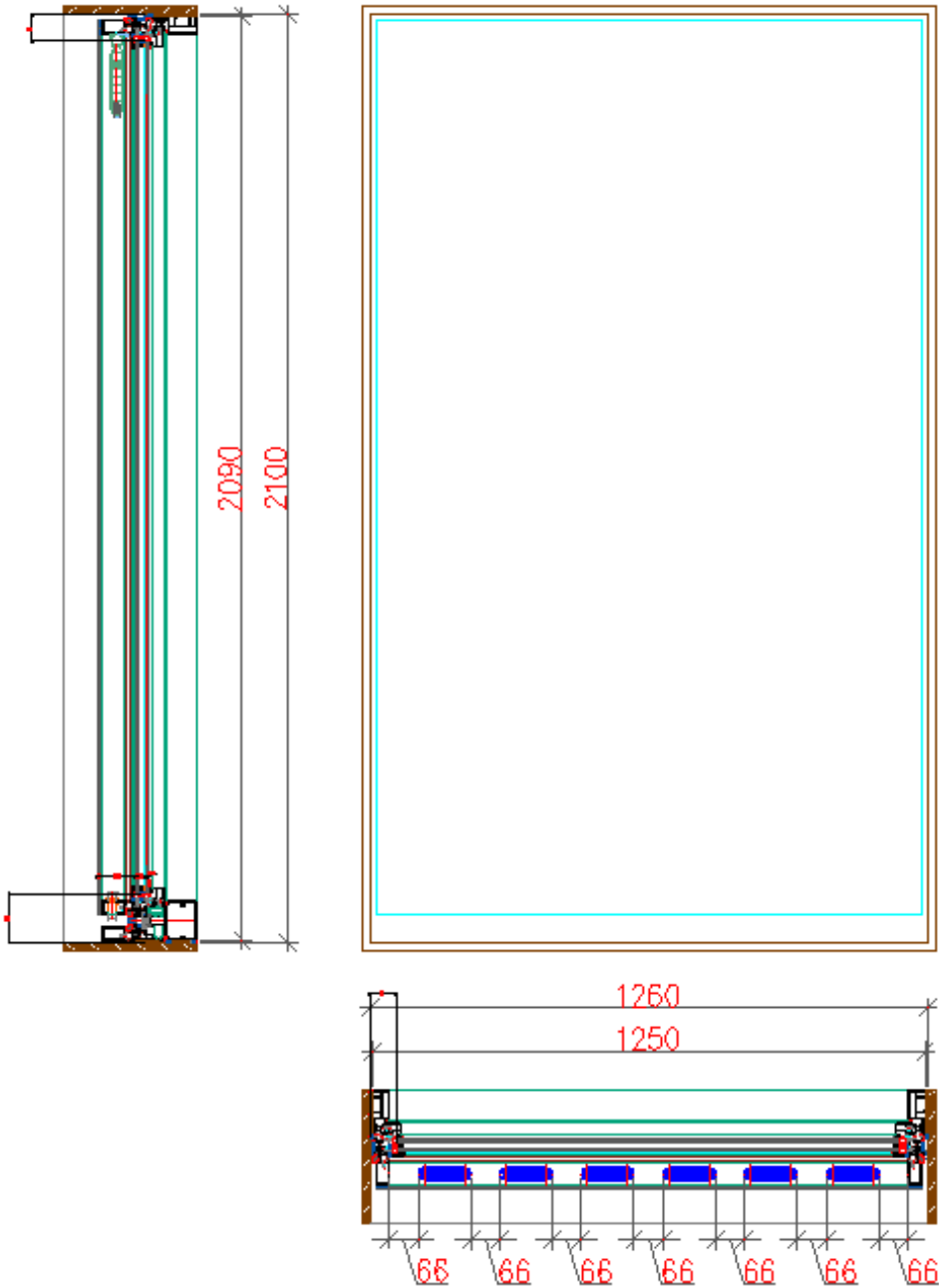


Figure 7. 2 General view of “Constituted Façade Respirante” test mock-up after CFD analysis.

2.) Frame Details of closed cavity façade system is shown in Figure 7.3, Figure 7.4 and Figure 7.5.

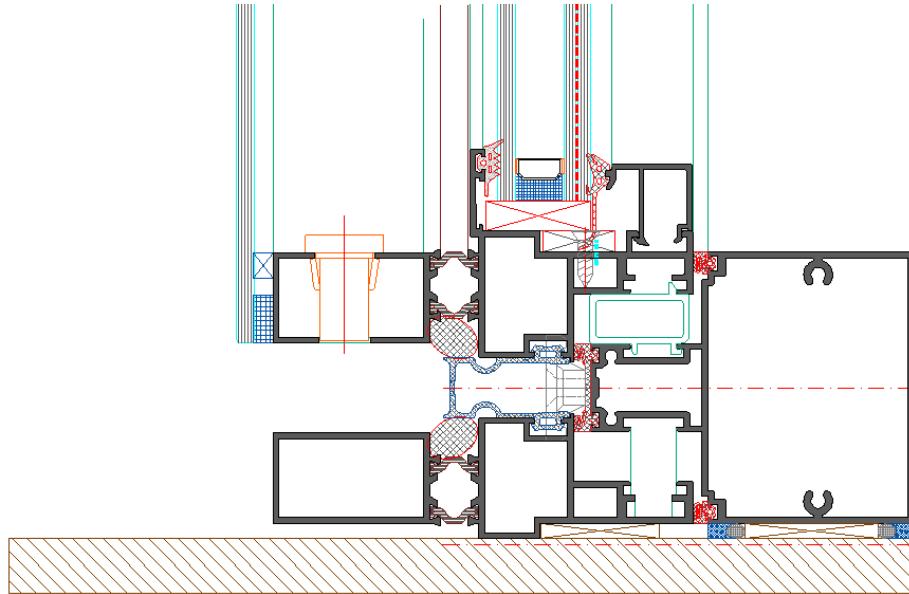


Figure 7. 3 Horizontal frame-1 (Bottom).

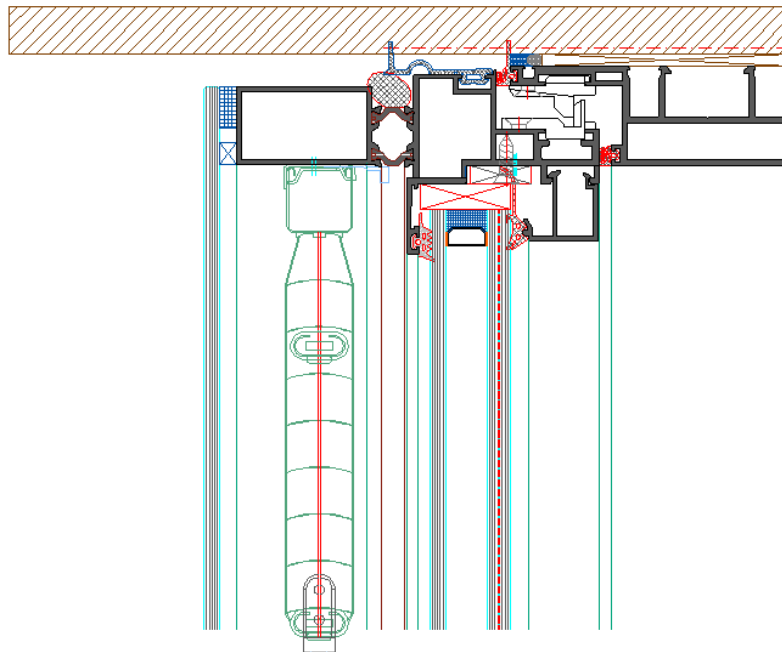


Figure 7. 4 Horizontal frame-2 (Top).

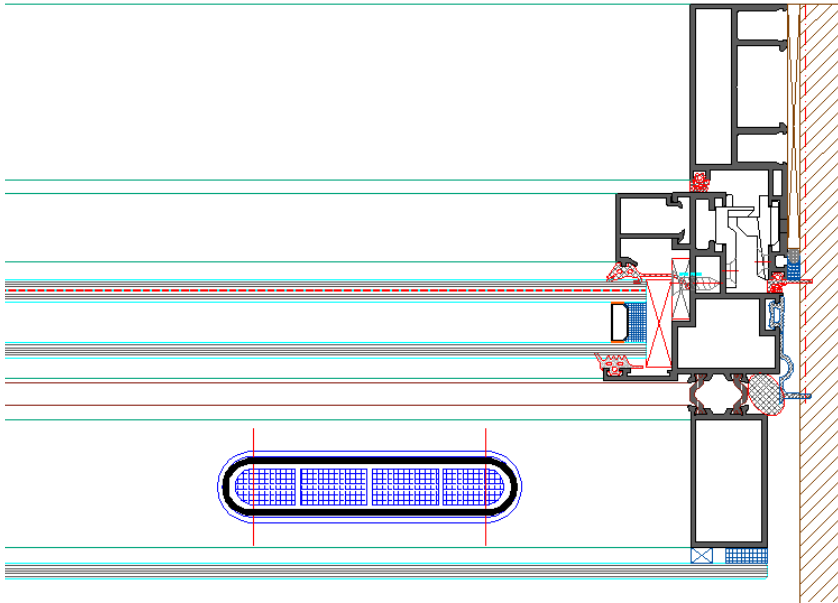


Figure 7. 5 Vertical frame.

7.1.5 Condensation risk assessment

Condensation risk assessment of the closed cavity façade frames are modelled in Bisco 2D steady state heat transfer analysis program.

7.1.5.1 Determination of interior glass air gap thermal conductivity

Determination to glass air gap conductivity is shown below in this façade system.

Table 7. 3 Calculation of thermal conductivity of glass air gap

Double glass air gap properties				
Glass U value	1.1		W/m²K	6 / 16 / 4.4.2
Resistance	0.909		m ² K/W	
Elements	Number	d (mm)	lambda(W/mK)	R
Exterior glass	1	6	1	0.006
Interior glass	2	4	1	0.008
Pvb	2	0.38	0.2	0.0038
			Resistance R _i	0.13
			Resistance R _d	0.04
			Total R =	0.1878
Air gap thickness (mm)				16
Thermal conductivity (W/mK)			□ cavity = d / (Rg - R) =	0.022

Thermal conductivity of inner glass air gap is determined as 0.022 W/mK as it is shown above.

7.1.5.2 Horizontal profile -1 (Bottom)

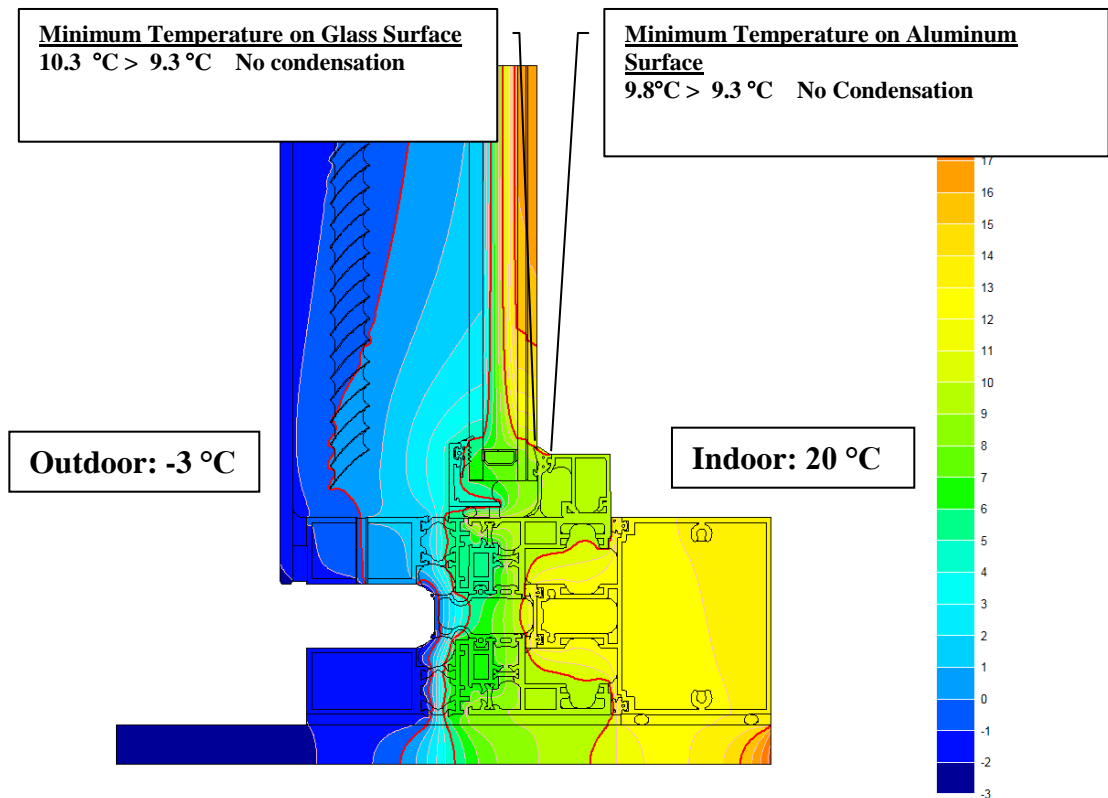


Figure 7. 6 Temperature distribution on the detail with isothermal lines (Red).

If there is 20°C and 50% relative humidity at indoor conditions, corresponded dew point is 9,3 °C according to August Magnus approach which is shown at section 5.3.5. Minimum temperature on aluminium surface is 9.8°C which is greater than 9.3°C. Therefore, there is no condensation on aluminium surface (Figure 7.6).

If there is 20°C and 50% relative humidity at indoor conditions, corresponded dew point is 9,3 °C. Minimum temperature on glass surface is 10.3 °C which is greater than 9.3°C (dew point). Therefore, there is no condensation on glass surface (Figure 7.6).

7.1.5.3 Horizontal profile -2 (Top)

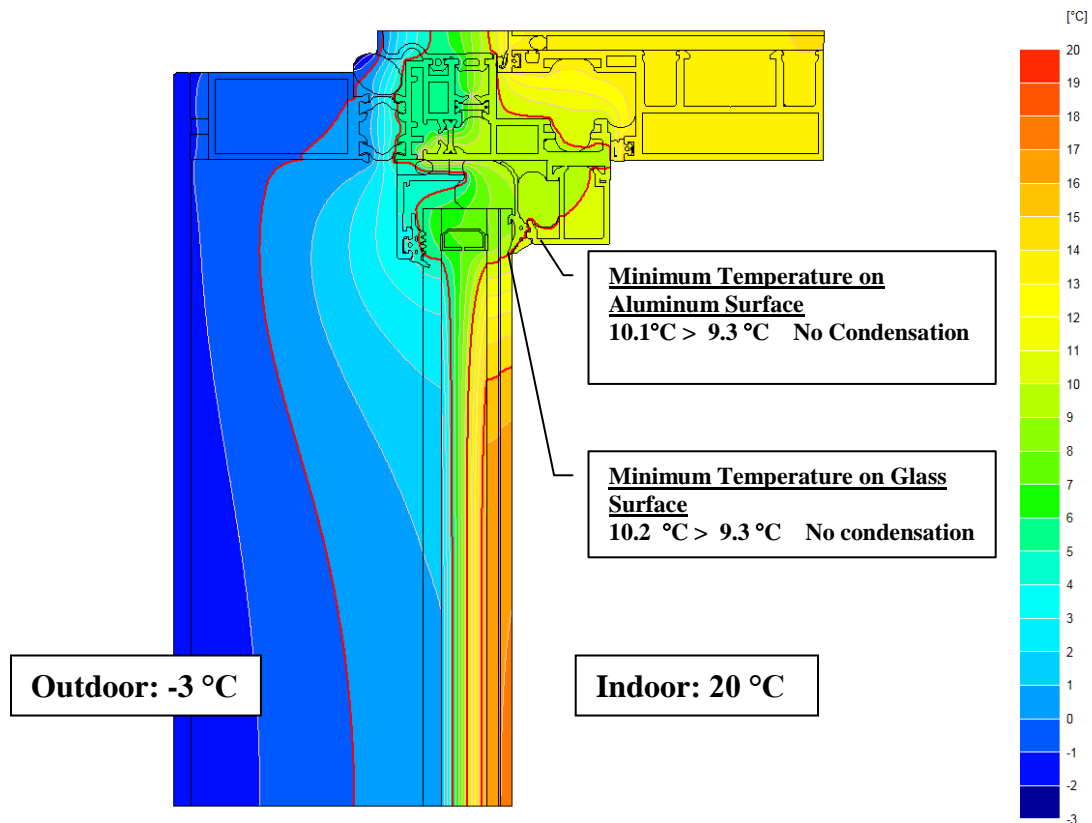


Figure 7.7 Temperature distribution on the detail with isothermal lines (Red).

If there is 20 °C and 50% relative humidity at indoor conditions, corresponded dew point is 9,3 °C according to August Magnus approach which is shown at section 5.3.5. Minimum temperature on aluminium surface is 10.1 °C which is greater than 9.3 °C. Therefore, there is no condensation on aluminium surface. (Figure 7.7)

If there is 20 °C and 50% relative humidity at indoor conditions, corresponded dew point is 9,3 °C. Minimum temperature on glass surface is 10.2 °C which is greater than 9.3 °C (dew point). Therefore, there is no condensation on glass surface. (Figure 7.7)

7.1.5.4 Vertical profile

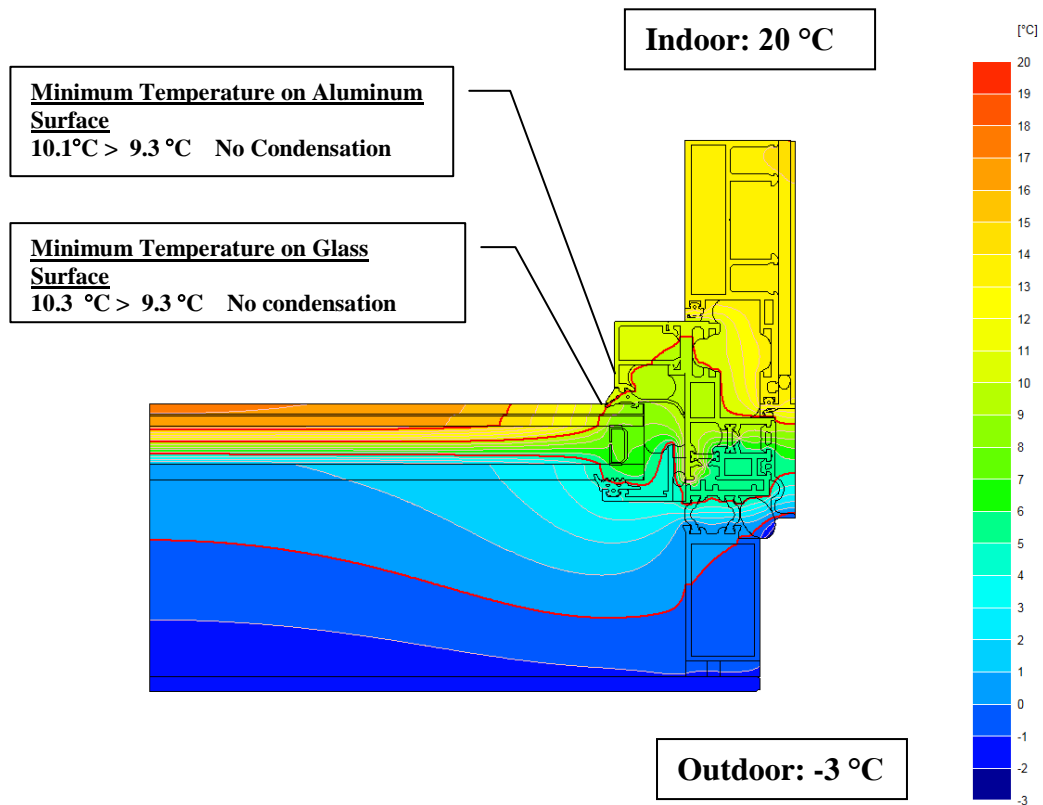


Figure 7. 8 Temperature distribution on the detail with isothermal lines (Red).

If there is 20°C and 50% relative humidity at indoor conditions, corresponded dew point is 9,3 °C according to August Magnus approach which is shown at section 5.3.5. Minimum temperature on aluminum surface is 10.1°C which is greater than 9.3°C. Therefore, there is no condensation on aluminum surface. (Figure 7.8)

If there is 20°C and 50% relative humidity at indoor conditions, corresponded dew point is 9,3 °C. Minimum temperature on glass surface is 10.3 °C which is greater than 9.3°C (dew point). Therefore, there is no condensation on glass surface. (Figure 7.8)

7.1.6 Determination of U_w value

This section presents global thermal transmission calculation (U_{window}) through façade.

The equations below shows how to calculate thermal transmission values (U values) basically in brief.

$$R = \frac{d}{\lambda_h} \quad (7.1)$$

$$\frac{1}{U} = R_i + R + R_e \quad (7.2)$$

$$U = \frac{1}{R_i + R + R_e} \quad (7.3)$$

R: Thermal Resistance ($\text{m}^2 \cdot \text{K}/\text{W}$),

d: Thickness of frame component (m),

λ_h : Thermal conductivity ($\text{W}/\text{m} \cdot \text{K}$)

1/U: Total thermal resistance ($\text{m}^2 \cdot \text{K}/\text{W}$),

R_i : Thermal resistance of interior surface ($\text{m}^2 \cdot \text{K}/\text{W}$),

R_e : Thermal resistance of exterior surface ($\text{m}^2 \cdot \text{K}/\text{W}$)

U: Thermal transmittance ($\text{W}/\text{m}^2 \cdot \text{K}$)'dır [17].

7.1.6.1 U_g of glazing combination

U_g value of glazing combination is determined by means of Vitrage Decision program. Input data and output data are demonstrated in Figure 7.9.

Dimensions: 1260 mm x 2100 mm

Glazing Combination: Clear Float Glass 6 mm + 81 mm Respired Cavity Gap including blind) + Clear Float Glass 6 mm + Sun-Guard HS Superneutral 70 (low-e layer) + 16 mm Cavity (90% Argon) + Clear Laminated Glass 8mm 44.2 8

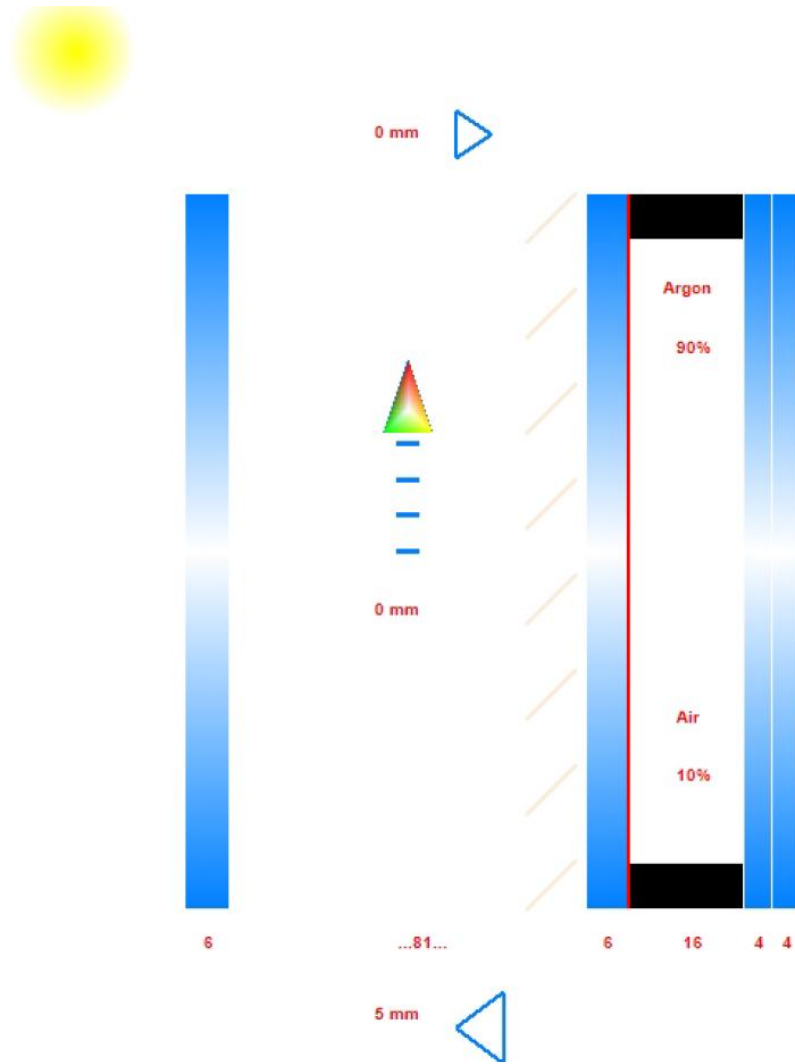


Figure 7. 9 Glazing combinations of Façade Respirante.

Technical features of glazing combinations is illustrated at Figure 7.10.

Final U value of glazing combination was found as **0.79 W/m²K** and final solar factor of glazing combination is found as **0.39** according to EN 410:2011.

Compositions

Number of panes: 3

Pane 1: **GUARDIAN - Clear Float - (Util)**

Composition: Monolithic Thickness: 6 mm

Gas gap 1: Thickness: 81 mm

Ventilated air gap in natural ventilation from indoors to outdoors

Dimensions of peripheral gaps: High: 0mm Low: 5mm Lateral: 0 mm

Pane 2: **GUARDIAN - Sun-Guard HS Superneutral 70 - (Util)**

Composition: Monolithic Thickness: 6 mm

Gas gap 2: Thickness: 16 mm

Mixed gas gap with 90% Argon 0% Krypton 0% Xenon and 10% Air

Pane 3: **GUARDIAN - Clear Lami 8mm 44.2 - (VD)**

Composition: laminated glass Thickness: 8 mm

Total glazing thickness: 117 mm

	Solar characteristics							Light characteristics				
	Te(%)	Re1(%)	Ab1(%)	Emn1(%)	Re2(%)	Ab2(%)	Emn2(%)	Tl(%)	Rl1(%)	Ab1(%)	Rl2(%)	Ab2(%)
Pane 1	82	7	11	89	7	11	89	89	8	3	8	3
Pane 2	43	31	26	89	39	18	3	77	6	17	4	19
Pane 3	74	7	19	89	7	19	89	88	8	4	8	4

Solar and light characteristics of the slats:

	Solar characteristics							Light characteristics				
	Te(%)	Re1(%)	Ab1(%)	Emn1(%)	Re2(%)	Ab2(%)	Emn2(%)	Tl(%)	Rl1(%)	Ab1(%)	Rl2(%)	Ab2(%)
	0	80	20	90	80	20	90	0	80	20	80	20

Solar and light characteristics of the venetian blind:

	Solar characteristics							Light characteristics				
	Te(%)	Re1(%)	Ab1(%)	Emn1(%)	Re2(%)	Ab2(%)	Emn2(%)	Tl(%)	Rl1(%)	Ab1(%)	Rl2(%)	Ab2(%)
Blind	16	59	25	90	59	25	90	16	59	25	59	25

Solar characteristics

Glazing (EN 410: 2011)

Solar global characteristics:

Transmittance: 0,27

Reflectance: 0,29

Absorption: 0,43

Effective absorption - Pane 1: 0,1398

Effective absorption - Pane 2: 0,2228

Effective absorption - Pane 3: 0,0705

Light characteristics

Glazing (EN 410: 2011)

Light global characteristics:

Transmittance: 0,61

Reflectance: 0,17

Absorption: 0,22

Glazing solar factor

Solar factor (EN 410: 2011): 0,39

Figure 7. 10 Technical features of glazing combinations.

7.1.6.2 Horizontal profile-1 (Bottom)

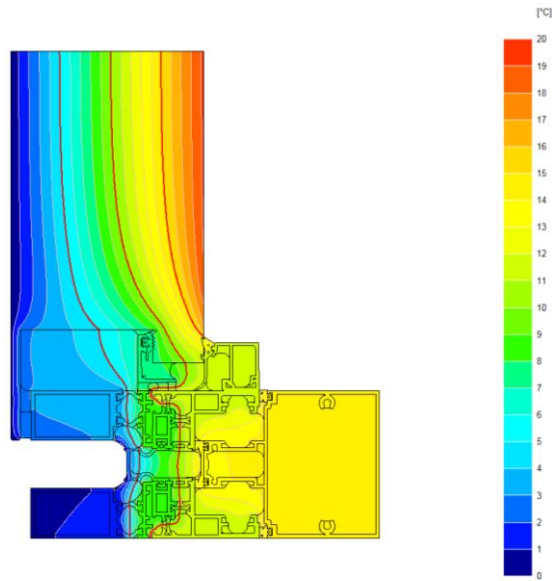


Figure 7. 11 Temperature distribution on detail with isothermal lines (Red).

BISCO Calculation Results

BISCO data file: MY FR alt detay U Value v2 .bsc

Number of nodes = 44998
 Heat flow divergence for total object = 7.38516e-005
 Heat flow divergence for worst node = 0.0255748

Col.	Type	Name	Tmin [°C]	Tmax [°C]	Ta [°C]	flow in [W/m]	flow out [W/m]
28	MATERIAL	insulation	0.18	19.25			
44	MATERIAL	polyamid reinf.	1.06	11.63			
60	MATERIAL	EPDM	0.89	14.31			
62	MATERIAL	silicone	1.75	11.49			
63	MATERIAL	Backing Rod	0.53	11.41			
170	BC_SIMPL	exterior	0.18	3.08		0.00	9.77
174	BC_SIMPL	interior (norma	13.52	19.25		4.70	0.00
182	BC_SIMPL	interior (reduc	11.82	18.46		5.06	0.00
192	EQUIMAT		2.70	8.10			

Thermal transmittance of frame (EN ISO 10077-2)

$$U_f = (Q/(T_i - T_e) - U_{p1} * w_{p1} - U_{p2} * w_{p2}) / w_f = 3.543 \text{ W/(m}^2 \cdot \text{K)}$$

$$Q = 9.768 \text{ W/m}$$

$$t_i = 20.00^\circ\text{C}$$

$$t_e = 0.00^\circ\text{C}$$

$$U_{p1} = 0.283 \text{ W/(m}^2 \cdot \text{K)} \text{ (top edge of bitmap)}$$

$$w_{p1} = 0.1726 \text{ m (distance no. 2)}$$

$$U_{p2} = 0.000 \text{ W/(m}^2 \cdot \text{K)}$$

$$w_{p2} = 0.0000 \text{ m}$$

$$w_f = 0.1240 \text{ m (distance no. 1)}$$

$$\text{Result: } U_f = \left(\frac{Q}{(T_i - T_e)} - U_{p1} \cdot w_{p1} \right) / w_f = 3.54 \text{ W/(m}^2 \cdot \text{K)} \quad (7.4)$$

7.1.6.3 Horizontal profile-2 (Top)

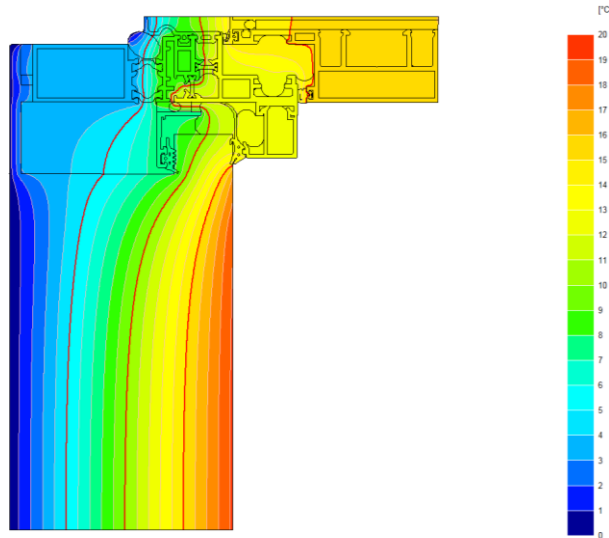


Figure 7. 12 Temperature distribution on detail with isothermal lines (Red)

BISCO Calculation Results

BISCO data file: Transom 2 U Value .bsc

Number of nodes = 42761
 Heat flow divergence for total object = 1.82972e-005
 Heat flow divergence for worst node = 0.0274799

Col.	Type	Name	Tmin [°C]	Tmax [°C]	Ta [°C]	flow in [W/m]	flow out [W/m]
8	MATERIAL	aluminium	3.15	15.34			
12	MATERIAL	hardwood	14.87	16.08			
28	MATERIAL	insulation	0.19	19.25			
44	MATERIAL	polyamid reinf.	3.39	12.23			
60	MATERIAL	EPDM	2.07	15.14			
62	MATERIAL	silicone	1.86	14.93			
63	MATERIAL	Backer Rod	0.50	14.93			
170	BC_SIMPL	exterior	0.19	3.31		0.00	7.35
174	BC_SIMPL	interior (norma	15.31	19.25		2.63	0.00
182	BC_SIMPL	interior (reduc	12.41	18.48		4.72	0.00
192	EQUIMAT		3.02	14.44			

Thermal transmittance of frame (EN ISO 10077-2)

$$U_f = (Q / (T_i - T_e) - U_{p1} * w_{p1} - U_{p2} * w_{p2}) / w_f = 3.976 \text{ W}/(\text{m}^2 \cdot \text{K})$$

$$Q = 7.352 \text{ W/m}$$

$$t_i = 20.00^\circ\text{C}$$

$$t_e = 0.00^\circ\text{C}$$

$$U_{p1} = 0.284 \text{ W}/(\text{m}^2 \cdot \text{K}) \text{ (bottom edge of bitmap)}$$

$$w_{p1} = 0.1895 \text{ m (distance no. 2)}$$

$$U_{p2} = 0.000 \text{ W}/(\text{m}^2 \cdot \text{K})$$

$$w_{p2} = 0.0000 \text{ m}$$

$$w_f = 0.0789 \text{ m (distance no. 1)}$$

Result:
$$U_f = \left(\frac{Q}{(T_i - T_e)} - U_p \cdot w_p \right) / w_f = 3.98 \text{ W}/(\text{m}^2 \cdot \text{K})$$

7.1.6.4 Vertical profile

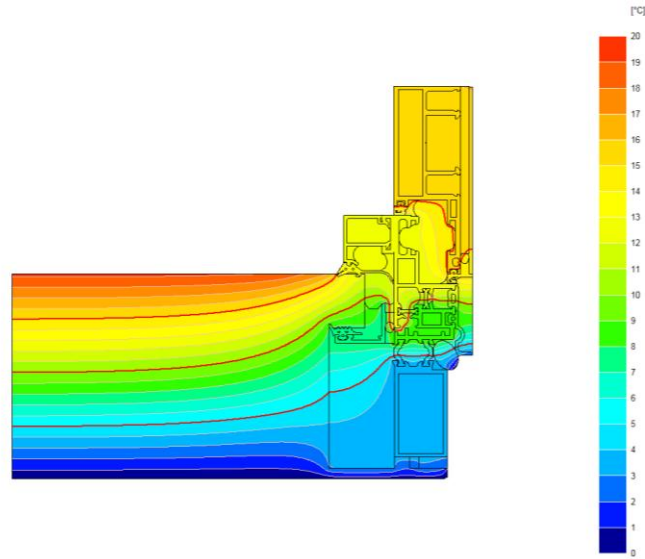


Figure 7.13 Temperature distribution on detail with isothermal lines (Red).

BISCO Calculation Results

BISCO data file: Mullion U Value r1 .bsc

Number of nodes = 41869
 Heat flow divergence for total object = 9.52415e-007
 Heat flow divergence for worst node = 0.0570153

Col.	Type	Name	Tmin [°C]	Tmax [°C]	Ta [°C]	flow in [W/m]	flow out [W/m]
8	MATERIAL	aluminium	3.16	15.44			
12	MATERIAL	hardwood	14.97	16.23			
28	MATERIAL	insulation	0.19	19.25			
44	MATERIAL	polyamid r.	3.40	12.26			
60	MATERIAL	EPDM	2.46	15.24			
62	MATERIAL	silicone	1.87	15.04			
63	MATERIAL	Backer Rod	0.50	15.04			
170	BC_SIMPL	exterior	0.19	3.32	0.00	7.27	
174	BC_SIMPL	interior (norma	14.17	19.25	2.64	0.00	
182	BC_SIMPL	interior (reduc	12.44	18.49	4.63	0.00	
192	EQUIMAT		14.53	16.19			

Thermal transmittance of frame (EN ISO 10077-2)

$U_f = (Q / (T_i - T_e) - U_{p1} * w_{p1} - U_{p2} * w_{p2}) / w_f = 3.939 \text{ W}/(\text{m}^2 \cdot \text{K})$
 $Q = 7.268 \text{ W}/\text{m}$
 $t_i = 20.00^\circ\text{C}$
 $t_e = 0.00^\circ\text{C}$
 $U_{p1} = 0.284 \text{ W}/(\text{m}^2 \cdot \text{K})$ (left edge of bitmap)
 $w_{p1} = 0.1845 \text{ m}$ (distance no. 2)
 $U_{p2} = 0.000 \text{ W}/(\text{m}^2 \cdot \text{K})$
 $w_{p2} = 0.0000 \text{ m}$
 $w_f = 0.0789 \text{ m}$ (distance no. 1)

Result: $U_f = \left(\frac{Q}{(T_i - T_e)} - U_p \cdot w_p \right) / w_f = 3.94 \text{ W}/(\text{m}^2 \cdot \text{K})$

Temperature distribution of all details are shown in Figure 7.11, Figure 7.12 and Figure 7.13.

7.1.6.5 Global U_w value

General view of closed cavity mock up is demonstrated below including all frames. Global U_w value is determined in accordance with EN 10077-1 Component Assessment Method.

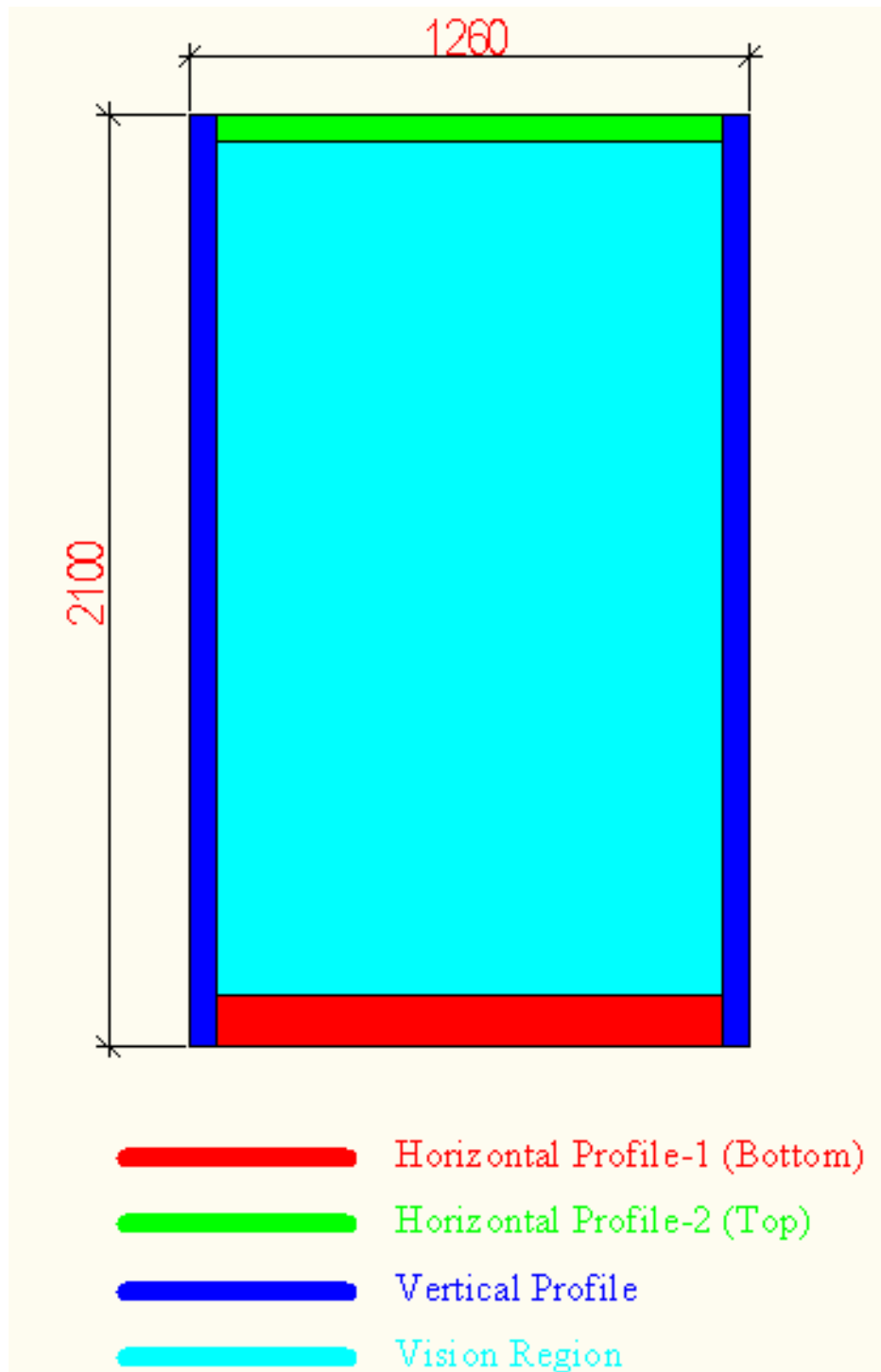


Figure 7. 14 Closed Cavity Façade mock-up distribution of system components.

The component assessment method is based on below formula.

$$U_w = \frac{U_g A_g + U_f A_f + U_s A_s + \psi L}{A} \quad (7.5)$$

- U_w : Thermal transmittance of the window modulus, in (W/m²K)
 U_g : Thermal transmittance of the glazing section, in (W/m²K)
 A_g : Area of glazing (m²)
 U_f : Thermal transmittance of the frame section, in (W/m²K)
 A_f : Area of frame (m²)
 U_s : Thermal transmittance of the spandrel section, in (W/m²K)
 A_s : Area of spandrel zone (m²)
 Ψ : Linear thermal transmittance W/(m.K)
 A : Area (m²) [20].

Determination of U value of closed cavity façade:

U value of closed cavity facade

Width	1,260	m
Height	2,100	m
A total	2,646	m ²

Frames

$U_{f1} =$	3,543	W/m ² K	$A_{f1} =$	0,128	m ²
$U_{f2} =$	3,976	W/m ² K	$A_{f2} =$	0,068	m ²
$U_{f3} =$	3,939	W/m ² K	$A_{f3} =$	0,252	m ²
			$\Sigma U_f A_f =$	1,717	W/K

Glass

$U_{g1} =$	0,79	W/m ² K	$A_{g1} =$	2,198	m ²
			$\Sigma U_g A_g =$	1,736	W/K

Spandrel

$U_{s1} =$	0,00	W/m ² K	$A_{s1} =$	0	m ²
			$\Sigma U_s A_s =$	0,000	W/K

Spacer

	Aluminium				
$L =$	6,136	m	$\psi =$	0,11	W/mK

U_{window} value

$U_w =$	1,56	W/m²K
---------	-------------	-------------------------

Global thermal transmittance value (U_{window}) of configured façade is determined as 1.56 W/m²K.

7.2 Energy Performance

According to TS 825, maximum U value in all regions in Turkey is supposed to be not more than **2.40 W/m²K**. [27] Global thermal transmittance value (U_{window}) is determined as **1.56 W/m²K** which is shown section 7.1.6.5 previous section Energy performance of constituted closed cavity façade is compared with this U value 2,4 W/m²K in all specified regions by considering solar radiation. The calculation is based on unit window area.

The calculation below covers thermal transmittance through windows by means of solar radiation and temperature difference with respect to all directions in cooling season and heating season.

7.2.1 Thermal transmittance through conduction and convection

Initial conditions and boundary conditions are defined in accordance with TS 825 standard. There are four different regions in Turkey in terms of temperature variation throughout a year. Indoor temperature is assumed as 19 °C for heating load calculations. [17] Indoor temperature is assumed as 23 °C for cooling load calculations. [26] Heat flow through window is calculated by using temperature difference and U value of both system as shown below.

$$q=U. (\theta_i - \theta_e) \quad (7.6)$$

q: heat flow rate (W/m²)

U: Thermal Transmittance value

θ_i : Indoor temperature

θ_e : Outdoor temperature

First comparison study is done without considering solar radiation. Monthly average ambient air temperatures [17] shows in average temperature of each month with respect to different regions in Turkey from average temperature variation aspect.

Table 7.4

Table 7. 4 Monthly average ambient air temperatures [17].

	1. Region (°C)	2. Region (°C)	3. Region (°C)	4. Region (°C)
January	8.4	2.9	-0.3	-5.4
February	9.0	4.4	0.1	-4.7
March	11.6	7.3	4.1	0.3
April	15.8	12.8	10.1	7.9
May	21.2	18.0	14.4	12.8
June	26.3	22.5	18.5	17.3
July	28.7	24.9	21.7	21.4
August	27.6	24.3	21.2	21.1
September	23.5	19.9	17.2	16.5
October	18.5	14.1	11.6	10.3
November	13.0	8.5	5.6	3.1
December	9.3	3.8	1.3	-2.8

Heat transfer (W/m^2) through constituted closed cavity façade and reference window with respect to months in all regions is shown in Table 7.5 and Table 7.6. Indoor set temperature is assumed as $19\text{ }^\circ\text{C}$ in heating period and $23\text{ }^\circ\text{C}$ in cooling period. Heat flow rate is not considered when outdoor temperature is between $19\text{ }^\circ\text{C}$ and $23\text{ }^\circ\text{C}$ in this calculation.

Table 7. 5 Heat flow through closed cavity façade (W/m^2).

	1. Region (W/m^2)	2. Region (W/m^2)	3. Region (W/m^2)	4. Region (W/m^2)
January	16.5	25.1	30.1	38.1
February	15.6	22.8	29.5	37.0
March	11.5	18.3	23.2	29.2
April	5.0	9.7	13.9	17.3
May	-	1.6	7.2	9.7
June	5.1	-	0.8	2.7
July	8.9	3.0	-	-
August	7.2	2.0	-	-
September	0.8	-	2.8	3.9
October	0.8	7.6	11.5	13.6
November	9.4	16.4	20.9	24.8
December	15.1	23.7	27.6	34.0

Table 7. 6 Heat flow through reference window (W/m²).

	1. Region (W/m²)	2. Region (W/m²)	3. Region (W/m²)	4. Region (W/m²)
January	25.4	38.6	46.3	58.6
February	24.0	35.0	45.4	56.9
March	17.8	28.1	35.8	44.9
April	7.7	14.9	21.4	26.6
May	-	2.4	11.0	14.9
June	7.9	-	1.2	4.1
July	13.7	4.6	-	-
August	11.0	3.1	-	-
September	1.2	-	4.3	6.0
October	1.2	11.8	17.8	20.9
November	14.4	25.2	32.2	38.2
December	23.3	36.5	42.5	52.3

Highest heat transfer rate difference is 4.8 W/m² in cooling season and 20.5 W/m² in heating season respectively. Highest difference in density of cooling energy consumption is calculated as 1.040 (kWh/m²) in first region in July and highest difference in density of cooling energy consumption is calculated as 4.442 (kWh/m²) in fourth region in January with 50 hours weekly occupancy in office environment assumption.

7.2.2 Solar heat gain calculation

Monthly average solar heat gain is calculated with equation 7.7 according to TS 825 standard.

$$(\varphi_{s,month}) = \sum r_{i,month} \times g_{i,month} \times I_{i,month} \times A_i \quad (7.7)$$

$r_{i,month}$: monthly average shading factor of transparent surfaces in “i” direction

$g_{i,month}$: monthly average solar factor (SHGC) of transparent surfaces in “i” direction

$I_{i,month}$: monthly average solar radiation intensity of vertical surfaces in “i” direction (W/m²)

A_i : Total window area in “i” direction (m²)

Area of the window is taken into account as unit area (1 m²).

Monthly average shading factor of transparent surface ($r_{i,month}$) value is taken into account as 0.5 which is defined for the environment of 10 or higher storey buildings for closed cavity façade and reference window calculation.

Monthly average solar factor (SHGC) value of closed cavity façade is calculated by means of “Vitrag Decision” program which is shown at section 7.1.6.1. Glass combination of reference window is taken from section A.4 of TS 825. It is the features of the combination which has $2.4 \text{ W/m}^2\text{K}$ U value. Monthly average solar factor (SHGC) value for reference window is calculated by means of Guardian Glass Configurator program. Program output is illustrated at Figure 7.15.

Monthly average solar radiation intensity ($I_{i,month}$) values are obtained from Appendix C in TS 825 for all climatic regions which is shown at Table 7.7.

Monthly average solar heat gain is calculated by considering all directions separately in Table 7.8.

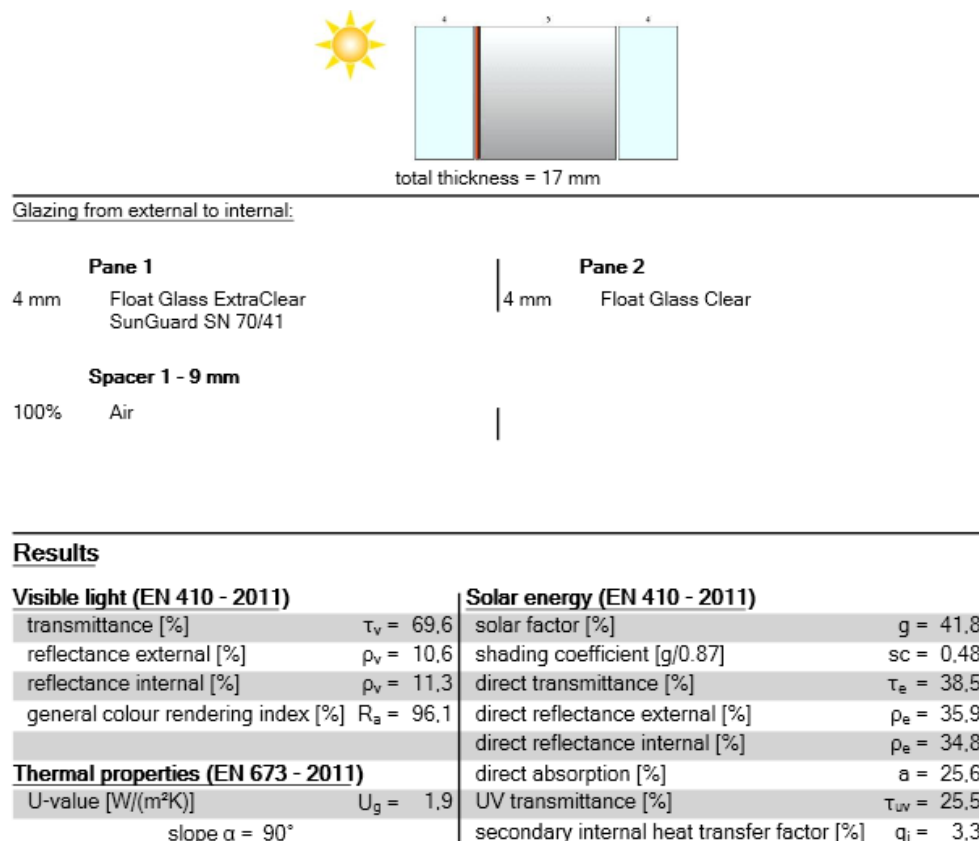


Figure 7. 15 Thermal and light characteristics of reference window.

Table 7. 7 Solar Radiation values from different directions [17].

	Solar Radiation (South) (W/m ²)	Solar Radiation (North) (W/m ²)	Solar Radiation (West- East) (W/m ²)
January	72.0	26.0	43.0
February	84.0	37.0	57.0
March	87.0	52.0	77.0
April	90.0	66.0	90.0
May	92.0	79.0	114.0
June	95.0	83.0	122.0
July	93.0	81.0	118.0
August	93.0	73.0	106.0
September	89.0	57.0	81.0
October	82.0	40.0	59.0
November	67.0	27.0	41.0
December	64.0	22.0	37.0

Table 7. 8 Solar Radiation values for CCF and Reference window with respect to solar directions.

	SOUTH		NORTH		WEST-EAST	
	$I_{(CCF)}$ (W/m ²)	$I_{(RW)}$ (W/m ²)	$I_{(CCF)}$ (W/m ²)	$I_{(RW)}$ (W/m ²)	$I_{(CCF)}$ (W/m ²)	$I_{(RW)}$ (W/m ²)
January	14.0	15.0	5.1	5.4	8.4	5.6
February	16.4	17.6	7.2	7.7	11.1	7.4
March	17.0	18.2	10.1	10.9	15.0	10.0
April	17.6	18.8	12.9	13.8	17.6	11.7
May	17.9	19.2	15.4	16.5	22.2	14.8
June	18.5	19.9	16.2	17.3	23.8	15.9
July	18.1	19.4	15.8	16.9	23.0	15.3
August	18.1	19.4	14.2	15.3	20.7	13.8
September	17.4	18.6	11.1	11.9	15.8	10.5
October	16.0	17.1	7.8	8.4	11.5	7.7
November	13.1	14.0	5.3	5.6	8.0	5.3
December	12.5	13.4	4.3	4.6	7.2	4.8

7.2.3 Cooling load comparison considering solar radiation

Heat flow to indoor and solar heat gain through window is considered for the calculation of cooling load in cooling season with respect to climatic regions in Turkey for all directions. If monthly mean temperature value is higher than assumed indoor temperature (23°C), specified months are defined as cooling season in this section.

7.2.3.1 South direction

Total heat flow to indoor and solar heat gain from south direction through constituted closed cavity façade and reference window in cooling season is indicated in Table 7.9 and Table 7.10 separately.

Table 7.9 Total heat flow and solar heat gain from south through closed cavity façade.

	1. Region (W/m ²)	2. Region (W/m ²)	3. Region (W/m ²)	4. Region (W/m ²)
April				
May				
June	23.7			
July	27.0	21.1		
August	25.3	20.2		
September	18.1			
October				
Total	94.1	41.3	-	-

The highest monthly heat transfer rate difference between closed cavity façade (CCF) and reference window (RW) in cooling season is 6.1 W/m² in first region in July. Highest difference in density of monthly cooling energy consumption between closed cavity façade (CCF) and reference window (RW) is 1.321 kWh/m² in first region in July. Annual difference is highest in first region with total 17 W/m² heat transfer rate and with total 14.7 kWh/m² saving amount with 50 hours weekly occupancy assumption in office environment in specified months.

Table 7. 10 Total heat flow and solar heat gain from south through reference window.

	1. Region (W/m ²)	2. Region (W/m ²)	3. Region (W/m ²)	4. Region (W/m ²)
April				
May				
June	27.8			
July	33.1	24.0		
August	30.5	22.6		
September	19.8			
October				
Total	111.2	46.6	-	-

7.2.3.2 North direction

Total heat flow to indoor and solar heat gain from north direction through constituted closed cavity façade and reference window in cooling season is indicated in Table 7.11 and Table 7.12 separately.

Table 7. 11 Total heat flow and solar heat gain from north through closed cavity façade.

	1. Region (W/m ²)	2. Region (W/m ²)	3. Region (W/m ²)	4. Region (W/m ²)
April				
May				
June	21.3			
July	24.7	18.8		
August	21.4	16.3		
September	11.9			
October				
Total	79.3	35.0	-	-

The highest monthly heat flow difference between closed cavity façade (CCF) and reference window (RW) in cooling season is 5.9 W/m² in first region in July. Highest difference in density of monthly cooling energy consumption between closed cavity façade (CCF) and reference window (RW) is 1.279 kWh/m² in first region in July. Annual difference is highest in first region with total 16 W/m² heat flow difference and with total 13.869 kWh/m² saving amount with 50 hours weekly occupancy assumption in office environment in specified months.

Table 7. 12 Total heat flow and solar heat gain from north through reference window.

	1. Region (W/m²)	2. Region (W/m²)	3. Region (W/m²)	4. Region (W/m²)
April				
May	-			
June	25.3	-		
July	30.6	21.5	-	-
August	26.3	18.4	-	-
September	13.1	-		
October				
Total	95.3	39.9	-	-

7.2.3.3 West / East direction

Total heat flow to indoor and solar heat gain from east and west direction through constituted closed cavity façade and reference window in cooling season is indicated in Table 7.13 and Table 7.14 separately.

Table 7. 13 Total heat flow and solar heat gain from east and west through closed cavity façade.

	1. Region (W/m²)	2. Region (W/m²)	3. Region (W/m²)	4. Region (W/m²)
April				
May	-			
June	28.9	-		
July	31.9	26.0	-	-
August	27.8	22.7	-	-
September	16.6	-		
October				
Total	105.3	48.7	-	-

Table 7. 14 Total heat flow and solar heat gain from east and west through reference window.

	1. Region (W/m ²)	2. Region (W/m ²)	3. Region (W/m ²)	4. Region (W/m ²)
April				
May				
June	33.4			
July	38.3	29.2		
August	33.2	25.3		
September	18.1			
October				
Total	190.6	54.5	-	-

The highest monthly heat flow difference between closed cavity façade (CCF) and reference window (RW) in cooling season is 6.4 W/m² in first region in July. Highest difference in density of monthly cooling energy consumption between closed cavity façade (CCF) and reference window (RW) is 1.387 kWh/m² in first region in July. Annual difference is highest in first region with total 17.8 W/m² heat flow difference and with total 13.429 kWh/m² saving amount with 50 hours weekly occupancy assumption in office environment in specified months.

Cooling load section indicates that highest saving is possible application of this kind of façade to first region on east or west direction.

7.2.4 Heating load considering solar radiation

Heat flow to outdoor and solar heat gain through window is considered together for the calculation of heating load in heating season with respect to climatic regions in Turkey for all directions. If monthly mean temperature value is lower than assumed indoor temperature, specified months are defined as heating season in this section. If total heat flow and solar heat gain together is less than zero in total, related month is not assigned as heating month.

7.2.4.1 South direction

Total heat flow to outdoor and solar heat gain from south direction through constituted closed cavity façade and reference window in heating season is indicated in Table 7.15 and Table 7.16 separately.

Table 7. 15 Total heat flow and solar heat gain from south through closed cavity façade.

	1. Region (W/m ²)	2. Region (W/m ²)	3. Region (W/m ²)	4. Region (W/m ²)
January	2.5	11.1	16.1	24.0
February		6.4	13.1	20.6
March		1.3	6.3	12.2
April				
May				
June				
July				
August				
September				
October				
November		3.3	7.8	11.7
December	2.7	11.2	15.1	21.5

Table 7. 16 Total heat flow and solar heat gain from south through reference window.

	1. Region (W/m ²)	2. Region (W/m ²)	3. Region (W/m ²)	4. Region (W/m ²)
January	10.4	23.6	31.3	43.5
February	6.4	17.5	27.8	39.3
March		9.9	17.6	26.7
April			2.6	7.8
May				
June				
July				
August				
September				
October			0.6	3.7
November	0.4	11.2	18.2	24.2
December	9.9	23.1	29.1	38.9

The highest monthly heat transfer difference between closed cavity façade (CCF) and reference window (RW) in heating season is 19.5 W/m² in fourth region in January. Highest difference in density of monthly heating energy consumption between closed cavity façade (CCF) and reference window (RW) is 4.226 kWh/m² in fourth region in January. Annual difference is highest in fourth region with total 94.1 W/m² heat

transfer difference and with total 142.740 kWh/m² saving amount with 50 hours weekly occupancy assumption in office environment in specified months.

Annual difference is lowest in first region with total 22,0 W/m² heat transfer difference and with 19.070 kWh/m² saving amount.

7.2.4.2 North direction

Total heat flow to outdoor and solar heat gain from north direction through constituted closed cavity façade and reference window in heating season is indicated in Table 7.17 and Table 7.18 separately.

Table 7. 17 Total heat flow and solar heat gain from north through closed cavity façade.

	1. Region (W/m²)	2. Region (W/m²)	3. Region (W/m²)	4. Region (W/m²)
January	11.5	20.0	25.0	33.0
February	8.4	15.6	22.3	29.8
March	1.4	8.1	13.1	19.0
April			1.0	4.4
May				
June				
July				
August				
September				
October			3.7	5.8
November	4.1	11.1	15.6	19.5
December	10.8	19.4	23.3	29.7

The highest monthly heat transfer difference between closed cavity façade (CCF) and reference window (RW) in heating season is 20.1 W/m² in fourth region in January. Highest difference in density of monthly heating energy consumption between closed cavity façade (CCF) and reference window (RW) is 4.356 kWh/m² in fourth region in January. Annual difference is highest in fourth region with total 100.6 W/m² heat transfer rate difference and with total 152.600 kWh/m² saving amount with 50 hours weekly occupancy assumption in office environment in specified months.

Annual difference is lowest in first region with total 34.4 W/m² heat transfer rate difference and with 37.272 kWh/m² saving amount.

Table 7. 18 Total heat flow and solar heat gain from south through reference window.

	1. Region (W/m ²)	2. Region (W/m ²)	3. Region (W/m ²)	4. Region (W/m ²)
January	20.0	33.2	40.9	53.1
February	16.3	27.3	37.6	49.1
March	6.9	17.2	24.9	34.0
April		1.1	7.6	12.8
May				
June				
July				
August				
September				
October		3.4	9.4	12.5
November	8.8	19.6	26.5	32.5
December	18.7	31.9	37.9	47.7

7.2.4.3 West/east direction

Total heat flow to outdoor and solar heat gain from east and west direction through constituted closed cavity façade and reference window in heating season is indicated in Table 7.19 and Table 7.20 separately.

Table 7. 19 Total heat flow and solar heat gain from east and west through closed cavity façade.

	1. Region (W/m ²)	2. Region (W/m ²)	3. Region (W/m ²)	4. Region (W/m ²)
January	8.2	16.7	21.7	29.7
February	4.5	11.7	18.4	25.9
March		3.2	8.2	14.2
April				
May				
June				
July				
August				
September				
October				2.1
November	1.4	8.4	12.9	16.8
December	7.9	16.5	20.4	26.8

The highest monthly heat transfer rate difference between closed cavity façade (CCF) and reference window (RW) in heating season is 23.6 W/m² in fourth region

in February. The highest difference in density of monthly heating energy consumption between closed cavity façade (CCF) and reference window (RW) is 5.114 kWh/m² in fourth region in February. Annual difference is highest in fourth region with total 130.5 W/m² heat transfer rate difference and with total 226.130 kWh/m² saving amount with 50 hours weekly occupancy assumption in office environment in specified months.

Annual difference is lowest in first region with total 49.8 W/m² heat transfer rate difference and with 53.933 kWh/m² saving amount.

Table 7. 20 Total heat flow and solar heat gain from south through reference window.

	1. Region (W/m²)	2. Region (W/m²)	3. Region (W/m²)	4. Region (W/m²)
January	19.9	33.1	40.7	53.0
February	16.6	27.6	38.0	49.5
March	7.8	18.1	25.8	34.9
April		3.2	9.7	14.9
May				0.1
June				
July				
August				
September				
October		4.1	10.1	13.2
November	9.1	19.9	26.8	32.8
December	18.5	31.7	37.7	47.5

Heating load section indicates that highest saving is possible with the application of CCF to fourth region on east or west direction.

7.2.5 Carbon footprint

Total heating and cooling loads of east and west direction are highest for all regions. Annual total heating and cooling loads of east and west direction are found at Table 7.21. The table indicates that there is up to 130.5 W/m² heat transfer rate difference and 339.352 kWh/m² potential saving by using CCF instead of RW.

Table 7. 21 Annual total heating and cooling load together just because of heat flow and solar radiation.

	1. Region (W/m²)	2. Region (W/m²)	3. Region (W/m²)	4. Region (W/m²)
CCF	127.2	105.2	81.7	115.4
RW	194.8	192.1	188.7	245.9
Saving	67.6	86.9	107.0	130.5

The assumption of heating and air conditioning hours for daily office occupancy is 10 hours and the office is occupied 5 days in a week. There is 52 weeks in total. There is up to 339.3 kWh/m² saving from heating and air conditioning in fourth climatic region in Turkey. It means that highest saving can be determined at fourth region in Turkey.

Annual savings with respect to regions;

Table 7. 22 Annual savings with respect to regions.

	1. Region (kWh/m²)	2. Region (kWh/m²)	3. Region (kWh/m²)	4. Region (kWh/m²)
Annual Saving	175.8	225.9	278.2	339.3

339.3 kWh annual saving for only 1 m² corresponds to 333.7 kg CO₂ emission by lignite burning coal to generate power. [36] It also corresponds to 234 kg CO₂ emission in average of different kind of power generation. This amount of carbon can be sequestered by 6 tree seedlings grown for 10 years. [37] The number for whole building can be obtained by multiplying specified numbers with total window area of applicable buildings.

7.3 Result

Expected U_{cw} value of the closed cavity façade system module is supposed to be less than 2.40 W/m²K according to TS 825 (Turkish Standard). Final U_{cw} value of closed cavity façade system is 1.56 W/m²K, which is quite lower than expected value.

Condensation risk assessment indicates that minimum temperatures on aluminium and glass of horizontal and vertical details are considerably higher than limited value for condensation risk.

Therefore, this constituted closed cavity façade is highly convenient with respect to TS 825, EN 10077-1, EN 10077-2 from thermal performance aspect in terms of condensation risk and U value.

There is monthly up to 1.387 kWh/m² and annually up to 13.429 kWh/m² saving in density of cooling energy consumption by applying CCF system in office building.

There is monthly up to 5.114 kWh/m² and annually up to 226.130 kWh/m² saving in density of heating energy consumption by applying CCF system in office building.

8. CONCLUSION

This study is evaluated in 3 different aspects which are CFD results, lab results and energy performance analysis.

8.1 Evaluation of CFD Results

CFD results are based on tested closed cavity façade (Façade Respirante) (CLC 12-260039255) coded model in CSTB in France.

Ca.1 and Ca.2 dew point values in CFD analysis from 0.4°C to 1.0°C higher than dew points in experimental data. This is actually proof to be stayed on safe side.

Dew point values at “Model with linear channel” is lower with respect to other models. The reason is having higher velocities leads to lower dew points.

There is no considerable temperature difference between 3 different filter modeling which is obviously seen at Figure 5.8. As it is seen from Figure 5.8, major effect to temperature distribution at cavity is stack effect. Stack effect mostly occurs by air buoyancy. Intensity of air buoyancy is depended air density difference ($1.21 \text{ kg/m}^3 - 1.29 \text{ kg/m}^3$) which varies with temperature difference (0.5 °C - 18.5 °C) and moisture difference (Mass Fraction of Steam 0.0035 - 0.0038). [16]

Velocity distribution which is driven by natural convection is mostly low. As it is indicated at Figure 5.7, velocity distribution is quite low which is under 0.1 m/s at all around cavity. The reason why velocity inside of cavity is lower relatively that the cavity fed only by one air flow inlet.

The probable disadvantage of modeling filter with linear channel is funnel effect due to narrow channel. As it is seen at Figure 5.7 and Figure 5.9, relatively higher velocities at below side leads to shift red zone to the right side compared to other ones. This is indicator of lower relative humidity distribution. This case might be neglected due to the similar relative humidity distribution with other model charts.

As it is demonstrated at Figure 5.7, Figure 5.8 and Figure 5.9, the points between blind and interior glass has high convenience for temperature, velocity and relative humidity values between each other's.

Higher velocities with ignorable level is observed at the model with linear channel. (Figure 5.7)

As it is obviously seen from Table 4.2 and Figure 5.9, there is significantly less difference between model results and experimental results with respect to “Air Flow and Heat Transfer in double skin façade”. This issue is explained at chapter 5.3.4.

CFD results indicates that there is no condensation under specified conditions at modeled cavity. According to the result of CFD model condensation will start at -0.8°C . These results are verified by experimental data, as well.

Consequently, measured data from CFD models indicates that filter modeling approaches can be alternative to simulate heat transfer and fluid behavior.

8.2 Evaluation of Lab Results

Closed cavity façade (Façade Respirante) experiment module is configured based on comprehensive CFD results.

Experiment results indicates that there is high tendency to condensation formation at venetian blinds vertically positioned case. On the other hand. when the blinds are removed. there is less probability to form condensation on outer glass surface. Moreover. as long as number of filter decrease. there is higher condensation risk. There is no condensation on glass surfaces. if there is at least 5 filters at bottom side of configured façade Respirante system.

Consequently, Configured Façade Respirante system is convenient in terms of condensation risk to CSTB Façade Respirante test methodology.

8.3 Evaluation of Energy Performance Analysis

Energy performance analysis is based on configured CCF module. Thermal analysis indicates that thermal transmittance value of window module ($U_w=1.56 \text{ W/m}^2\text{K}$) is considerably better than expected thermal transmittance value ($U_w=2.40 \text{ W/m}^2\text{K}$) according to TS 825.

There is also no condensation on neither on aluminum surface nor on glass surface under specified conditions with respect to EN 10077 standard.

Both situation means that maximum thermal performance is achieved without condensation occurrence.

There is monthly up to 6.4 W/m^2 in cooling and up to 23.6 W/m^2 in heating load saving and annually up to 17.8 W/m^2 saving in cooling load and 130.5 W/m^2 saving in heating load potential by applying CCF system under Turkey conditions.

There is up to 130.5 W/m^2 heat transfer rate difference in Turkey. It means, it can be up to 339.3 kWh annual saving for each m^2 of window. Configured CCF system with 339.3 kWh for each m^2 energy saving potential, decrease 234 kg CO_2 emission in a year which corresponds to 6 trees CO_2 emission toleration.

ACKNOWLEDGEMENT

Special thanks to **METAL YAPI** for providing licensed Solidworks Flow Simulation CFD program. supplying all the materials related with glass and frame. constituting experiment mock-up, creating time for this scientific study as employer and encouraging me to finalize master thesis.

Special thanks to **FTI (Façade Testing Institute)** supplying experiment filters from a company from France and permitting me to use all measuring devices and charging her staff to arrange experiment chambers for this scientific study.

REFERENCES

- [1] **Cleveland. Cutler J., and Christopher G. Morris.** (2009) "Building envelope (HVAC)". Dictionary of Energy, Expanded Edition. Burlington: Elsevier.
- [2] **Syed. Asif.** (2012) Advanced building technologies for sustainability, Hoboken, N.J.: John Wiley & Sons. Inc. 115. Print.
- [3] **Wilson. Jeff.** (2013) The Greened House Effect: Renovating Your Home with a Deep Energy Retrofit. Chelsea Green Publishing. White River Junction. 42. print.
- [4] **Blecker H.,** (2012) MFREE-S Closed Cavity Façade, CTBUH
- [5] **Çengel Y.,** (2002) Heat Transfer: A Practical Approach, second edition
- [6] **Velkovsky K.,** (2013) Innovations and Energy Efficiency in Contemporary Office Buildings, World Sustainable Energy Days, 28 February
- [7] **Poirazis H.,** (2004) Double Skin Façades for Office Buildings: literature review Report EBD-R—04/3, Lund University
- [8] **J. Laverge, S. Schouwenars, M. Steeman, A. Janssens, N. Van Den Bossche** (2015), Research Gate, Ghent University, Belgium
- [9] **CSTB (Centre Scientifique et Technique du Bâtiment Report).** (2012) Rapport D'essais N° CLC 12-260039255 Concernant Un Element De Façade Vitree June
- [10] **Teshome E. J., Tao Y., Haghghat F.,** Airflow and heat transfer in double skin façades, Energy and Buildings 43 (2011) 2760-2766
- [11] **Zeng Z., Li X., Li C., Zhu Y.,** Modeling ventilation in naturally ventilated double-skin façade with a venetian blind, Building and Environment 57 (2012) 1-6
- [12] **Yilmaz Z., Çetintaş F.,** Double Skin Façade's effects on heat losses of office buildings in İstanbul, Energy and Buildings 37 (2005) 691-697
- [13] **Barenbrug. A.W.T.,** (1974) Psychrometry and Psychrometric Chart., 3rd Edition, Cape Town, S.A.: Cape and Transvaal Printers Ltd.
- [14] **Stanley C.,** (2012) Mechanics of Fluids and Transport Processes Lecture Notes. The University of Iowa
- [15] **Bakker A.,** (2002) Applied Computational Fluid Dynamics Lecture-7 Meshing, Fluent Inc.
- [16] **Quirouette R.,** (2004) Air Pressure and The Building Envelope, November
- [17] **Turkish Standard Institute** (2008) Thermal Insulation Requirements in Buildings. TS 825, Ankara

- [18] **Comitte Europeen de Normalisation**, (2000) Thermal Performance of Windows, EN ISO 10077-1, Brussels
- [19] **Comitte Europeen de Normalisation**. (2000) Thermal Performance of Windows, EN ISO 10077-2, Brussels
- [20] **URL-1** <http://www.techniques-ingenieur.fr/base-documentaire/construction-th3/l-enveloppe-du-batiment-42226210/murs-rideaux-c3604/mur-rideau-respirant-c3604niv10002.html>. date retrieved 13.09.2014
- [21] **International Standard Organization**, (2012) Thermal Performance of Curtain Walling- Calculation of Thermal Transmittance. EN ISO 12631. Brussels
- [22] **Comitte Europeen de Normalisation**. (2000) Building Materials and Products. BS EN 12524. Brussels
- [23] **Comitte Europeen de Normalisation**. (2007) Building Materials and Products. EN 10456, Brussels
- [24] **Turkish Standard Institute** (2006) Building Components and Building Elements. TS EN ISO 6946. Ankara
- [25] **Turkish Standard Institute** (1983) Principles for the preparation of the projects of the central heating systems. TS 2164. Ankara
- [26] **Anonymous**, (2013) ANSI/ASHRAE Standard 55 Thermal Environmental Conditions for Human Occupancy, Atlanta, GA
- [27] **Matsson J. E.**, (2011) An Introduction to Solidworks Flow Simulation. SDC Publication
- [28] **BS Solidworks**, (2012) Solidworks Flow Simulation Tutorial
- [29] **Hella Group**, (2015) Venetian Blind Technical Data Sheet, Tirol Austria
- [30] **Sofabin**, (2013) Fische Technique Filtre 04, Chatou Cedex
- [31] **URL-2** <<http://www.sensormag.com/sensors/humidity-moisture/choosing-a-humidity-sensor-a-review-three-technologies-840>> date retrieved 24.04.2015
- [32] **Dixell**, (2005) XH20P Hygrometer Technical Data Sheet, Italy
- [33] **OMET**, T3111P Hygrometer Technical Data Sheet, Temperature and Humidity Transmitters with 4-20mA Output
- [34] **HP**, (2014) Agilent 34972A Data Logger Technical Data Sheet, Keysight Technologies in USA
- [35] **OAC Air Conditioning Inc.** (2014) Olefini-12 NA Dehumidifier Technical Data Sheet
- [36] **U.S. Energy Information Administration**, (2015) FAQ How much carbon dioxide is produced per kilowatt hour when generating electricity with fossil fuels?
- [37] **U.S. Environmental Protection Agency**, (2014) Greenhouse Gas Equivalencies Calculator

CURRICULUM VITAE



Name Surname: Ahmet Biler
Place and Date of Birth: 08.09.1989 Kocaeli/TURKEY
E-Mail: ahmetbiler@hotmail.com

EDUCATION

High School: Bolu Science High School (2003-2007)
B.Sc.: Istanbul Technical University-Civil Engineering
Faculty-Civil Engineering (2007-2012)
Technische Universität Darmstadt-Bauingenieurwesen
(2011)
M.Sc.: Istanbul Technical University-Energy Institute-Energy
Science and Technology (2012-2015)

PUBLICATIONS. PRESENTATIONS AND PATENTS ON THE THESIS:

- Biler A., Sözer H. (2015) Modeling Condensation Risk on Closed Cavity Façade. Sustainable and Renewable Energy Reviews (Under Editor Evaluation), March 02. 2015
- Biler A., Sözer H. (2014) Thermal Modelling of Double Skin Façades. Istanbul Technical University Energy Institute- Seminar Presentation. May 8th, 2014. İstanbul

OTHER PUBLICATIONS. PRESENTATIONS AND PATENTS:

- Biler A., (2014) Integrated Trickle Vent in Structural Silicone Glazed Unitized Panel Curtain Wall, European Property Awards Summit Oct 14th, 2014 London
- Özgül Z., Biler A., (2014) Concealed Sliding Vent System Integrated to Structural Silicone Glazed Unitized Curtain Wall System. European Property Awards Summit Oct 14th, 2014 London
- Biler A., (2014) DAP Burgu Kule, Journal of “Çatı ve Cephe”. July 2014
- Biler A., (2014) Trickle Vent, Journal of “Mimarlık ve Dekorasyon”. October 2014

PROFESSIONAL EXPERIENCE AND REWARDS:

R&D Department / Metal Yapı Holding A.Ş./ 07.2013-... İstanbul - Turkey

- Coordination of Patent Affairs
- Heat Transfer Analysis and Structural Analysis of Façade Systems
- CFD Analysis with Solidworks Flow Simulation to simulate thermal comfort conditions
- Article writing for the magazines in façade sector
- Developing Thesis about “Identification of Closed Cavity Façades in terms of Condensation Risk and Energy Performance Analysis”
- Comparative Thermal Analysis of Alternative Glazing Combinations for Maslak Orjin Project Double Façade Systems
- Daylighting Performance Analysis of Light Shelves through Ecotect

Research Group Member/ Istanbul Technical University Energy Institute / 09.2012 -02.2013

- IPRO Project: Application of renewable energy systems to the certain building with Illinois Institute of Technology (Chicago U.S.)

R&D Engineer/ Asteknik Engineering Co. / 10.2012 -07.2013 İstanbul - Turkey

- Conducting all test processes for products which will be introduced both domestic and international market in Universities.
- Analysis of international project specifications. offering the rightest profiles from product range of company and affording for quality of products to satisfy international standards (ASTM, EN, DIN etc...)
- New product search in global market and the most optimized product is gained to company as a result of technical and economic analysis
- Contacting for technical problems with international companies which are currently represented in Turkey by us and preparation of installation instruction both Turkish and English
- (Attendance to Munich Construction Fair) in order to conduct one technical interview and one commercial interview)

Project Intern Engineer / Istanbul Technical University Civil Engineering Faculty Hydraulic Laboratory / 06.2012 - 08.2012 İstanbul- Turkey

- Designing components of Floating Breakwater with Greek Assist. Prof. Eva Loukogeorgaki
- Designing Oblique Water break which is Master Thesis of Bsc. Engineer Lami Açıanal
- Processing wave data on Mat lab

Translator / Edu Fairs International Education Fairs

Translator (Sequential translator during the presentations of academicians from USA, Canada and UK.)

10 - 11 March 2012 (Hilton İstanbul Conference Hall)

10 - 11 November 2012 (Hilton İstanbul Conference Hall)

16 - 17 March 2013 (İstanbul Congress Center Yıldız Conference Hall)

Intern Engineer / Akış Real Estate Investment Trust / 06.2010-08.2010 İstanbul

Akbatı Shopping and Life Center, Akbatı Residences projects office and site works